

8-2017

Visual Detection of Small Unmanned Aircraft: Modeling the Limits of Human Pilots

Gregory Stephen Woo

Follow this and additional works at: <https://commons.erau.edu/edt>



Part of the [Aerospace Engineering Commons](#), and the [Aviation Commons](#)

Scholarly Commons Citation

Woo, Gregory Stephen, "Visual Detection of Small Unmanned Aircraft: Modeling the Limits of Human Pilots" (2017). *Dissertations and Theses*. 350.

<https://commons.erau.edu/edt/350>

This Dissertation - Open Access is brought to you for free and open access by Scholarly Commons. It has been accepted for inclusion in Dissertations and Theses by an authorized administrator of Scholarly Commons. For more information, please contact commons@erau.edu.

**VISUAL DETECTION OF SMALL UNMANNED AIRCRAFT:
MODELING THE LIMITS OF HUMAN PILOTS**

By

Gregory Stephen Woo

A Dissertation Submitted to the College of Aviation
in Partial Fulfillment of the Requirements for the Degree of
Doctor of Philosophy in Aviation

Embry-Riddle Aeronautical University
Daytona Beach, Florida
August 2017

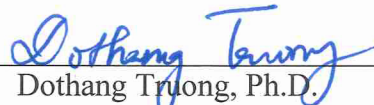
© 2017 Gregory Stephen Woo
All Rights Reserved.


**VISUAL DETECTION OF SMALL UNMANNED AIRCRAFT:
MODELING THE LIMITS OF HUMAN PILOTS**


By

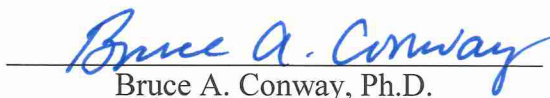
Gregory Stephen Woo

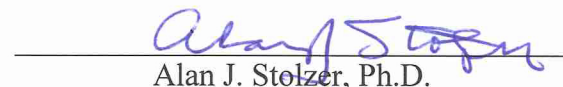
This dissertation was prepared under the direction of the candidate's Dissertation Committee Chair, Dr. Dothang Truong, and has been approved by the members of the dissertation committee. It was submitted to the College of Aviation and was accepted in partial fulfillment of the requirements for the
Degree of
Doctor of Philosophy in Aviation


Dothang Truong, Ph.D.
Committee Chair

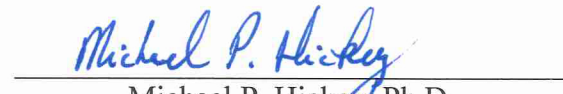

Haydee M. Cuevas, Ph.D.
Committee Member


Antonio I. Cortés, Ph.D.
Associate Dean, School of Graduate
Studies


Bruce A. Conway, Ph.D.
Committee Member


Alan J. Stolzer, Ph.D.
Dean, College of Aviation


Michael K. Zuschlag, Ph.D.
Committee Member


Michael P. Hickey, Ph.D.
Dean of Research and Graduate Studies

08/17/2017
Date

ABSTRACT

Researcher: Gregory Stephen Woo

Title: VISUAL DETECTION OF SMALL UNMANNED AIRCRAFT:
MODELING THE LIMITS OF HUMAN PILOTS

Institution: Embry-Riddle Aeronautical University

Degree: Doctor of Philosophy in Aviation

Year: 2017

The purpose of this study was to determine the key physical variables for visual detection of small, Unmanned Aircraft Systems (UAS), and to learn how these variables influence the ability of human pilots, in manned-aircraft operating between 60-knots to 160-knots in the airport terminal area, to see these small, unmanned aircraft in time to avoid a collision. The study also produced a set of probability curves for various operating scenarios, depicting the likelihood of visually detecting a small, unmanned aircraft in time to avoid colliding with it. The study used the known limits of human visual acuity, based on the mechanics of the human eye and previous research on human visual detection of distant objects, to define the human performance constraints for the visual search task.

The results of the analysis suggest the probability of detection, in all cases modeled during the study, is far less than 50 percent. The probability of detection was well under 10 percent for small UAS aircraft similar to the products used by many recreational and hobby operators.

The results of this study indicate the concept of see-and-avoid is not a reliable technique for collision prevention by manned-aircraft pilots when it comes to operating near small, unmanned aircraft. Since small, unmanned aircraft continue to appear in

airspace where they do not belong, regulators and the industry need to accelerate the development and deployment of alternative methods for collision prevention between sUAS aircraft operations and manned-aircraft.

The analysis effort for this study included the development of a new simulation model, building on existing models related to human visual detection of distant objects. This study extended existing research and used currently accepted standards to create a new model specifically tailored to small, unmanned aircraft detection. Since several input variables are not controllable, this study used a Monte Carlo simulation to provide a means for addressing the effects of uncertainty in the uncontrollable inputs that the previous models did not handle. The uncontrollable inputs include the airspeed and direction of flight for the unmanned aircraft, as well as the changing contrast between the unmanned aircraft target and its background as both the target aircraft and the observer encounter different background and lighting conditions.

The reusable model created for this study will enable future research related to the visual detection of small, unmanned aircraft. It provides a new tool for studying the difficult task of visually detecting airborne, small, unmanned aircraft targets in time to maneuver clear of a possible collision with them. The study also tested alternative input values to the simulation model to explore how changes to small, unmanned aircraft features might improve the visual detectability of the unmanned aircraft by human pilots in manned aircraft. While these changes resulted in higher probabilities of detection, the overall detection probability remained very low thereby confirming the urgent need to build reliable collision avoidance capability into small UAS aircraft.

DEDICATION

I dedicate this dissertation to my amazing wife Sarah, who encouraged, supported, and challenged me when I needed it most. Sarah made it possible for me to pursue my passion for aviation-related studies and research. Without her steadfast support, patience, and encouragement, this dream would not have been possible.

ACKNOWLEDGEMENTS

I wholeheartedly thank my dissertation committee for their thought-provoking questions, encouraging support, and helpful feedback throughout my efforts to formulate and produce this dissertation. I would not have learned nearly as much had it not been for the dissertation committee's guidance and insightful efforts to keep me energized and focused on the right possibilities and questions.

I especially thank my dissertation chair, Dr. Dothang Truong, for his invaluable mentorship throughout my dissertation effort as well as during my graduate course work. He made it intriguing and satisfying to work my way through a number of intimidating textbooks and topics such as statistical analysis, data modeling, and decision-making. Throughout the dissertation effort, he provided just the right amount of encouragement and thought-provoking inquiry to keep me motivated and focused.

Thank you to Dr. Haydee Cuevas for growing my knowledge regarding the study of human factors and the science of human behavior integrated with mechanical devices and control systems. The human factors aspect of my doctoral learning experience was one of the major highlights of this program for me.

Thank you to Dr. Bruce Conway, who stimulated both my thinking about my research objectives and my formulation of the outcome and conclusion discussions. He provided thought provoking and helpful questions to guide my study efforts. Additionally, he gave me a strengthened perspective on systems engineering which has helped me advance in my career.

Thank you to Dr. Michael Zuschlag, who was instrumental in getting me to clarify my thinking and my descriptions of the findings for this study. His questions,

thoughtful challenges, and editorial comments drove me to research, explore, and test many more facets of this problem than I would have considered probing on my own.

Thank you to Dr. Alan J. Stolzer for his inspiration and encouragement regarding my academic writing efforts. He inspired my strong interest in safety management systems and aviation safety research. This educational experience has been one of the major highlights of my life, and the combination of safety management, human factors, and systems engineering has been a perfect fit with my career-related passions.

Thank you to Sam DeBartolo, a great friend, a superb pilot, and a promising student who is part of our future in the aviation industry. His enthusiastic help in gathering data about popular recreational drone products was both helpful and informative.

Most of all, I wish to thank my wife, Sarah, and my entire family, for their enduring love, patience, understanding, and sacrifices these past several years. I know it was not easy having me lost in my studies and removed from our day-to-day lives for these past numerous years. I would not have made it through this without Sarah's love, support, and encouragement. I am so lucky to have her in my life and cannot begin to describe how much I cherish her love.

TABLE OF CONTENTS

	Page
Signature Page	iii
Abstract	iv
Dedication	vi
Acknowledgements	vii
List of Tables	xii
List of Figures	xiv
Chapter I Introduction	1
Statement of the Problem.....	4
Purpose Statement.....	6
Significance of the Study	6
Research Questions.....	9
Delimitations.....	9
Limitations and Assumptions	11
Definitions of Terms	14
List of Acronyms	14
Chapter II Review of the Relevant Literature	16
The Significance of Small UAS.....	16
Potential Technology-based Solutions.....	21
Existing Studies in Human Observer Capabilities.....	27
Visual Acuity	28
Retinal Eccentricity.....	33

	Contrast Threshold.....	36
	Target Discrimination Against Background Clutter	39
	Other Factors Affecting Visual Target Detection.....	41
	Useful Models for Visual Recognition of Airborne Objects	44
	The Relevance of Monte Carlo Simulation	53
	Other Factors Affecting the Visual Recognition Model.....	54
	Conclusions from the Existing Literature.....	55
Chapter III	Methodology	57
	Research Approach.....	57
	Design and Use of the Model.....	63
	Apparatus and Materials	74
	Sources of the Data	75
	Model Reliability	79
	Model Validity.....	80
	Background Clutter.....	81
	Treatment of the Data	82
Chapter IV	Results	83
	Verification Testing	83
	Reliability Testing.....	90
	Descriptive Statistics of the Results.....	94
	High Contrast Testing.....	105
	Results Summary	107

Chapter V	Discussion, Conclusions, and Recommendations.....	109
	Discussion.....	110
	sUAS size.....	111
	Manned aircraft airspeed.....	113
	Search time.....	114
	sUAS contrast	115
	Conclusions.....	118
	Methodology and data.....	120
	Validity	121
	Practical implications.....	123
	Theoretical implications.....	124
	Limitations	125
	Recommendations.....	126
	Future research opportunities.....	128
	References.....	130
	Appendices.....	140
A	Common Small UAS Products and Specifications	140

LIST OF TABLES

Table	Page
1 Technologies to Prevent Manned vs. Unmanned Traffic Conflicts	22
2 Snellen Relationship to Visual Arc Size in Minutes	32
3 Sky Luminance.....	48
4 Input and Output Variables for the Model	61
5 Aircraft Identification and Reaction Time	77
6 Atmospheric Visibility Data from Selected Airports	79
7 Closure Rate Calculation Node Verification Results	87
8 Minimum Range Node Verification Results	87
9 Contrast-Adjusted UAV Size Node Verification Results	88
10 Maximum Range Node Verification Results	89
11 Probability of Sighting Node Verification Results.....	89
12 Comparison of Results with Different Random Number Seed Values.....	93
13 Area of Small UAS Side View Profile.....	95
14 Probability of Sighting a 0.2 Square Foot sUAS.....	96
15 Probability of Sighting a 0.7 Square Foot sUAS.....	98
16 Probability of Sighting a 1.0 Square Foot sUAS.....	99
17 Probability of Sighting a 1.5 Square Foot sUAS.....	100
18 Probability of Sighting a 3.5 Square Foot sUAS.....	102
19 Probability of Sighting a 10.8 Square Foot sUAS.....	103
20 Probability of Sighting a 1.0 Square Foot sUAS, Contrast = 0.8.....	105
21 Probability of Sighting a 1.0 Square Foot sUAS, Contrast = 1.0.....	106

22	Probability of Sighting a 100 Square Foot sUAS.....	113
----	---	-----

LIST OF FIGURES

Figure	Page
1 Determination of visual angle	30
2 Visual acuity related to retinal eccentricity	35
3 Changing visual target area based on perspective	49
4 Research approach overview	58
5 Monte Carlo Simulation Model Flowchart	64
6 Conceptual layout of the mathematical model	74
7 Probability density distribution of target contrast values	84
8 Probability density distribution of UAV airspeed values	85
9 Probability density distribution of relative UAV heading values	86
10 Probability of detection curve: 0.2 square foot target	97
11 Probability of detection curve: 0.7 square foot target	98
12 Probability of detection curve: 1.0 square foot target	99
13 Probability of detection curve: 1.5 square foot target	100
14 Probability of detection curve: 3.5 square foot target	102
15 Probability of detection curve: 10.8 square foot target	103
16 Average arc size of image at latest possible detection time	104
17 Probability of detection curve: 1.0 square foot target, contrast = 0.8	106
18 Probability of detection curve: 1.0 square foot target, contrast = 1.0	107
19 Composite probability of detection graph	111
20 Available search time	115
21 Extreme contrast test – contrast = 100	117

CHAPTER I

INTRODUCTION

Federal Aviation Administration (FAA) records, over the past several years, show pilots are reporting visual contact with small Unmanned Aircraft System (sUAS) aircraft flying near their manned aircraft in locations where no sUAS aircraft should be operating (FAA, 2017b). This study provides new perspectives about the limits, issues, and key factors associated with human visual detection of sUAS, for collision avoidance by pilots in manned aircraft operating in the airport terminal area at airspeeds ranging from 60-knots to 160-knots.

This study also includes the construction and use of a mathematical model to determine the ability of a human pilot, flying a manned aircraft, to spot and maneuver clear of a sUAS in time to avoid colliding with it in the airport terminal area. The 60-knot to 160-knot airspeed range used in this study represents common operating profiles for aircraft, ranging from light sport aircraft to airliners, during airport approach and departure operations where these manned aircraft are most likely to encounter sUAS aircraft (FAA, 2016a). The mathematical model applies the known limits of human visual performance to conditions pilots encounter when looking for small, distant objects from the cockpit of an aircraft.

Technically, an Unmanned Aircraft System (UAS) includes the unmanned aircraft, its control station, and the infrastructure and communications systems needed for the aircraft to complete its mission as determined by the aircraft's operator. Historically, people have referred to the actual unmanned aircraft as an Unmanned Aerial Vehicle (UAV) or drone. The FAA refers to the actual Unmanned Aircraft as a UA (FAA, 2013).

Since the literature often uses these terms interchangeably, for the purposes of this research project, the reader should assume UAS, UAV, and UA mean unmanned aircraft.

To date, no specific solutions exist to help manned aircraft pilots see and avoid UA, especially small UA. Instead, many research and development initiatives are underway to develop strategies for the safe, efficient integration of UAS operations into our National Airspace System (NAS) in a manner designed to prevent unmanned aircraft from colliding with manned aircraft. These studies include the use of existing collision avoidance systems for manned aircraft and a variety of future sensing technologies for unmanned aircraft (Yu & Zhang, 2015). Other research explores the use of communications networks and cooperative management strategies in which aircraft communicate with each other and with ground-based and satellite-based systems to achieve collision avoidance, coordination, and in-flight decision-making (Frew & Brown, 2008). The appropriate solution for keeping UA and manned aircraft from colliding in the NAS will ultimately depend on the mission requirements and operational boundaries for the UA.

This study focuses on sUAS aircraft because they make up the fastest growing component of the UA population and are the most likely to appear improperly in airspace near manned aircraft. *Aviation Week & Space Technology* concurs and further states that non-commercial operators have easy access to sUAS aircraft and are often the operators who fly UAs in unauthorized or prohibited areas (Esler, 2015).

According to a recent retail tracking study by The NPD Group, Inc., sUAS sales are growing dramatically. Their study found a 224 percent increase in drone sales to nearly \$200 million from April 2015 to April 2016 (NPD Group, 2016). The NPD

Group, an international market research corporation, predicted continued strength in retail sales of drones for both 2016 and 2017. An FAA industry forecast report estimates 2.5 million sUAS sales in 2016, 4.8 million sales in 2017, and yearly growth to 7.0 million sales in 2020 (FAA, 2016b). The FAA (2016a) also states reports of UAS sightings “have increased dramatically since 2014” (para. 2). The FAA is concerned about the sightings because “safely integrating unmanned aircraft into the national airspace system is one of the FAA's top priorities, and the agency wants to send a clear message that operating drones around airplanes and helicopters is dangerous and illegal” (FAA, 2016a, para. 2).

Based on the large volume of literature about UAS sense and avoid technology, the UAS industry, government agencies, and educational institutions are aggressively researching and developing technology-based proposals for keeping small UA away from manned aircraft. These technology efforts include sense-and-avoid systems, machine vision, radar, electronic collaboration and decision-making, and air traffic control augmentation systems (FAA, 2016c; Gettinger & Michel, 2015; Lai, Mejias, & Ford, 2011; Mcfayden & Mejias, 2015; Yu & Zhang, 2015). However, current guidance to pilots calls for visual separation by the operators of both the manned and unmanned aircraft (Consiglio, Chamberlain, Muñoz, & Hoffler, 2012; Operation and Certification of Small Unmanned Aircraft, 2016; Yu & Zhang, 2015).

Le Tallec (2005) raised concern about the lack of specific solutions for general aviation pilots for the safe avoidance of UAVs, over 10 years ago. In 2005, Le Tallec proposed a converging traffic alert system as a strategy to make it easier for manned aircraft pilots to find, see, and avoid UAV-related traffic conflicts. Though the industry

did not adopt Le Tallec's proposal, the underlying concern remains true in 2017. Until industry deploys such a solution in the NAS, see-and-avoid remains the primary tool for collision avoidance between aircraft (Le Tallec, 2005). To date, no solution exists in the NAS to address the UAV detection challenge for manned aircraft pilots.

Visual detection and identification studies on full-sized, passenger-carrying aircraft exist in the literature and have many years of relevant application validating their findings; however, few studies address the identification and avoidance of small UAV hazards by manned aircraft pilots. One recent study conducted by Loffi, Wallace, Jacob, and Dunlap (2016) attempted to establish performance benchmarks related to the detection of sUAS aircraft by pilots on manned aircraft. Their study collected data from actual flight test encounters between manned and unmanned aircraft. Loffi et al. did not attempt to connect their findings with the physiological limits of human performance nor did they attempt to create a flexible model for simulating human visual performance in varying operational environments where closure rates, background contrast, and apparent sUAS size might change depending on viewing angles and mission conditions. The pilots of manned aircraft, both now and for the next few years, must rely on their vision to avoid small UAs. The question is, how reliably can a pilot of a manned aircraft see and avoid a small UA?

Statement of the Problem

Every month, the FAA receives over 100 reports of small UA operating in airspace where they do not belong (FAA, 2017b) and the industry has not deployed any specific, ubiquitous solution to preclude this potential collision hazard for pilots of manned aircraft. While some manufacturers build geo-fencing and other operational

safety constraints into their UA products, such features are not standard for the industry, and many UA products exist in the field without such safeguards. Therefore, manned aircraft pilots must have some means of detecting and avoiding these UA intrusions.

At present, no specific solutions exist to help the pilots of civilian manned aircraft spot and avoid a small UA in flight. In the near-term, pilots of civilian manned aircraft must rely on their own ability to visually detect and avoid UA because no other technology-based UA avoidance solutions are available.

The FAA's current strategy to keep small, recreational UA separated from manned aircraft is to educate UA operators about regulations and airspace constraints designed to keep small UA away from manned aircraft (Loffi, Wallace, & Ison, 2016). Given the number of sightings of small UA operating outside of the FAA-defined regulations, these procedures and regulations are not producing the reliable separation of manned and unmanned aircraft needed to ensure safety in the NAS (Gettinger & Michel, 2015; Loffi, Wallace, & Ison, 2016).

Since UA continue to appear outside the airspace they are supposed to be constrained to, and since UA continue to be sighted in areas where they pose a conflict hazard for the pilots of manned aircraft, see-and-avoid is an essential, last defense against mid-air collisions. Additionally, the literature review effort did not reveal any studies specifically designed to determine the key factors and human performance limits for the small UA avoidance task. The studies on visual detection of UA that do exist focus on the future of how UA can avoid encroaching upon other aircraft.

Purpose Statement

The purpose of this study was to determine the key physical attributes related to visual detection of sUAS aircraft and their operations. The study also related these key attributes to the ability of human pilots in manned aircraft to see these sUAS aircraft in time to avoid a collision. Graham (1989) and Morris (2005) suggest smaller-sized aircraft are generally difficult to see in time to allow a pilot to avoid colliding with them. The smaller aircraft in the Graham and Morris studies were much larger than the small UAS aircraft targets in this study. Loffi et al. (2016) conducted flight test studies and found pilots generally had difficulty spotting small UAS targets from the cockpit of their Cessna 172 aircraft. This study therefore hypothesized small UA targets would be very difficult to visually spot in time to allow action for collision avoidance.

An additional purpose of this study was to determine the likelihood a manned aircraft pilot would detect a small UA in time to avoid colliding with it. The analytical model developed for this study produced probability of visual detection numbers using specific input variable values appropriate for the scenarios defined in the study. The study also produced a reusable mathematical model for future research, related to the visual detection of small UA, in applications such as visual detection by law enforcement / safety officers and visual tracking of small UA by the UA operator.

Significance of the Study

This study extends the research from previous studies on visual target recognition and human visual search performance by building on existing models developed by Howett (1983) and Andrews (1991a), to create a new model specifically tailored to predicting the probability of visually detecting a small UA from a distance of a

few thousand feet or more. For each case of a manned aircraft encountering a small UA, the contrast of the target against its background is likely to change (Poe, 1974). Contrast is therefore an uncontrollable input variable. This study expands the utility of existing visual detection models by adding a Monte Carlo simulation framework to address uncontrollable input variables such as target contrast and target airspeed, to address the uncertainty in the visual search task.

The study integrates the research findings from Wulfeck et al. (1958), Erickson and Burge (1974), Poe (1974), Chisolm (1977), and Hirsch and Curcio (1989) to provide the justification for the selection of the input variables and to explain the assumptions used for the treatment of the data in this study. Data from previous studies and existing research reports provided the information on human visual search performance and human physiological constraints needed to construct the simulation model for this study. The selected inputs target the limits of human visual performance based on the mechanics of the human eye. As a result, the simulation model for this study used the following inputs:

- Size of the target UAS vehicle,
- Airspeed of the unmanned aircraft,
- Relative heading of the unmanned aircraft,
- Airspeed of the manned aircraft,
- Minimum time needed to avoid colliding with the target (includes both human see / react time and aircraft trajectory alteration time), and
- Contrast factor between the target and the background scenery.

The simulation model determined the probability, given specific conditions, that a human pilot will see a sUAS aircraft in time to avoid colliding with it. The output of the model, rendered in both numerical table form and graphical form, relates the probability of sUAS target detection to the values of the controllable input variables. The probability curves illustrate how visual detection probability varies as a function of UAS size, manned aircraft airspeed, closure rate between the manned and unmanned aircraft, and contrast between the UA and its background.

The resulting model produced by this research also provides a mechanism for modeling future research questions related to the visibility of small UA by the UA operator under various conditions. The model could address questions related to the visual detection of other small objects, from the aircraft cockpit, such as foreign object debris on the runway at airports. Though these visual detection tasks are outside the scope of this study, the model produced by this study would be applicable to those types of tasks.

Additionally, this research provides aviation regulators with science-based analysis of the visibility of small UA from the manned aircraft cockpit given the current lack of sUAS target detection technology available to pilots in the cockpit. The probability of detection curves produced by this study, relating the likelihood of visual detection to the controllable input parameters of this model, provides rule-makers with context as they produce practical, near-term regulations for sUAS operations in airspace used by manned aircraft. At the very least, agencies who promote aviation safety now have additional insights to share with aircraft operators regarding the limits of human vision performance and the timely detection of sUAS collision hazards.

Research Questions

The research questions for this study were:

1. What variables in the small UAS probability of detection model, related to the physical features of a small UAS or the manner in which pilots operate their manned aircraft, limit the manned aircraft pilot's ability to see a small UAV in time to avoid a potential collision with it?
2. What is the probability a manned aircraft pilot will see a small UAV in time to avoid colliding with it, given different scenarios determined by the controllable input variables?
3. What simulation model parameters, if changed, would improve the manned aircraft pilot's ability to see and avoid a small UAV?

Delimitations

This study focused only on the visual detection and avoidance of small UAS aircraft. Small UAS aircraft are those UA with a maximum gross weight of less than 55 pounds, including any cargo or equipment carried by the aircraft (Operation and Certification of Small Unmanned Aircraft, 2016). *Aviation Week & Space Technology* noted small UAs often appear in FAA sighting reports of improper or illegal operations (Esler, 2015). Small UA products are now available to consumers at affordable prices, enabling non-professional remote pilots to obtain these aircraft. Without the formal training and operational proficiency testing imposed on professional UAS operators, recreational and hobby operators are more likely to fly their aircraft into conflict situations with manned aircraft (Esler, 2015). The FAA Mandatory Occurrence Report (MOR) summaries appear to confirm this belief with hundreds of UAS sighting reports

describing small UA flying illegally in areas reserved for manned aircraft operations (FAA, 2017b).

The study did not include large-sized UAV because they typically operate in reserved airspace under the control of a professional, well-trained, UAV pilot. Large UAV operations are also typically coordinated with Air Traffic Control (ATC), so air traffic controllers can pass along UAV location data to other aircraft in the area. Large UAV may also carry position-reporting technology such as a radar transponder or an Automatic Dependent Surveillance-Broadcast (ADS-B) device, which can alert manned aircraft pilots about their presence in the area (Yu and Zhang, 2015). Small UAV products sold to date generally lack transponders and ADS-B technology (Gettinger and Michel, 2015).

This study also modeled the probability of detection based on human visual detection and recognition capabilities as described in multiple previous research efforts. However, this investigation did not include human subject testing because the intent of this study was to extend existing, validated models of human visual target identification to the identification of small UAVs. The focus of this study compares the known limits of human vision to the physical requirements for sighting a small UA from an adequate distance to allow time to react and maneuver clear of a collision with the UA. The study did not test human subjects in this role since previous research used by this study already did human subject testing for validation of the underlying concepts related to the human aspects of the visual search performance algorithm used in this study (Andrews, 1991).

Additionally, this study modeled operations in daytime, good visibility weather conditions. This study did not attempt to model poor visibility weather conditions,

nighttime or dim light conditions, or adverse conditions such as storms. Recreational UAV operators are less likely to fly their UA in these types of conditions due to aircraft vulnerability and aircraft control difficulties.

The manned aircraft speeds used in this study range from 60 knots to 160 knots. The study used this range of airspeeds because they are typical for the civilian aircraft from which pilots often report sUAS sightings (FAA, 2017b). Civilian aircraft operating at the lower altitudes, where sUAS encounters are most likely to occur, are typically departing, approaching, or arriving at airports at airspeeds within this proposed range.

The study ignored the potential for degraded visual capability in the population of manned-aircraft pilots because pilots with abnormal or degraded visual capacity should not be capable of passing the FAA's medical requirements for pilots. The study also excluded consideration of poor pilot proficiency and poor pilot scanning techniques. Instead, it focused on the limitations imposed by the performance constraints of the human eye.

While there are a number of delimitations identified for this study, they are all consistent with operational constraints relevant to the use of current-day small UA. Therefore, the focused nature of this study does not detract from its utility nor its suitability for generalized use when it comes to modeling the performance limitations of human vision for small UA detection.

Limitations and Assumptions

The simulation model in this study assumed no technology-based image enhancement and no electronic UA position sensing information are available to the manned aircraft pilot for the purposes of detecting and identifying small UA collision

threats. This assumption reflects the current state of small UA operations and the current lack of technology in manned civilian aircraft cockpits to detect and avoid small UA. This study did not include consideration for manned military aircraft, with high-resolution surveillance and small target detection capabilities.

The study used a Monte Carlo simulation to model uncertainty in the uncontrollable input variables representing the speed, relative direction, and contrast of the UA. Though there are a wide variety of additional human factors variables that affect the ability of a human pilot to see and avoid airborne collision hazards, such as small UAs, this study did not account for them in its model. The reason for excluding these other human factors issues, including cognitive workload, misplaced attention, other distractions, fatigue, poor physical health, and loss of situation awareness, is they are numerous and vast in terms of how they may manifest themselves. The resulting model would be cumbersome and difficult to understand, and the output would potentially be of little use. The inclusion of these human factors variables would require a separate human subject experiment for validation of the model, and the additional variables could potentially obscure the effect of the controllable input variables of primary interest.

Furthermore, the study did not model the effects of background clutter. The validated models for visual search and detection of airborne targets found during the literature review also excluded any special logic for the effects of background clutter. Instead, existing models of airborne target detection focus on target contrast against the background. This study used the contrast-based approach as well, and it used a Monte Carlo simulation to model the uncertainty associated with target contrast values.

All of the additional variables identified and not included in the model to date reduce the likelihood of detecting and recognizing a small UA at a distance. Since some of the references and preliminary testing of the visibility concepts found during the literature review suggest small UAV are difficult to see at distances of a few thousand feet or more, the extraneous variables not included in the model would all serve to strengthen the study's findings by further reducing the likelihood of detection. None of the potential extraneous variables improves the human pilot's ability to see and avoid small airborne objects from manned aircraft. The variables chosen for use in this study target investigation of the limits of human vision performance to determine the degree to which human visual acuity affects the small UA sighting task.

Definitions of Terms

sUAS	A small Unmanned Aircraft System weighing less than 55 pounds including its payload, cargo, etc. (Operation and Certification of Small Unmanned Aircraft, 2016).
NPD Group	The NPD Group, Inc. is an international market research corporation. The NPD initials came from the company's history with its previous National Purchase Diary data service; however, the current company name is not an acronym and the previous data service is not a core component of the company's current identity (http://www.npd.com).

List of Acronyms

ADS-B	Automatic Dependent Surveillance - Broadcast
AMA	Academy of Model Aeronautics
AMSA	Australian Maritime Safety Authority
ATC	Air Traffic Control
ATSB	Australian Transport Safety Board
BASI	Bureau of Air Safety Investigation
CFR	Code of Federal Regulations
EO	Electro-Optical system
ERAU	Embry-Riddle Aeronautical University
FAA	Federal Aviation Administration
GBSAA	Ground-based Sense and Avoid
IR	Infrared

IRB	Institutional Review Board
LIDAR	Laser Detection And Ranging
MOR	Mandatory Occurrence Report
NAS	National Airspace System
SAR	Synthetic Aperture Radar
sUAS	Small Unmanned Aircraft System
TCAS	Traffic Alert and Collision Avoidance System
TIS	Traffic Information Service
TSSIM	Target Structure Similarity
UA	Unmanned Aircraft
UAS	Unmanned Aircraft System
UAV	Unmanned Aerial Vehicle

CHAPTER II

REVIEW OF THE RELEVANT LITERATURE

This chapter describes the existing literature documenting the concerns, flight hazards, and current mitigation work related to the prevention of collisions between manned and unmanned aircraft. It details the importance of visual detection of both manned and unmanned aircraft until the government or industry can establish and enforce technology standards to prevent unmanned aircraft from creating safety hazards for aircraft with onboard human pilots.

In order to understand and describe the limits of human visual capability this study used a Monte Carlo simulation model to gather insight about the limits and sensitivity of key parameters affecting a human pilot's ability to see and avoid an unmanned aircraft. Therefore, this chapter also describes the supporting rationale for the input variables to the Monte Carlo model, how the variables are treated, and the algorithms used in the simulation model. It explores the available literature describing human vision and visual performance limits. The chapter also addresses the applicability of Monte Carlo simulation modeling to the characterization of human visual search capabilities.

The Significance of Small UAS

The Federal Aviation Administration (FAA) defines Small Unmanned Aircraft Systems (sUAS), commonly referred to as drones, as aircraft weighing less than 55 pounds (FAA, 2016b) with no onboard pilots. Within the last two years, sUAS sales have grown rapidly. Sales of sUAS grew 224 percent from April 2015 to April 2016, and the NPD Group expects sUAS sales to remain strong through 2017 (NPD Group, 2016).

The FAA industry forecast report also estimates strong growth in annual sales to 7.0 million in 2020 (FAA, 2016b).

To manage the influx of these sUAS aircraft in our nation's skies, the FAA, user community organizations such as the Academy of Model Aeronautics (AMA), and many of the vendors and manufacturers of sUAS have created public awareness campaigns to educate sUAS operators with the knowledge and information needed to fly their vehicles safely in accordance with FAA regulations. Despite government and industry efforts to educate the sUAS operator community, manned aircraft pilots and ground observers continue to report sUAS aircraft operating improperly in controlled airspace (FAA, 2017b; Gettinger & Michel, 2015).

The continued presence of improperly operated sUAS presents both operational and safety challenges for pilots of manned aircraft. According to the FAA's UAS Sightings Report web page from both March 2016 and February 2017, the agency receives more than 100 sighting reports each month (FAA, 2017a; FAA, 2017b). The FAA also states potential drone sighting reports increased over 45% between February through September 2016 compared to the same period in 2015 (FAA, 2017a). While many of these reported sightings did not describe immediate collision hazards, the ongoing occurrence of these incidents suggests there are a number of sUAS operators who are not abiding by the regulatory constraints and best practice guidelines taught by industry user organizations such as the AMA. Additionally, finding the irresponsible or misinformed sUAS operators can be difficult given the products already deployed to the consumer market (Esler, 2015).

Very few sUAS aircraft already sold to consumers contain any means of tracing the link between the operator and the actual aircraft; therefore, it is often difficult to hold sUAS operators accountable for improper operation of their aircraft (Loffi, Wallace, & Ison, 2016). The FAA is attempting to create both awareness and accountability among sUAS operators by requiring them to register as operators and to identify their aircraft with registration identification markings. As of March 2016, the FAA (FAA, 2016a) had over 406,000 registered sUAS operators, though they had estimated that as many as 1.6 million sUASs would be sold in 2015 (Registration and Marking Requirements for Small Unmanned Aircraft, 2015). It is likely many sUAS operators have not registered their unmanned aircraft, and the FAA expected up to 1.9 million additional sUASs to be sold to hobbyists in 2016 (Registration and Marking Requirements for Small Unmanned Aircraft, 2015).

Given the large number of sUAS vehicles purchased by consumers in 2015 and 2016, the ongoing reports of improper sUAS operations (Loffi, Wallace, & Ison, 2016; Gettinger & Michel, 2015), and the lack of tracking and / or collision avoidance technology deployed in these vehicles, sUAS and manned aircraft pilots must rely on visual detection and human action to avoid collision hazards. “See and avoid capability ... is considered the last line of defence against a mid-air collision once all auxiliary layers of the collision avoidance process have failed” (Mcfadyen & Mejias, 2016, p.2). Since nascent sUAS aircraft sold in 2016 and earlier do not generally have reliable detect-and-avoid technology to guide them away from manned aircraft, visual detection and avoidance will serve as a crucial function in the manned aircraft cockpit for as long as these early generation UAV aircraft continue to fly in the public airspace. The FAA

describes the requirement for manned aircraft pilots to see and avoid other aircraft in its final rule for operation and certification of small UAS – Federal Register, Volume 81, No. 124, published on June 28, 2016 (Operation and Certification of Small Unmanned Aircraft, 2016).

Though the FAA and other aviation industry groups have repeatedly expressed safety concerns related to ongoing reports of UAV sightings in airspace prohibited for UAV operations, other industry organizations believe the concerns are overstated. The AMA countered concerns by the FAA, news media, and various researchers such as Gettinger and Michel (2015) stating, “Only a small number of sightings were legitimately reported as ‘near misses,’ the most serious reports involved government-sponsored military drones and some reports appeared to involve people flying responsibly” (AMA, 2016, p. 1). The same AMA report also states there are decreased sightings of drones despite the large number of purchases by consumers. In general, the AMA calls for a more comprehensive analysis and less “inflammatory terminology” (p. 11) when characterizing the reported sightings of UAS. The AMA report based these conclusions on the AMA’s analysis of the FAA’s UAS sightings report (FAA, 2017b) covering the period August 2015 to January 2016.

Conversely, while the sUAS sighting reports issued by the FAA contain preliminary information, and a number of those reports may be found irrelevant upon further investigation, there are still hundreds of sUASs reported to be operating improperly in controlled airspace or in the vicinity of manned aircraft – even if no imminent collision hazard was perceived (FAA, 2017b). Between the period of November 2014 and September 2016, the FAA received 2,617 reports of UAS sightings,

and the agency reported on February 23, 2017, they were receiving over 100 additional reports of sightings each month (FAA, 2017b).

There are well over one million consumer-owned sUAS aircraft capable of operating in the nation's airspace with no automated means of abiding by airspace restrictions or avoiding other aircraft. Since these sUASs do not generally have technology to render their whereabouts on existing traffic position awareness systems, such as the Traffic Alert and Collision Avoidance System (TCAS) and the Traffic Information System (TIS), see-and-avoid remains the fundamental means for manned aircraft pilots to avoid collisions with sUASs (Yu & Zhang, 2015). In fact, "the US Code of Federal Regulations (CFR) [requires] that pilots see and avoid other aircraft" (Consiglio, Chamberlain, Muñoz, & Hoffler, 2012, p. 2).

The need for reliable detection, identification, assessment, and avoidance action is widely recognized in the literature. However, nearly all of the research and analysis work to date addresses the sense and avoid capability of the unmanned aircraft and its operator. Very little recent work exists on the challenges of sUAS see and avoid for pilots of manned aircraft. Safe operation of aircraft in the National Airspace System (NAS) is the driving force behind the need for reliable detect / sense and avoid systems in UAS aircraft. Since UAS aircraft do not have an onboard pilot, it can be difficult to impossible for UAS operators to use the see and avoid concept to remain clear of low-flying manned aircraft. This is especially true if the UAS is operating in a field surrounded by trees or buildings that prevent the operator from seeing approaching aircraft behind the tree line or building skyline. The lack of visual capability in the sUAS operating environment

amplifies the need for technology-based sense-and-avoid solutions to prevent collisions (Lai, Mejias, & Ford, 2011; Mcfadyen & Mejias, 2016; Yu & Zhang, 2015).

Potential Technology-based Solutions

The technology to prevent collisions exists; however, the sUAS industry still needs to agree on and produce the standards and products required to address the collision avoidance challenge introduced by sUASs. Yu and Zhang (2015) divided these technologies into cooperative and non-cooperative technologies based on whether aircraft work collaboratively to avoid collisions or independently to generate their own collision avoidance solutions. Table 1 summarizes the set of technologies available to address the collision avoidance problem between manned and unmanned aircraft. Though these technologies exist today, none of them stands as a standard for small UA and none of them are widely deployed as a requirement for small UA.

The following paragraphs provide additional details regarding these technologies, which may resolve concerns about collisions between manned and unmanned aircraft in the future. The implementation of these technologies would eventually eliminate the concerns of this study about a manned aircraft pilot's ability to see and avoid a small UAV in time to prevent a collision. However, since these technologies do not exist across the current fleet of small UA products for sale today, the research questions in this study remain for the near-term. The following literature illustrates the current focus on enabling UA and UA operators to avoid manned aircraft with little to no work focused on enabling manned aircraft pilots to avoid UA – especially small UA.

Table 1

Technologies to Prevent Manned vs. Unmanned Traffic Conflicts

Technology	Type	Function
Traffic Collision Avoidance System (TCAS)	Cooperative	Detection / Alert
Automatic Dependent Surveillance – Broadcast (ADS-B)	Cooperative	Detection / Alert
Network Meshing	Cooperative	Communication Bandwidth Management
LIDAR (Laser Detection and Ranging)	Non-Cooperative	Sense and Avoid
Synthetic Aperture Radar (SAR)	Non-Cooperative	Sense and Avoid
Electro-Optical (EO) systems	Non-Cooperative	Sense and Avoid
Acoustic sensing systems	Non-Cooperative	Sense and Avoid
Ground-based Sense and Avoid (GBSAA)	Non-Cooperative	Sense and Avoid
Geo-fencing	Non-Cooperative	Airspace restriction
Counter-UAS Technologies	Non-Cooperative	Defensive

Note. Material obtained from Campbell (2012, October); Doll, McWhorter, Wasilewski, and Schmieder (1998); Frew and Brown (2008); Gettinger and Michel (2015); Lai, Mejias, and Ford (2011); Mcfadyen and Mejias (2015); and Yu and Zhang (2015).

The cooperative systems identified by Yu and Zhang (2015) include TCAS and Automatic Dependent Surveillance – Broadcast (ADS-B). These systems engage other aircraft with an information exchange process that enables the participating aircraft to work out a well-defined collision avoidance solution. These systems may also inform ground-based surveillance systems about their location, altitude, and track so ground-based processors can calculate potential traffic conflicts and relay alerts and warnings to aircraft in the sky. However, ground-based sense and avoid systems require the UA to be equipped with ADS-B or radar transponder equipment to provide a signal for the ground systems to detect (Campbell, 2012).

Some larger UAS vehicles have TCAS and / or ADS-B capabilities; however, these technologies are limited in terms of their capacity to operate in environments with

high numbers of targets. TCAS and ADS-B technology may also exceed the payload capacities of small UAS (Yu & Zhang, 2015). Though the UAS industry is addressing the weight and size issues, the limited radio bandwidth to accommodate TCAS and ADS-B technologies remains problematic when many hundreds of vehicles operate within a small geographic area.

Yu and Zhang do not discuss the radio bandwidth requirements for these technologies when many hundreds or thousands of aircraft are within communications range of each other. However, Frew and Brown (2008) described the bandwidth limitation issues for sUAS operations a number of years ago, long before the rapid growth in the number of sUAS that exists today. In their research, Frew and Brown examined direct link, satellite-based, and cellular strategies for control and aircraft-to-aircraft communications with UA. They concluded the use of meshed, ad-hoc communications was the only viable bandwidth solution for sUAS communication requirements in the future. Network meshing means the participants and nodes in the communication network have the ability to forward and route data between themselves, from aircraft to aircraft, aircraft to satellite, or from aircraft to ground network nodes, in an ad hoc fashion. Such a network could dynamically accommodate high-density communications traffic over long distances; however, current cooperative air traffic control and collision avoidance systems do not use meshed networking architectures.

The wide variety of laser, electro-optical, acoustic, and infrared sensor-based non-cooperative systems described by Yu and Zhang (2015) all have potential benefits that circumvent the radio bandwidth limitations and the requirement for all aircraft to be properly equipped for cooperative collision avoidance. Non-cooperative systems do not

communicate and negotiate with each other. Rather, they independently sense and assess the operating situation and make their own decisions regarding their collision avoidance actions. These non-cooperative technologies do not generally exist in sUAS aircraft and do little to help the pilots of manned aircraft detect and avoid sUASs operating outside of their authorized airspace.

The majority of the other traffic detection and conflict avoidance strategies found in the literature describe advanced technology sensor systems and strategies for autonomous sense and avoid capabilities for the unmanned aircraft. The sensor technology for these systems include Laser Detection and Ranging (LIDAR), Synthetic Aperture Radar (SAR), Electro-Optical (EO) systems, acoustic sensing systems, and Infrared (IR) sensors designed to create an image or model of the physical world from the UA's perspective (Yu & Zhang, 2015). LIDAR scanning and SAR use active light or radio energy emissions to scan the environment for objects that reflect the emitted energy back to sensors for interpretation. These systems analyze the reflected energy to determine the distance, relative direction, and ultimately the size and shape of the objects scanned by the system. However, LIDAR sensors have a limited field of view, and SAR sensors lack the resolution and accuracy needed to create the same quality imagery as an EO system. EO systems are essentially sophisticated camera systems designed to capture optical images of the environment and its content. Acoustic sensors detect engine sounds and sounds related to propulsion devices such as rotors and propellers. Acoustic sensing, using an array of sensitive microphones, can provide location and tracking information on airborne targets; however, acoustic systems lack target range determination capability and are susceptible to adverse weather, winds, and temperatures (Yu & Zhang, 2015).

Passive IR sensing systems provide better image quality than acoustic or radar systems, a wider field of view than LIDAR, and improved performance over other optical systems at night. However, IR systems do not provide range-to-target information. While EO systems use optical image sensors such as visible-light camera systems to create detailed visual representations of the environment, such systems generally lack range calculation capability (Yu & Zhang, 2015). Though the captured image can be very detailed, researchers and engineers must implement sophisticated methods and algorithms to identify targets of interest and to determine if those targets present a potential collision hazard. Though a great deal of research has been invested into the development of such artificial vision concepts, replicating the multitude of input channels such as color, movement, temporal location, conceptual shape, context, orientation, etc. is a complex, systems-oriented task (Doll, McWhorter, Wasilewski, & Schmieder, 1998).

Doll et al. produced their work on artificial vision nearly two decades before the current surge in sUAS sales. Lai, Mejias, and Ford (2011) describe recent applications of machine vision systems to the task of airborne target collision detection as being attractive due to their “relatively low cost, size, weight, and power requirements” (p. 137). Lai et al. point out the numerous advances made over the past decades regarding multi-stage processing of image data, advances in noise filtering, advances in image stabilization, and the treatment of background clutter. During in-flight testing, their machine vision-based detection algorithms found targets “at distances ranging from 400 to around 900 m (depending on the collision geometry)” (Lai et al., 2011, p. 155), providing between eight to ten seconds of warning prior to a collision.

Mcfadyen and Mejias (2015) recently confirmed assertions by Yu and Zhang and Lai et al. regarding the merits of vision-based sense and avoid technology – especially for sUAS applications. Mcfadyen and Mejias described active radar-based technology as being functionally “attractive” (p. 3) though “typically either too heavy or too expensive for many small unmanned aircraft operations” (p. 3). Instead, Mcfadyen and Mejias suggest electro-optical system strategies are a more realistic approach for sense and avoid capability on sUAS aircraft. Furthermore, they suggest the same type of sense and avoid system could be installed on manned aircraft to help pilots detect, see, and avoid small UA more readily.

The current literature documents the many artificial vision and target sensing research efforts from the past two decades; however, the sUAS industry has yet to select specific standards for sense and avoid operations. Yu and Zhang (2015) also provide a comprehensive description of many of the published approaches and methods for using the data from the sensor options available today. In the end, they conclude none of the available sensor technologies nor the methods for using them in sense and avoid applications are available as certified products yet. While there are numerous publications on studies of how to implement reliable sense and avoid systems in the future, there is comparatively little literature on the challenge of detecting UAs, especially small UAs, from the manned aircraft cockpit. There is also very little literature on the realistic limits and likelihood of visual detection of sUAS aircraft by pilots of manned aircraft.

Another strategy for the application of technology-based solutions to the problem of sUAS and manned aircraft collision avoidance uses technology to prevent sUAS from

operating in areas off limits to sUAS. These strategies include geo-fencing software designed to disable or redirect the sUAS when they reside in or approach inappropriate airspace. People have mixed opinions on the concept of geo-fencing across the industry. While some believe it will provide important protection against dangerous or careless operations, others believe it will only keep inept but well-meaning operators out of trouble because those who do not wish to comply with regulations can easily defeat the feature. At present, a few manufacturers offer geo-fencing as a feature on their sUAS products (Gettinger & Michel, 2015).

Other technology-based solutions to keep sUAS out of restricted airspace or to remove them from the air when they appear will likely emerge in the future. In 2016, the U.S. Senate passed a transportation bill to fund research on counter UAS technologies (Senate passes transportation, 2016). Counter UAS technologies are envisioned to “detect, locate, and track both UAS and their operators and mitigate unauthorized operations” (Warwick, 2016, para. 9). Since these new defensive technologies are not yet available for deployment, pilots of manned aircraft cannot benefit from them at present.

Existing Studies in Human Observer Capabilities

Given the current lack of technology-based collision avoidance options for sUAS aircraft already sold to consumers, and given the ongoing stream of reports filed with the FAA regarding sUAS sightings (FAA, 2016a), visual detection and identification of airborne traffic conflicts remains an important task for present-day pilots of both manned and unmanned aircraft (FAA, 2016c). However, the see and avoid concept is far from perfect. The Australian Transport Safety Board (ATSB) describes a variety of limitations constraining a pilot’s ability to successfully see and avoid collision hazards. These

include workload and other distractions from the visual search task, obstructed views from the cockpit, glare, the retinal blind spot, accommodation or focus delays, complex or cluttered backgrounds, atmospheric visibility, the contrast between the target and the background, the size of the target when it is safely distant, and a variety of other detractors (ATSB, 1991).

Since see-and-avoid is the only current, consistent tactic manned aircraft pilots have to prevent collisions with airborne sUAS, it is important to understand the limitations associated with the tactic; therefore, this dissertation examines a number of models designed to predict the detection and recognition of airborne objects viewed from a distance. The distance must be large enough to afford the pilot time to recognize the object as a potential collision hazard and to take appropriate evasive action. Conversely, the further away the manned aircraft pilot is from the small UA, the smaller the UA will appear to be.

Visual acuity. Before examining other extraneous factors affecting the human ability to detect and recognize a small distant object, it will be helpful to understand how small an object can appear within the human field of vision before it is no longer reliably recognizable. Howett (1983) states humans with a Snellen visual acuity of 20/20 vision can generally see and resolve image details as fine as one minute of arc within their field of vision. Though many humans can resolve detail smaller than one minute of visual arc, the National Bureau of Standards has used this standard as a conservative limit for detail resolution when it comes to defining guidelines for the development of readable signage. Gibb, Gray, and Scharff (2010) describe collision avoidance with full-sized, manned aircraft as challenging because of the small angular size of the target when viewed from

an adequate distance to make proper evasive actions. Gibb et al. suggest the minimum visual angle for target detection in the aircraft collision-avoidance scenario is 0.2 degrees or 12 arc minutes based on information from National Transportation Safety Board investigations. Their assertion is different from the one arc minute threshold described by other researchers, though Gibb et al. focus on recognizing the overall target instead of recognizing the detailed features of the target. Howett's one arc minute minimum refers to recognizing the strokes that form a letter so the observer has enough detail to identify what the letter is (Howett, 1983). In either case, all of the researchers agree that aircraft collision avoidance requires pilots to detect and comprehend the location and trajectory of potential collision targets while they appear as small, distant objects.

Objects tend to appear larger when they are close to the observer because they occupy more of the observer's field of vision. Conversely, when the object is distant, it appears to be smaller. The difference in size is a mathematical result of trigonometry, as shown in Figure 1. Given an object AB of size w , and a viewing distance of d between the object and the observer O, it is possible to determine the visual angle θ subtended on the eye's retina in terms of minutes of arc. Since there are 60 minutes of arc in a degree, and there are 2π radians in a circle, the following logic defines a constant to convert radians to minutes of arc. Given 2π radians = 360 degrees, the following transforms can be made: 1 radian = $360 / 2\pi$ degrees which equals $(360 / 2\pi) \times 60$ minutes. This yields a conversion constant of 1 radian = 3437.75 minutes of arc (Howett, 1983). By dividing the object height AB in half, as shown in Figure 1, the size of the visual arc subtended is the sum of two lines of a right triangle - AC and BC. Using trigonometry, one half of the subtended visual arc for triangle ACO is: $\tan^{-1}(w/2) \times 3437.75$, which converts the arc

size from radians to minutes of visual angle. Finally, since the visual angles are so small in this study of sUAS visibility, $(w/2)/d$ nearly equals $\tan^{-1}((w/2)/d)$, so it makes sense to simplify $\tan^{-1}((w/2)/d)$ to $(w/2)/d$ (Howett, 1983). The two values are within $1.0 \text{ E-}07$ of each other for the values encountered when the sUAS is less than 50 feet in size at a distance of 2400 feet.

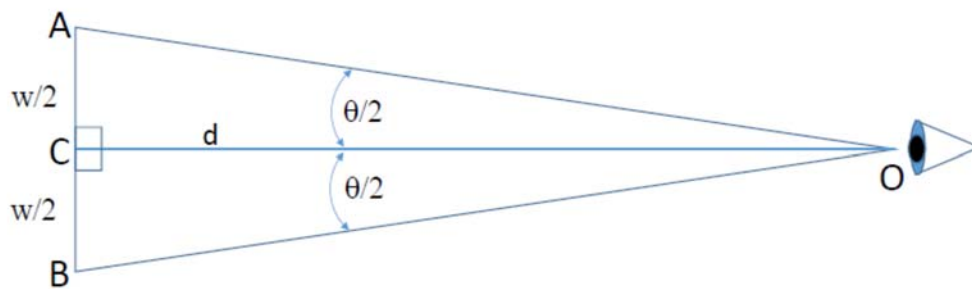


Figure 1. Determination of visual angle. The visual angle θ (in minutes) of an object having width w (extending from A to B) can be calculated using the formula $2 \times 3438 \times \tan^{-1}((w/2)/d)$, where d is the distance between the observer (O) and the object AB (Howett, 1983, p.7).

To get the complete visual angle subtended by the distant sUAS on the retina in terms of visual arc, Howett (1983) combined the two half-arcs resulting in the simplified equation $2 \times 3438 (w/2)/d$ which was simplified further, as shown in Equation 1.

Note, the derived constant 3437.75 was rounded up to 3438 in these simplified equations.

$$\text{Visual Angle in minutes of arc} = 3438 \times (w/d) \quad (1)$$

where:

w = size of the target sUAS

d = distance between the target sUAS and the observer O.

The important consideration when making these calculations is repeated studies of human visual target recognition capabilities suggest that most humans with normal vision can recognize fine detail in an image down to about one arc minute in size. This limit assumes normal visual acuity, high contrast lines against a plain background, and moderate illumination (Howett, 1983). Howett suggests other studies have shown that many humans can identify even finer details, with visual arcs less than one minute, under ideal conditions; however, the National Bureau of Standards uses the one arc minute limit as a common minimum standard.

Howett (1983) provides data indicating that a person with a visual acuity of 20/10 on the Snellen scale can identify image components down to a critical visual angle of 0.5 arc minutes under the same conditions that a person with 20/20 vision can identify image components down to a critical visual angle of one arc minute. It is important to note that while there are many people with visual acuity better than the norm of 20/20 for the general population, they represent only a small portion of the population.

Table 2 shows the Snellen visual acuity relationships to the detail or stroke width of letters on a standard eye test chart. It also shows the percentage of the population with visual acuity at each level. Visual acuity worse than 20/40 is not depicted because such individuals would not pass the required FAA medical exam to fly an airplane.

Table 2 also shows that a portion of the population may be able to see fine detail down to 0.75 arc minutes of subtended image on the foveal center of the retina; however, very few people have the 20/10 vision required to see 0.50 arc minutes of detail.

Table 2

Snellen Notation Relationship to Visual Arc Size in Minutes

Snellen Notation	Critical Visual Angle (minutes)	Cumulative % of population un-corrected	Cumulative % of population corrected
20/10	0.5	1.1	1.5
20/15	0.75	30.3	40.0
20/20	1.0	53.9	72.9
20/30	1.5	69.3	90.6
20/40	2.0	75.8	95.1

Note. Depiction of the relationship between visual acuity in Snellen notation, the critical visual angle or minimum number of arc minutes that can be seen with each Snellen rating, and the percentage of the population who have such visual acuity (or better) – both un-corrected and corrected with glasses, contact lenses, or now eye surgery. Adapted from “Size of letters required for visibility as a function of viewing distance and observer visual acuity.” by G. L. Howett, 1983. Copyright 1983 by U.S. Government Printing Office.

Howett’s (1983) research and studies relate to the minimum size of detail for human recognition of letters in signage (e.g. Exit signs and other signage for public safety applications). The critical visual angle refers to the minimum size of the letters’ stroke width or ink width. The typical full letter is generally five times larger than the stroke width, in terms of letter height. Howett describes the stroke width as being the critical level of detail for letter recognition, however. Howett’s use of the one arc minute minimum for human visual acuity aligns well with research done by Hirsch and Curcio (1989) on the ability of the human retina to resolve fine details. Hirsch and Curcio compared the foveal section of human retinas to gather data on the density or spacing of cone cells, which the eye uses to detect detail and color. Based on their findings regarding the spacing of cone cells in the foveal area of the retina where the cones are the most densely populated, Hirsch and Curcio predicted the best case acuity for the human eye. They compared their predictions with a variety of visual acuity test measures

performed on living human subjects. Their findings suggested the best-case visual acuity, based on analysis of the retina's cone cells in the dense foveal section of the retina, was about 68 cycles per degree or about 0.88 arc minutes. Actual human subject performance ranged from one to two arc minutes with most of the samples falling in the range of 1.15 to 1.50 arc minutes (Hirsch & Curcio, 1989).

Retinal eccentricity. In addition to the apparent size of the image as measured by visual angle, another key factor in a human's ability to detect distant, airborne objects is the location the image appears on the retina relative to the center of the fovea where the cone cells are the most densely populated. Retinal eccentricity refers to the distance from location of the target image on the retina to the center of the fovea. Vision researchers measure retinal eccentricity in degrees or minutes of visual arc (Hirsch & Curcio, 1989; Westheimer, 2010). Other researchers refer to this same offset distance as the angle-off-the-visual-axis (Greening, 1976).

The minimum visual angle of one arc minute, described in the previous section on visual acuity, only applies if the object renders its image in the foveal region of the eye's retina where the cone cells are the most densely packed together. Hirsch and Curcio (1989) found the cone cells less densely spaced as they examined the retina further away from the foveal center. The resulting loss of resolution results in an increased minimum visual angle for fine detail recognition of two or more arc minutes when the image falls just two degrees away from the foveal center. As the image falls further from the center of the foveal region of the retina, human ability to resolve and recognize finely detailed images degrades rapidly.

The peripheral areas of the retina contain the highest concentration of rod cells. Rods are more sensitive to light than cones. Rods are also sensitive to image movement; however, rods do not detect color and are unable to resolve fine detail like cones (Gibb, Gray, & Scharff, 2010). For maximum visual acuity, it is important to use the foveal portion of the field of vision when searching for small, distant objects (Erickson & Burge, 1974; Graham, 1989). Using the center of the field of vision allows the fine detail of an image to appear on the foveal section of the retina where the color and detail-oriented sensory cells, or cones, are closely spaced with around 150,000 cones per square millimeter (Frisby & Stone, 2010).

Retinal eccentricity is important when searching for distant objects because distant objects appear to be small, and the ability to discern fine detail is therefore essential. Figure 2 provides a graphical depiction of the loss of visual acuity as images render on the retina further away from the foveal center. The graph depicts research findings based on peripheral vision work originally conducted by Theodor Wertheim in the late 1890s (Wulfeck, Weisz, & Raben, 1958). As the target image moves further from the one degree-wide foveal center in the field of vision, the density of cone cells decreases rapidly. From the four-degree eccentricity point out to the peripheral edge of the vision field, the number of cone cells remains somewhat constant. Rod cells predominate the retina at about 4 degrees of eccentricity going out to the edge of the field of vision, and are more sensitive to motion and to light in the upper end of the visible spectrum. Since this region of the retina, populated predominantly by rod cells, cannot resolve details as fine as the foveal region of the retina can, the smallest visual angle the

eye can see at 30 degrees of eccentricity is approximately 30 minutes of arc size (Wulfeck, et al., 1958).

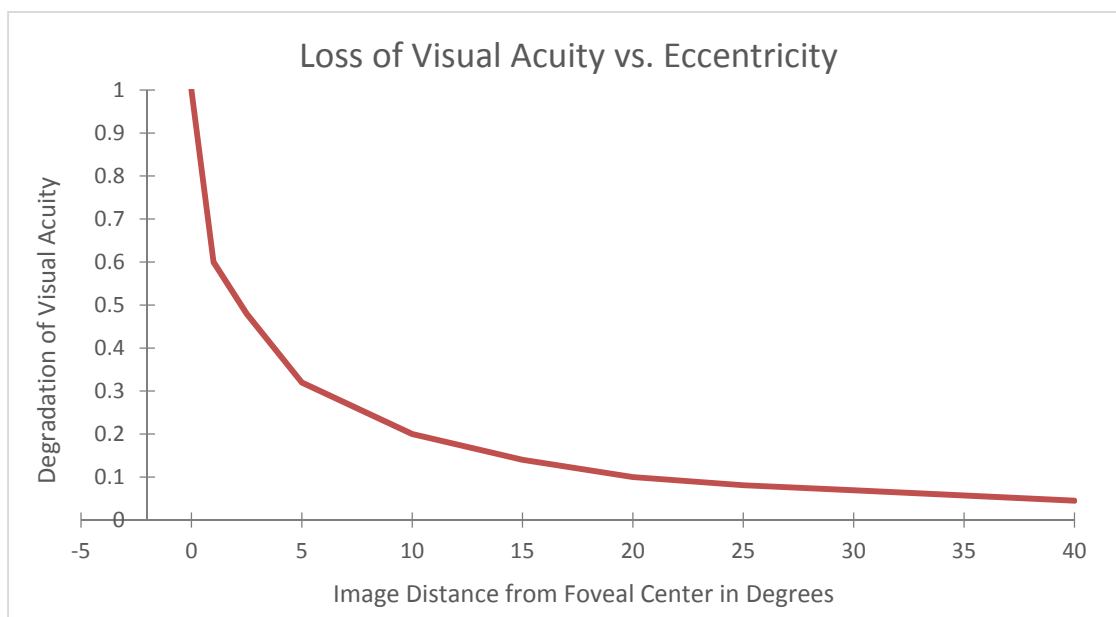


Figure 2. Visual acuity related to retinal eccentricity. Adapted from “Vision in military aviation,” by Wulfeck et al., 1958, p. 130. Copyright 1958 by Armed Services Technical Information Agency, Graph shows the decrease in visual acuity as eccentricity increases. Eccentricity is the angular offset from the center of the foveal region of the retina. As images appear to the left or right of the foveal center, the retina’s ability to resolve fine detail diminishes.

Wulfeck, Weisz, and Raben (1958) also map the eye’s blind spot, where the optic nerve connects to the retina, between approximately 11 degrees to 17 degrees of eccentricity on the nasal side of the retina. As a result, the missing image data will occur 11 to 17 degrees on the temporal side or outer axes of the visual scene, in any given eye. Since the two eyes have blind spots in different locations, and since the brain cognitively merges image data from the two eyes, the blind spot is not generally an issue for normal

vision. This is true unless the second eye also has no view of the target due to some object blocking only its view (ATSB, 1991).

Contrast threshold. Another key attribute used in human visual search models is contrast between the target and its background (Greening, 1976). Researchers have a variety of methods to choose from for determining contrast. The best choice depends on the circumstances of the search operation, the characteristics of the target, and the environmental conditions in which the target is operating.

For this study, the target object was a small UA operating in daylight conditions between the ground and a few thousand feet. Small UAs are limited to operation no higher than 400 feet above the ground unless special permission has been obtained from the FAA (Operation and Certification of Small Unmanned Aircraft, 2016); however, a number of unauthorized small UA have been reported at altitudes above 400 feet, as high as several thousand feet (FAA, 2017b). This means likely backgrounds for the UA target detection task will include both light, medium, and dark luminosity levels. Based on a convenience sample of information gathered from popular sUAS websites, small UAV devices come in a variety of shapes and colors, though the most common UAV colors are black, white, and gray. The details of how this information was gathered are in Chapter 3.

In general, most studies calculate contrast using a formula similar to the one shown in Equation 2 (Akerman & Kinzley, 1979; Chisum, 1977; Poe, 1974). To calculate contrast, divide the difference between the luminance of the target and the luminance of the background by the luminance of the background resulting in contrast in terms of a ratio. Not all models use the absolute value of the difference. Some models

have a positive or negative contrast to show whether the target or the background is lighter.

$$C = |L_T - L_B| / L_B \quad (2)$$

where:

C = contrast

L_T = luminance of the target UA

L_B = luminance of the background

The confusing issue in the literature regarding contrast is that some researchers use the opposite order of terms in the numerator to calculate contrast. Howett (1983) and Erickson and Burge (1974) calculate contrast using $(L_B - L_T) / L_B$ which yields negative contrast values when the target is lighter than the background. Howett reverses the terms so that the formula yields positive values for black letters on white backgrounds to represent the more common scenario for letters on signs. The study will need to use a variety of contrast values to model the luminance and background contrasts that could potentially exist in a given sUAS scenario. Poe (1974) acknowledges, in general, “substantial variations in contrast over a flight path lasting 20 sec (sic) are common. Common levels of aircraft intrinsic contrasts are between 0.05 and 0.75” (p.11).

Previous researchers model the effect of contrast using different strategies. Poe (1974) used data from Blackwell and McCready (1958), Blackwell and Moldauer (1958), Sloan (1961), and Taylor (1963) to create his own model to determine contrast thresholds at which the probability of sighting an object drops below 50%. Poe spent months

crosschecking his model against multiple databases. The resulting formulas in Poe's model are somewhat similar to those used by Howett (1984) and Andrews (1991a); however, the integration of the multiple datasets creates a cumbersome set of formulas which Ackerman and Kinzly (1979) found mismatched actual experimental data. Ackerman and Kinzly recommended further recalibration of Poe's contrast thresholds. Andrews (1991a), unlike Poe's work, calibrated and tested his model using actual experimentation.

Andrews (1984) cites studies relating small target detectability to the product of target area and contrast. Andrews defines small targets as those subtending an arc size of one to ten minutes to the human observer. Since detectability is a function of the target area multiplied by the target's contrast, if the contrast decreases by one-half, then the target size must double to produce the same level of detectability. Andrews (1984) provides Equation 3 to illustrate this relationship. Note the expression $\exp (2.996 r / R)$ represents the contrast reduction element of this equation, based on Koschmieder's Law.

$$\lambda = \frac{\beta A}{r^2} \exp \left[\frac{-2.996 r}{R} \right] \quad (3)$$

where:

λ = target acquisition rate

β = experimentally derived constant (17,000 for single pilot operations)

A = area of the target

r = range or distance between the target and the observer

R = meteorological range (atmospheric visibility)

Koschmieder's Law describes an equation accounting for the loss of visibility resulting from the scattering and absorption of light energy as it travels through the atmosphere. When light, reflected off an object the eye is watching, travels through hazy or misty air, some of its energy is scattered and some is absorbed, resulting in a reduced amount of the reflected light from the object reaching the eye's retina. The resulting reduced amount of light from the target makes it more difficult to see (Lee and Shang, 2016). Andrews (1984) accounts for Koschmieder's Law in Equation 3. Andrews also states if the visibility through the atmosphere is two or three times the distance to the object under observation, then the effect of atmospheric scattering is minimal. Therefore, the Koschmieder term in the equation is unnecessary when clear atmospheric conditions prevail (Andrews, 1991b).

Target discrimination against background clutter. Depending on the altitude and operating phase of the manned aircraft (takeoff, departure climb, cruise, descent, approach, or landing), given the variety of improper places that small UA have been spotted near airports and aircraft, the likely background for the target UA will vary widely. Possible backgrounds could include a bright homogeneous sky; a complex, textured cloudy sky; a homogeneous, monochromatic landscape; or a complex metropolitan skyline. Many other background scenes are possible too, including suburban neighborhoods, lakes, forests, hills, and ocean settings.

In order to capture the effect of background clutter in the Monte Carlo simulation for this dissertation, the literature research examined a variety of background clutter modeling and analysis strategies. Chang and Zhang (2006) developed the Target Structure Similarity (TSSIM) metric for characterizing clutter in an image when

searching for a target. The concept divides the image into blocks and compares the background area characteristics to those of the target, block-by-block. TSSIM divides the background image into blocks that are twice the size of the apparent target area. Since the apparent target area is tiny for small UA viewed from large distances, the background blocks are also very small.

The analysis examines the structure, luminance, and contrast features in each block and in the target, and analyzes the similarities statistically. Higher levels of similarity will require higher amounts of time for the observer to search through the background scene. In the case of small UA images, the target and the tiny background blocks are generally featureless blocks of homogeneous grayscale level. If the background image contains many areas of similar grayscale to the UA grayscale, the similarity score will be high, and longer search times will be required to find the UA.

When Chang and Zhang compared their model results with the results obtained from 62 test observers searching for targets in 44 different high-resolution color images of natural complex scenes, their model produced outputs with Pearson correlation coefficients ranging from 0.75 to 0.87 when related to the results of the human observer tests. Subsequent testing showed the TSSIM structural similarity metric “correlates significantly with human visual search performance, and outperforms other clutter metrics” (Toet, 2010, p. 467). Toet’s (2010) conclusion was when the TSSIM metrics identified increased levels of similarity between search target features and features of the natural scenic backgrounds, visual search time increased, and the correlation between actual human search time and TSSIM predictions of search time per the clutter metric was very strong.

Additional research by Itti and Koch (2000) examines search methods and search times in the presence of background clutter using a multi-layered processing approach in which color, contrast intensity, and visual feature orientation are inputs to the creation of feature and conspicuity maps. These maps provide the information needed to produce a saliency map that predicts the human search focus within the search area. While Itti and Koch used a very different search technique for their model, their model produced similar results to the TSSIM outcomes in terms of added search time requirements for scenes with a higher volume of background features similar to the visual features of the target. Both research teams found a minimum increase of 2 seconds for non-homogeneous search area backgrounds in which the target is somewhat conspicuous, and up to 15 seconds or more for the backgrounds with features in which the target is less conspicuous (Itti and Koch, 2000; Toet, 2010). Though experimental testing is required to determine the precise amount of increased search time needed because of background clutter or feature similarity, the increased time requirement is clear.

Other factors affecting visual target detection. “Many other target attributes are known to influence detectability including shape, motion, and color” (Akerman & Kinzley, 1979, p. 278). Graham lists “variability of pilot visual acuity and of air-to-air visibility, target size and aspect, target contrast, background complexity, crew workload and search patterns, and sun position” (Graham, 1989, p. 6) as additional factors affecting successful see and avoid operations. For the purposes of the Akerman and Kinsley study, some of these additional target attributes were secondary or irrelevant to their study because of the scope and focus of their research questions. The scope and purpose of this study also makes many of the additional target attributes not addressed by this study less

important or irrelevant. Small UA operate in daylight, fair weather conditions since the operator is required to have visual line of sight to their aircraft and to the obstacles in the environment in which the UA is operating (Operation and Certification of Small Unmanned Aircraft, 2016). Additionally, small UA viewed from distances of hundreds or thousands of feet appear as very small angular sizes. They occupy or subtend only a few minutes of visual arc on the retina. When targets subtend less than 0.5 degrees or 30 arc minutes of angular size, “the contribution of any chromatic difference to the overall perceived difference [in contrast with the background] drops off more rapidly than the contribution of the lightness difference (Howett, 1983, p. 27). Graham (1989) also cites multiple field studies in which the use of color, even fluorescent color, has no significant effect on visual detection of aircraft.

Graham (1989) also concludes the use of aircraft lighting and anti-collision strobe lights do not improve the visibility of an aircraft during daylight hours. The Australian Bureau of Air Safety Investigation (BASI) agrees with Graham’s findings, claiming that an anti-collision strobe light on an aircraft would have to output more than 100,000 candelas to be effective in full daylight. On a dark, cloudy day, the strobe would have to emit around 5,000 candelas to stand out. In practice, BASI claims most aircraft strobe lights emit between 100 to 400 candelas—far short of the required light output to be effective (ATSB, 1991). Therefore, adding lights to small UA will not likely make the UA more visible to manned aircraft pilots.

One other consideration that could improve target detection in search scenarios is the perception of relative motion. When an object moves within the field of vision, it captures the attention of the brain more readily than a stationary object (ATSB, 1991;

Regan, 2000). However, “an aircraft on a collision course will usually appear to be a stationary object in the pilot’s visual field” (ATSB, 1991, p. 13). The perception of relative motion is also minimal due to the small level of angular velocity a slow moving UA creates when observed from several thousand feet away. The tiny visual angle subtended on the retina for a small UAV at distances of several thousand feet may also be a factor (Wulfeck, Weisz, and Raben, 1958). Though the peripheral field of vision sensed by the rods in the human eye is very sensitive to image movement, rods cannot discriminate image features smaller than 30 minutes of arc. The image sizes of small UA, at the distances relevant to this model, tend to be in the range of one to six minutes of arc—too small for low velocity motion detection by the motion-sensitive rods (McKee and Nakayama, 1984; Wulfeck, Weisz, and Raben, 1958). Therefore, the relative motion concept is not a key factor for the visual detection of distant, small UA rendering very low velocity motion across the field of vision.

The effects of relative motion in the context of small UA target detection as described above may account for the “unexpected finding” (p. 12) in the Loffi et al. (2016) study where test subjects (flying manned aircraft) did not detect small UAS targets until the UA was in close proximity to the manned aircraft. Loffi et al. expected the motion of the UA in the pilots’ peripheral vision to have captured their attention. Instead, the pilots generally detected the motionless UA more reliably.

One more visual detection factor not modeled by this study is empty field myopia. Empty field myopia is a phenomenon in which the eye relaxes into a state where it focuses to a distance of around 56 cm in a plain daylight sky with no particular object for it to target on. In this state, distant small objects will be out of focus and will not be

visible. Since aircraft collision avoidance requires pilots to consciously focus their eyes on distant objects to avoid the hazards of empty field myopia, and since it is not possible to characterize when a pilot may let down their guard and enter the empty field myopic state, the condition is not part of this study.

Useful Models for Visual Recognition of Airborne Objects

The literature contains numerous studies and models to describe the human capacity to detect, identify, and comprehend the status and movement of objects within one's field of vision. These models use a variety of input variables to determine the detection outcomes. Since this study involves the detection, identification, and comprehension of sUAS aircraft in time for the pilot to avoid any collision hazard, the relative size of the target aircraft is likely to be very small within the observer's field of vision (ATSB, 1991). This is especially true since sUASs tend to present a small visual cross section compared to the full-sized passenger-carrying aircraft the ATSB referred to in its report on the see and avoid concept. The size of the target object for most of the scenarios of this study occupies only a few arc-minutes (fractions of a degree) of one's field of view, even when the target is within a few hundred feet of the observer. Many of the models in previous studies of visual aircraft detection assume target sizes much larger than the small UAVs in this study, thereby allowing other constraints to be limiting factors. Given the tiny size small UAVs appear to be from a distance, they may not be visible at the ranges used for previous studies and model testing (Stephenson, O'Young, & Rolland, 2015; Loffi, Wallace, Jacob, & Dunlap, 2016).

Chisum (1977) used a comparatively large AQM-37B target drone as one of the targets for a study on the predictability of airborne target detection. The AQM-37B is

only 13 inches in diameter, though it is 200 inches long and has a 40-inch wide tail section (Chisum, 1977). This target looks like a missile. Chisum's model uses a graphical chart to determine a target's detection range based on the visible area of the target's cross section, the ambient light level, the meteorological range, and the inherent contrast of the object against its background. Chisum's model predicts the target, when viewed from the side, should be detectable at an 8,000 yard range when the meteorological range or visibility is 20,000 yards.

Greening (1976) summarized and compared six different models designed to predict the probability of visual detection for airborne targets. These models include:

- Multiple Airborne Reconnaissance Sensor Assessment Model developed for the U.S. Air Force by Honeywell, Inc.;
- General Research Corporation, Model A;
- Combined Reconnaissance, Surveillance, and SIGINT developed for the U.S. Army by Stanford Research Institute;
- Visual Target Reconnaissance and Acquisition developed by Sandia Corporation;
- DETECT II and III – visual models developed by the U.S. Air Force Studies and Analysis Group with the Air Force Armament Laboratory; and
- AUTONETICS – a visual model supplied to the U.S. Naval Air Development Center by Rockwell International.

These models, as described by Greening (1976), vary in complexity and take into account numerous input variables beyond those in the Chisum model or the Howett (1983) letter recognition model. The extra input variables include concepts such as:

- Probability of the existence of a line of sight to the target;
- Probability of fixating and dwelling on a target element;
- Probability of confusion;
- Angular rate;
- Time and glimpse allocations;
- Object density or the number of similar-featured objects in the search area;
and
- Crew size.

While these models are more comprehensive and complex than needed for the purpose of this study, the overall results from these six models are useful. This study focuses on the limitations imposed by human vision since the detection of small UA encroaches on those limits. While each model presented by Greening produced its own unique probability of detection or probability of recognition curve, the summarized results from the various models are:

1. Targets with visual angles less than one arc minute are unlikely to be seen;
2. Targets with visual angles greater than 10 arc minutes are likely to be detected (but not necessarily recognized) (Greening, 1976, p. 139);
3. Targets become recognizable between 30% to 40% of the time when they render a visual angle of 15 arc minutes or more; and
4. In four of the six models, targets become recognizable 50% to 100% of the time when the visual angle exceeds 30 arc minutes (Greening, 1976, p. 140).

The models described by Greening are more complex and require more input data than are required for this study. Since the visual angle size of a small UA viewed from a distance is likely to be a key limitation for target detection and recognition, many of the additional inputs required for the models described by Greening are of secondary importance. Additionally, the Andrews (1991b) model used in this study accounts for most of the input considerations described by Greening through Andrews' experimentally derived B constant. Andrews refers to B as the *pilot search effectiveness* constant. It is also convenient that the Andrews model produces the required output for this study in a direct and usable form—probability of detection. While the Monte Carlo engine in this study will not use any of the models described by Greening because of their excessive complexity, Greening's summarized results will provide implicit validation data for the results of this study.

Howett (1983) offers a more practical model for determining if a human can recognize a shape at a given distance. Howett has a well-defined, validated model to determine the required size of letters in signs, given a specified range of human visual acuity, distance, lighting, and contrast values. Howett combines these input parameters in a manner that produces a required letter size for readability at a given distance. Howett uses contrast and lighting to modulate visual acuity. In order for a person to recognize a letter, the letter must be larger when contrast or lighting levels are lower.

This study assumes small UA operations are taking place during daylight hours, so luminance levels are generally high. Chisum (1977) provides the following table of typical luminance levels for various sky conditions (see Table 3).

Table 3

Sky Luminance

Day Time Sky Condition	Sky Luminance (Foot Lamberts)
Clear Day, Full Daylight	1000
Overcast Day	100
Dark Cloudy Day	10
Twilight	1

Note. This table provides typical luminance values for various sky conditions. Adapted from “Prediction of airborne target detection” by G. T. Chisum. Copyright 1977 by Naval Air Development Center.

Since the luminance levels during daylight hours, even on overcast days, provide ample illumination for object recognition, the key factor for Howett’s equations will be contrast. Poe (1974) offers a contrast formula that adjusts the inherent contrast of the target UAV to an apparent contrast as seen by the eye. The apparent contrast value takes into account the distance to the target and the meteorological visibility. The combination of Howett’s model, Chisum’s data, and Poe’s contrast equation can potentially provide a useful model for determining the visibility of the target object as seen from a distance.

Andrews (1991a) provides a model that builds on concepts used by Howett, Chisum, and Poe to create an output in the form of a probability of visual target acquisition. Testing involved 24 general aviation pilots, ranging in age from 24 to 60, flying a Beechcraft Bonanza airplane. There were 64 total encounters with the target aircraft – a Cessna 421. The test subjects were not aware that a Cessna 421 twin-engine aircraft would be intercepting their route of flight; however, they were aware that other aircraft might be operating in the vicinity (Andrews, 1991b).

Andrews used solid angles, based on two-dimensional measurements, to take into account the fact that objects appear to be different sizes based on the perspective from

which the observer views the object. An aircraft provides a much greater visual target area if viewed from above than it does if viewed from a head on perspective, as shown in Figure 3.

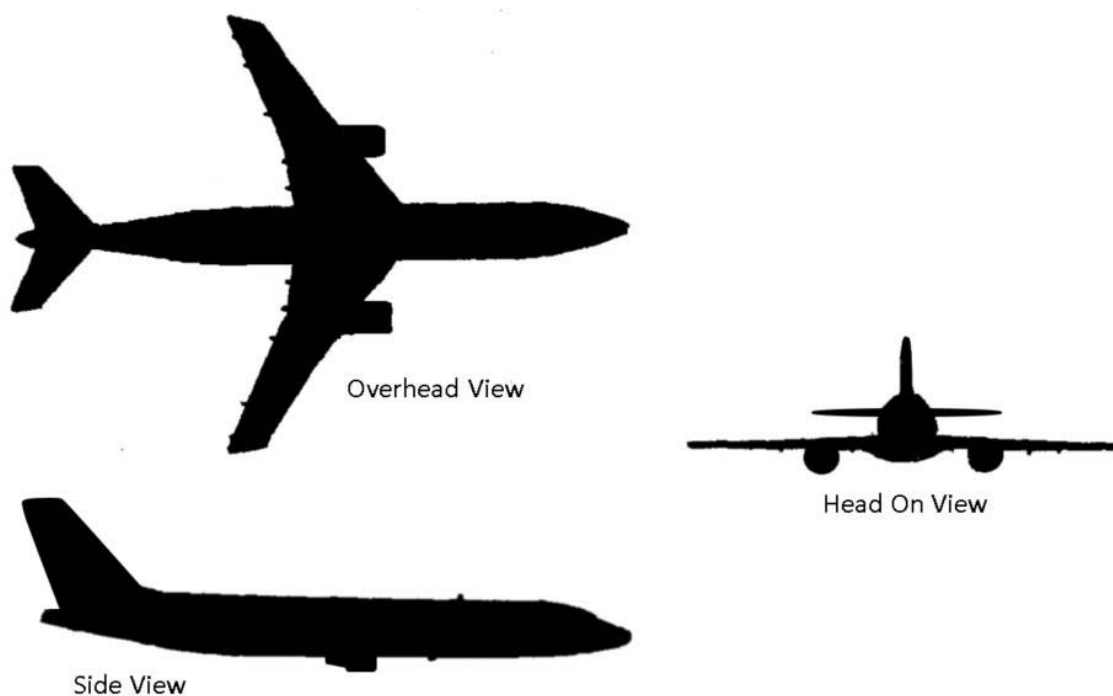


Figure 3. Changing visual target area based on perspective. The size of the visual target area can be very different based on the visual perspective or viewing angle. Adapted from “Air-to-Air Visual Acquisition Handbook” by J. W. Andrews, 1991, p. 19 to illustrate the concept of visual perspective for aircraft. Copyright 1991 by Department of Transportation.

Based on the use of two-dimensional solid angles, Andrews (1991a) extended the Howett model to the use of steradian units instead of the single dimension radian unit. This change better represents the target object when compared to Howett’s model where Howett was interested in the stroke width of a letter as being key to one’s ability to recognize a letter.

In the case of multiple rotor-copter sUAS aircraft, commonly flown by non-professional remote pilots, it is important to note the visual target area presented by the aircraft tends to be more consistent than the aircraft shown in Figure 3 when viewed from different angles. The consistent area, regardless of horizontal viewing angle, is the result of the round shape and consistent vertical profile of multi-rotor, copter-style sUAS aircraft. Even when viewed from a different altitude, the presented area tends to be very consistent because a pilot must view the UA from a long distance in order to have time to maneuver clear of a collision with it, and therefore tends to view the UA primarily from the side.

Additionally, Andrews (1991b) looks at the amount of time the pilot has to find the target aircraft in order to compute the probability of visual acquisition. The search time is bound by the moment the target aircraft becomes large enough to be visible to the human eye (1.0 square arc minute) and the latest possible time at which visual acquisition can occur and still allow the pilot to maneuver clear of the target aircraft. Unlike some other models, Andrews also accounts for the growth in the visual size of the target, as it gets closer to the observer, integrating the instantaneous probability of detection over each instance of time as the target aircraft approaches.

Andrews (1991b) determined that the probability of visual acquisition is a function of the size of the target, the contrast of the target against its background, and the time available to detect the object multiplied by some constant determined through flight test experimentation. Andrews refers to this constant as the *search effectiveness parameter* (B). “ B is the rate of visual acquisition per solid angle of target size per second of search” (Andrews, 1991a, p. 3). Andrews established the B constant in a

manner to create the following relationship: if $\beta = 17,000$ steradian-second units, then a target that subtends a one micro-steradian size at the human eye will generate a 1.7 percent probability of acquisition per second of search time.

β accounts for the human performance component of the search task, and it includes pilot workload, visual acuity, pilot training, effort spent searching, etc. Based on the flight test experimentation referred to above, Andrews (1991a) determined β to be 17,000 per steradian-second for pilots experiencing low workload, normal traffic search effort, and no alert about traffic in the area. This concept takes advantage of former research where the detectability of small targets, between one to ten minutes of arc in size, was determined to be a function of the target area and contrast (Andrews, 1984).

Andrews (1991a) uses Koschmieder's Law to model how the contrast of the target is reduced when the atmosphere is not clear. Per Koschmieder's Law, the atmosphere reduces the apparent contrast of an object according to Equation 4.

$$C(r) = C_0 \exp \frac{-2.996 r}{R} \quad (4)$$

where:

$C(r)$ = apparent contrast of the target observed from range r

C_0 = inherent contrast of the target

r = distance from which the target is observed

R = visibility or meteorological range dependent on clarity of the atmosphere

Furthermore, Equation 5 describes the opportunity for visual acquisition $Q(t)$ given time t , per the Andrews (1991a) model. This relationship is based on studies that

determined the probability of sighting an aircraft is related to the product of the visual angle subtended by the target area and the target's contrast against its background. In this equation, the opportunity for visual acquisition is the sum of the instantaneous opportunities given target area A , visibility R , and an observation range r (Andrews, 1991b).

$$Q(t) = A \left[\int_{-\infty}^t \frac{1}{r^2} \exp \frac{-2.996 r}{R} dt \right] \quad (5)$$

With the appropriate β constant, and when delimited by the appropriate range of times the pilot can theoretically see and still avoid the target aircraft, the probability of visual acquisition becomes P as shown in Equation 6 (Andrews, 1991a).

$$P = 1 - \exp \left[\frac{-\beta A}{rdot} \left(\frac{1}{r_2} - \frac{1}{r_1} \right) \right] \quad (6)$$

where:

$\beta = 17,000$ (per Andrews test flight studies for un-alerted crew, normal search)

A = the area of the target

$rdot$ = closure rate between the observer and the target

r_2 = range when the pilot must initiate a course change to avoid collision

r_1 = range when target becomes large enough in the field of vision to be visible

Equation 6 is relevant when the atmospheric visibility is good so that visual contrast of the target to the background remains relatively constant as the target approaches (Andrews, 1991a). Andrews (1991b) states that when the atmospheric

visibility is more than two or three times the distance between the observer and the target, the atmospheric visibility has little effect. Since even a large sUAS aircraft becomes too small to see when it is just two miles away, as long as the visibility is greater than four miles, Equation 6 will be relevant. This is true because the UA will generally be within observation range when it is only a few thousand feet away; therefore, long atmospheric visibilities are not required for the equation to be relevant. Given this determination, Equation 6 could serve as a means for calculating the probability of visual acquisition of a small UA under conditions where the B constant used in the model matches the mission parameters.

The Relevance of Monte Carlo Simulation

A Monte Carlo simulation will model a range of potential values for input variables where uncertainty exists. A Monte Carlo simulation will analyze a variety of combinations of these inputs by repeatedly executing the model and capturing the outcomes as a set of results. This provides a range of possible outcomes at the output of the model, along with a probability density curve depicting the most frequent outcome along with the possible outcomes.

Papadopoulos and Yeung (2001) list a number of advantages for using a Monte Carlo simulation to address uncertainty. Two of these advantages include the ability of a Monte Carlo simulation to handle “both small and large uncertainties in the input quantities” (p. 293) and the elimination of concerns about covariance and dependency between the input variables.

Veneri et al. (2010) used a Monte Carlo simulation to address uncertainty while building a model of human visual search performance. Veneri et al. needed to address

uncertainty in how the eye might scan different regions of interest within the search area scene. A Monte Carlo simulation was also used to model the absolute threshold of visual detection given low energy or faint image flashes (Cohn, 1981)

Other peer-reviewed research done by Pretegiani, Federighi, Rosini, Federico, and Rufa (2010) used Monte Carlo methods to address uncertainty in variables used in formulas designed to model human performance. The use of multiple simulations using a range of possible input data, weighted in the form of a distribution, enables the use of stochastic processing and the calculation of a range of possible results with uncertainty taken into account. This study will follow the example of previous human visual performance studies and address the challenge of uncertainty in the input variables using Monte Carlo simulation methods.

Other Factors Affecting the Visual Recognition Model

A wide variety of factors not yet discussed exists with the potential to influence the visibility model's output. These include issues such as glare from sunlight, high cockpit workloads and other distractions, pilot age, fatigue, and hypoxia (ATSB, 1991; Morris, 2005). While these considerations all affect a pilot's ability to see a distant, small UA in flight, they all detract from the pilot's ability to see the UA in time to avoid colliding with it. These factors are all outside the scope of the proposed study, though they potentially strengthen the case for the finding that manned aircraft pilots are likely to have difficulty seeing a sUAS aircraft in time for collision avoidance.

There are numerous reasons why pilots may fail to see and avoid other aircraft to prevent collision hazards from developing. Morris (2005) and Graham (1989) present cases describing the difficult nature of seeing smaller-sized aircraft in time to avoid mid-

air collisions in general. Loffi et al. (2016) conducted flight test studies with human pilot test subjects and reported qualitative data on the difficulty of spotting sUASs from Cessna 172 aircraft. Therefore, the literature suggests visual detection, recognition, and avoidance of sUASs by human pilots flying manned aircraft may be difficult. Since this study confirms the findings of Morris, Graham, and Loffi et al., many of the extraneous variables and factors not addressed by this study strengthen the conclusion that sUASs are difficult to see from manned aircraft cockpits because they would make the visual detection task even more difficult.

Conclusions from the Existing Literature

The literature review confirms very little published research exists on the specific topic of the ability of a manned aircraft pilot to see and avoid a collision with a small UA. One recent study done by Loffi et al. (2016) does address the topic with human subjects participating in flight tests; however, the Loffi et al. study does not explore the use of mathematical simulation modeling based on biological information and visual acuity models. The Loffi et al. study focused on visual detection of small UA from small, slower, general aviation aircraft. This concept of modeling the visual detection of small UA is therefore still a new, important research topic. The model also provides insight useful to other types of observation platforms such as airliner and business jet aircraft.

Additionally, the literature provides precedence for the use of Monte Carlo techniques to model uncertainty when simulating human performance in airborne visual search and detection tasks. Since there are a variety of examples of modeling for visual search and recognition tasks, and since there is adequate former research findings on

visual aircraft detection probabilities and limitations, the information and methods needed to create a Monte Carlo simulation model exists.

Finally, the literature suggests small UAV may be difficult to spot from a manned aircraft in time to reliably avoid a collision. This study focused on the physical modeling of whether it should be possible to see small UAV in time to avoid a collision, based on human physiology and physics. In order to avoid skewing the results of the study to match the pessimistic outcome of other studies, this study excluded a number of negative extraneous factors. Since the results of the study revealed that the physics and human physiology constraints, related to visual search and detection of distant objects, make small UAV targets hard to see in time for collision avoidance, the conclusions of Loffi et al., Morris, and Graham concur with and add strength to the study's findings.

CHAPTER III

METHODOLOGY

The research model constructed for this study mathematically simulates the visual limitations for the detection of a small UA by the pilot of a manned aircraft. The detection task is constrained by situational variables such as closure speed between the manned aircraft and the target UA, UA size, and contrast between the target UA and its background. The detection task must also be completed in time to allow the pilot of the manned aircraft to avoid a mid-air collision with the UA. The literature review identified the key variables associated with this task. The review also found existing models used for other vision-related tasks such as object recognition against a cluttered background and airborne target detection for military or other passenger-carrying aircraft (Akerman & Kinzley, 1979; Andrews, 1991a; ATSB, 1991; Chisum, 1977; Greening, 1976; Howett, 1983; Morris, 2005; Poe, 1974; Toet, 2010; Wulfeck et al., 1958).

This study does not involve human subject testing and no data collection or experimentation involving human subjects occurred; therefore, the research for this study did not require Institutional Review Board (IRB) approval. Data from previous studies and existing research reports provided the information on human visual search performance and human physiological constraints needed for this investigation.

Research Approach

The goal of the study was to determine the key physical attributes of small UAS aircraft and aircraft operations that limit the manned aircraft pilot's ability to see a small UA in time to avoid colliding with it and to determine the probability of detecting the small UA in time to avoid a collision with it. These goals were explored using specific

scenarios defined by aircraft speed, UA size, and different contrast values between the UA and its background. The analytical model used in this study produced probability curves depicting the likelihood of UA detection in time to avoid a collision for each of the chosen scenarios.

Figure 4 illustrates the overall approach to this research study. The actual theoretical construct and mathematical model is detailed in the Design and Procedures section later in this chapter. Chapter 1 addressed the first step of the overall approach by defining the problem, the scope, and the research questions for this study at a high level.

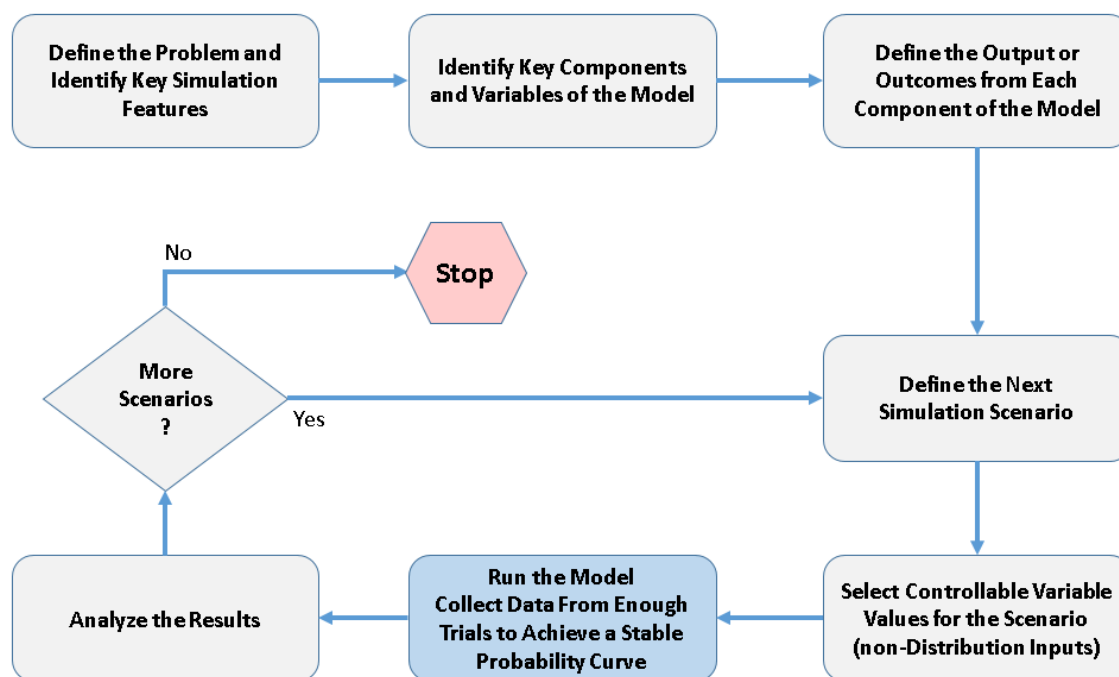


Figure 4. Research approach overview. The overall research approach is summarized in this figure. The blue block step represents the Monte Carlo simulation, and it is diagrammed in greater detail in Figure 5. Adapted from “Stats: data and models,” by R. D. De Veaux, P. F. Velleman, and D. E. Bock, 2012. Copyright 2012 by Pearson Education, Inc.

The mathematical model, referenced in the blue box in Figure 4, uses a Monte Carlo approach to address uncertainty. The details of the theory used to construct the mathematical components of the model are documented in the Design and Procedures section of this chapter. The literature review in Chapter 2 provided several airborne target detection studies conducted over the past few decades as options for modeling small UA detection.

Based on the work of Howett (1983), Andrews (1991a, 1991b), Poe (1974), Chisum (1977), and several others described by Greening (1976), there are multiple existing models capable of determining the ability of an observer to detect an airborne target. This study integrates the limits of human visual performance as described by Howett (1983) with the probabilistic determination target detection algorithm used in the Andrews (1991a) model. The study expands those models with a Monte Carlo simulation and adaptations for very small targets to produce a new model relevant to the detection of small UA. The previous research work, cited above, used several common input variables for their models. The common input variables relevant to this study are listed in Table 4. They are also the variables described by Weaver (1981) as important for the visual target acquisition task. Weaver identified “object density; and scale factor and display size (search area)” (p. 9) as additional influential inputs for one of the models in her paper; however, these inputs are addressed in a different manner by the Monte Carlo simulation model used in this study.

The selection of scenarios for this study focused on departure and arrival operations by various types of manned aircraft. This means the aircraft will be flying at airspeeds consistent with either a departure climb or an approach to an airport. The study

conducted simulation runs with aircraft speeds ranging from 60 knots to 160 knots to provide output data for aircraft ranging from small sport aircraft to large airliners. These operations were chosen because these are the types of lower altitude operations where manned aircraft seem to commonly encounter non-professionally-operated UA, according to the FAA's UAS sightings reports (2017b). The study acknowledges helicopter operations and inspection patrols may occur at low enough altitudes to encounter small UA even though these manned aircraft are not necessarily conducting an arrival or departure operation at the time of encounter.

Table 4

Input and Output Variables for the Model

Variable	Variable Type	Description
Manned Aircraft Speed	Input Controlled	- Airspeed of the manned aircraft in nautical miles / hour (kts)
UA Size	Input Controlled	- Size of the unmanned aircraft in terms of area (ft ²)
UA/Background Contrast	Input Uncontrolled	- Contrast between the Unmanned Aircraft and its background scenery (a normal distribution as described in the text)
UA speed	Input Uncontrolled	- Airspeed of the Unmanned Aircraft (kts) (a Gaussian distribution)
UA relative heading	Input Uncontrolled	- Heading of Unmanned Aircraft relative to the manned aircraft (a uniform distribution from 0 to 350)
Visual Arc Size of UA at the minimum acceptable detection time	Output	- The visual arc size of the UA when it is at the minimum distance from the manned aircraft to allow time for the pilot to maneuver clear of a collision (arc minutes)
Probability of visual detection in time to avoid a collision	Output	- The probability a pilot of a manned aircraft has the ability to visually detect and avoid a collision with a sUAS

Note. These are the variables used by the model for this study. The model also generates a table containing the results for each of the Monte Carlo trials. This output table contains the probability of UA detection given the input parameters to the model. The Design and Procedures section of this chapter contains an in-depth discussion of these variables.

The use of a Monte Carlo simulation is important for this study because of the uncertainty and variability in the following key input variables: UA airspeed, UA direction of movement, and contrast between the UA and its background at any given moment. The UA speed and direction of movement variables affect the closure rate

between the manned and unmanned aircraft and therefore the time available to the pilot to detect the UA. This simulation model is capable of illustrating the effect of uncertainty in the UAV movement by running the calculation many thousands of times to generate a composite representation of the range of detection probability outcomes given the uncertainty of the UAV movement and the contrast between the UA target and its background.

The mathematical algorithms and concepts used for this simulation are well established in studies conducted over the past few decades. The key to applying the simulation to the new application, of determining the probability of visually detecting small UA in time to avoid colliding with them, was selecting appropriate limits for human visual performance and identifying appropriate input variable distributions to represent the uncertainty and variability of the uncontrollable variables. The data and the rationale for these limits and input distributions were derived from the previously accepted studies and industry standards, as described in Chapter 2. The details of the selection rationale for the human performance limits and input distributions are documented in the Design and Procedures section of this chapter.

Analysis of the results, including validation of the model against results of previous studies of human visual detection performance, was done by performing a descriptive statistical analysis of the output table generated by the model for all of the trials for a given scenario. This output table contains the calculated probability of UA detection for each trial of the model. Additionally, data from the various scenarios, defined by different UAV sizes and different manned aircraft approach speeds, were organized to render an easy-to-understand graph depicting the relationship between the

controllable variables and the resulting probability of detection. Sensitivity analysis tested edge cases to determine if reasonable values of controllable variable inputs would produce an outcome where the small UAS target aircraft was likely to be visible greater than 50 percent of the time. Detailed explanations of the findings are discussed in Chapters 4 and 5.

Design and use of the model. The previous pages described the overall design of the research process for this study. This section details the design and use of the mathematical model. Figure 5 illustrates the theoretical structure and components of the model. The model uses Equation 6 to calculate the probability of UA detection for each trial. The model uses the software product Analytica® by Lumina Decision Systems. The Analytica software allows the researcher to define a mathematical model using a flowchart-like graphical representation.

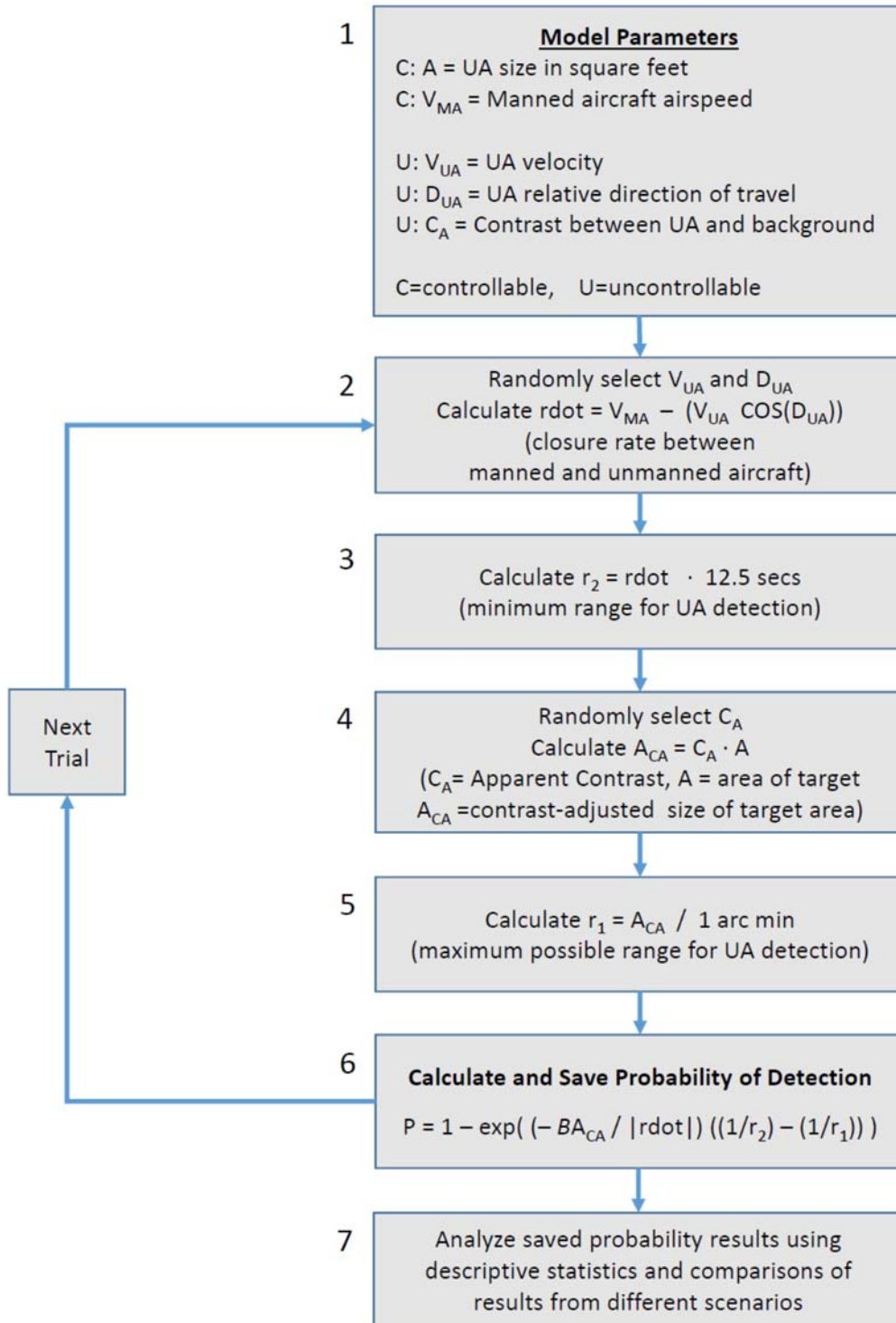


Figure 5. Monte Carlo Simulation Model Flowchart. Note: $\beta = 17,000$, per Andrews (1991a), for the purpose of this study. Adapted from "An introduction to management science: quantitative approaches to decision making," by D. R. Anderson, D. J. Sweeney, T. A. Williams, J. D. Camm, and K. Martin, 2012. Copyright 2012 by South-Western Cengage Learning.

Analytica allows the researcher to define distributions for use as input data, and it provides the processing environment for repeated trials of the model for Monte Carlo simulation analysis. The software package also collects and organizes the output from each of the Monte Carlo trials to allow for statistical analysis and examination of the set of results for a given Monte Carlo simulation scenario.

The simulation model depicted in Figure 5 relies upon two primary, controllable variables, as shown in Block 1. The controllable input variables were set to values appropriate for each of the scenarios related to manned aircraft speed and UA size.

The V_{MA} variable, or manned aircraft speed, was set to a range of airspeed values representative of low altitude operating airspeeds. These speeds include the departure and arrival airspeeds of small personal sport category aircraft to high performance personal aircraft to faster moving business jets through heavy airliners. The upper range of approach airspeeds varies from 125 knots for a Boeing 707-320 to 158 knots for a Boeing 747-400F freighter aircraft, with the remainder of the Boeing fleet falling between these two airspeeds (Boeing Aircraft, 2016). Light general aviation aircraft, such as the Cessna 172 Skyhawk typically operate at airspeeds ranging from 65 knots to 100 knots during departure, approach, and other low altitude operations (ERAU, 2016). This study used scenario airspeeds between 60 knots to 160 knots to capture the range of airspeeds typical for different scenarios based on different types of aircraft.

To determine the range of sizes for small UAS aircraft, a student in the North Shore Community College – Aviation Science program conducted an informal review of popular websites offering sUASs for sale. The hired student reviewed the following web

sites: <http://www.amazon.com> and <http://www.bestbuy.com>. The student also used manufacturer websites to confirm and check product specification information, recording the model, size, weight, and color data for these UA. The student also looked for information on larger, professional small UA products to round out the list of UA sizes for use in this study. The intent of this informally gathered information is not to represent the actual UA population operating in the United States. The information only serves to provide informal support for the assumed sizes of common UA products used in this study. Information from other independent sources such as PC Magazine (Fisher, 2017) and Google.com (Google, 2017) provided a means for confirming the student's data on products described as popular by some of the media.

The model randomly selects an airspeed and a relative direction for the UA, as shown in Box 2 of Figure 5. The UA track (D_{UA}) relative to the manned aircraft and UA speed (V_{UA}) were used to compute a closure rate (\dot{r}) as follows: $\dot{r} = V_{MA} - (V_{UA} \times \cos(D_{UA}))$. V_{MA} is the controllable variable for the airspeed of the manned aircraft. D_{UA} is a uniform distribution of discrete values ranging from zero degrees to 350 degrees, in 10-degree increments. This distribution provides the model with randomly chosen heading values to account for the uncertainty about which direction the small UA target is heading relative to the manned aircraft. The uniform distribution indicates the UA is equally likely to be traveling in any direction relative to the track of the manned aircraft.

V_{UA} is chosen randomly from a Gaussian distribution with a mean of zero miles per hour and a standard deviation of 14 to provide values for the airspeed of the UA. Casual observation by the researcher of actual small UA operations and numerous videos from small UA suggest that most small UA operators tend to fly their aircraft at low

airspeeds. Low airspeed operation is consistent with the common mission of gathering video data and with the need to keep visual surveillance and control of the UA. While some UA are capable of operating up to 40 miles per hour or more, such operations appear to be rare. The majority of operations seem to be hovering operations or slow speed movements within the zero to 14 mile per hour range. Two standard deviations would cover operations within the zero to 28 mile per hour range, and three standard deviations allows for occasional operation up to the limit of 42 miles per hour, though such operating speeds seem to be rare in practice.

The closure rate is important for the next step (see Box 3)—calculating the minimum range (r_2) for UA detection by the human pilot. This minimum range is the closest the two aircraft can get before the pilot must see and take action to avoid a collision. As described later in the Data Sources–Determination of Minimum Distance to Avoid a Collision section of this chapter, the pilot must have 12.5 seconds of time to see the small UA and react so a collision can be avoided (FAA, 2016c). If the pilot does not detect the UA until the aircraft is closer than r_2 , there may not be enough time to maneuver clear of a collision. The model calculates the minimum range (r_2) by normalizing the closure rate (\dot{r}) to units of feet per second and multiplying it by 12.5 seconds. While the visual angle size at r_2 is not required for calculations related to the probability of detection model, knowing the r_2 value will enable the calculation of the visual angle size of the target 12.5 seconds before the collision point. Knowledge of the visual angle size of the target at the latest possible detection point provides useful information for the outcome analysis in Chapter 4.

The model also requires the determination of the maximum possible detection range in order to compute the amount of time the pilot will have to search for the UA. The maximum possible detection range depends on the size of the UA and the distance between the UA and the observer because they determine the apparent size of the UA to the observer. The further away the target is, the smaller it appears to be. If the object appears to be so small that it renders an image of less than one arc minute on the eye's retina, it may be too small to see. Therefore, the maximum range is the distance at which the target UA renders one arc minute of image size on the retina. The apparent size of the UA, for distant detection purposes, is also dependent upon the contrast between the target and its background. A contrast value of less than 1.00 further reduces the apparent size of the target object. Box 4 illustrates the calculation of the apparent size of the UA target.

Andrews (1984) states that the detectability of small, distant objects, ranging from one to 10 arc minutes of image size, is a function of the product of the target area and the target's contrast against its background. Therefore, a reduction in contrast requires an increase in target area to produce the same level of target detectability. In this study, the area of the target is a controlled input value; however, the target area will effectively be smaller if the contrast of the target is poor. Based on Andrews (1984), the contrast-adjusted target size (A_{CA}) becomes $A_{CA} = C_A \times A$, where A is the target size in terms of its physical profile area, and C_A is the apparent contrast of the target against its background.

The model randomly selects C_A from a normal distribution of contrast values based on the range of potential values described by Poe (1974) to account for contrast

uncertainty. Poe states the luminance of both the aircraft and its background change constantly as it moves because of changes in both light sources and background reflectivity. While Poe described the challenge of selecting a single contrast value for use in detection models, Poe's study states, "common levels of aircraft intrinsic contrasts are between 0.05 and 0.75" (p. 11). The model will choose values from a normal distribution shaped such that 0.05 and 0.75 constitute a 95% confidence level. The normal distribution is constrained to ensure the chosen contrast value cannot be less than zero; however, verification testing, as described in Chapter 4, confirmed the distribution provides values that appear to match Poe's assertion about the typical range of contrast values. Given the many combinations of background textures and small UA target colors, the expected apparent contrast will generally fall between the two limits of Poe's contrast range, with a bell-shaped distribution.

Box 5 depicts the calculation of the maximum possible range (r_1) for target detection using the contrast-adjusted target size (A_{CA}). This maximum range is constrained by the 1.0 arc minute limit for human vision acuity. If the object renders a smaller image than this on the retina, the human eye will not be able to resolve it from its surroundings (Hirsch & Curcio, 1989; Howett, 1983; Jones, Freitag, & Collyer, 1974). Andrews (1991a) states laboratory tests show the typical limit of detection for a high contrast, circular object is 1.0 arc minutes in target size. Flight tests have shown pilots often do not detect objects below 2.0 arc minutes of visual angle size. The exact small size of this limit specification is not critical according to Andrews because "very little of the total opportunity to acquire [the target] accumulates when the target aircraft is near the resolution limit" (p. 43).

The maximum possible range (r_1) is the distance at which the rendered target image becomes so small that it equals 1.0 arc minutes of visual angle. If the distance increases any further, the object becomes too small for the human eye to resolve. The model calculates this maximum possible distance as $r_1 = A_{CA} / 1.0$ arc minute. The actual formula, derived from Andrews (1991a), is shown in Equation 7.

$$r_1 = (1.1284 * \text{SQRT}(A_{CA})) / ((1/60) * (2*\pi) / 360) \quad (7)$$

where:

A_{CA} = contrast-adjusted area of target's horizontal profile

1.1284 = constant to convert steradian units to a linear unit as explained below

Since the simulation model computes probabilities based on steradian or solid angles, using radian-based units, it is necessary to perform a units conversion to match the angular units in both the numerator and the denominator of the r_1 calculation. The denominator is 1.0 minutes of arc, which means its angular unit is degree-based. Since 1.0 arc minutes is $1/60^{\text{th}}$ of a degree, and since degrees can be converted to radians by multiplying them by $(2\pi/360)$, the denominator of the r_1 calculation is $(1/60) * (2\pi/360)$, yielding the radian equivalent of 1.0 arc minutes.

The numerator is a solid angle measured in steradians, or squared-radians, by Andrews. A solid angle is analogous to a cone with the measurement of interest being the area of the circle at the wide-end of the cone. To convert the solid area to a linear measurement from a squared measurement of area, the square root of the dimension is taken. Since conceptually the angle is conical, in addition to the square root of the area, it

is necessary to take the square root of the constant associated with the area of a circle. The area of the circle is π times the square of the radius of the circle. The radius is equal to the diameter (the linear measurement of the target) d , divided by two. This results in the area of the circle $A = \pi(d/2)^2$. Alternatively, $A/\pi = d^2/4$. Multiplying both sides of the equation by four yields $(4/\pi)A = d^2$. Taking the square root of both sides of the equation results in $\text{SQRT}(4/\pi) \times \text{SQRT}(A) = d$, the linear measurement needed to compute the r_1 distance. The r_1 distance is d divided by one arc minute in radians. The square root of $(4/\pi) = 1.1284$, as used in Equation 7.

Box 6 contains the probability calculation equation from Andrews (1991a). All of the information needed to calculate a probability of detection exists at this step of the model execution. This calculation uses the simplified integration result described earlier in the literature review. The calculation in Box 6 is dependent upon several assumptions described below.

One assumption is the aircraft are not accelerating during the search period beginning at r_1 and ending at r_2 . Given the small subtended sizes created by small UA and the airspeeds at which most manned aircraft operate, the difference between r_1 and r_2 is likely to be small enough to constrain the search period to well under 30 seconds. Given the short search time, the assumption is reasonable. The assumption is also a limitation of the study.

The constant β used in the equation in Box 6 will be 17,000 steradian-seconds as determined by Andrews (1991a) to be appropriate for situations where the pilots have no alert about UA traffic and they are scanning for traffic normally, with a low workload level. Andrews describes B as the pilot-search-effectiveness constant whose value was

determined by flight test studies conducted by Andrews in earlier research (Andrews, 1991b).

The final assumption needed for the equation in Box 6 is atmospheric visibility is generally good. The equation used in Box 6 assumes the atmospheric visibility is good enough so it does not reduce the apparent contrast C_A by occluding reflected light from the vicinity of the target from reaching the observer. Andrews (1991b) states that if the visual range is two to three times the range at which visual acquisition is to occur, then atmospheric scattering has a minimal effect on visual detection. Since early calculations have shown that visual acquisition of small targets, such as the small UA in this study, will need to occur at distances between 2,000 and 5,000 feet, flight conditions must generally be three statute miles or better for the Andrews (1991a) equation used in this model. The Sources of Data section of this chapter describes the weather repository this study used to confirm visibilities are generally far better than three miles based on weather observations from fifteen airports around the country. Though the assumption of good atmospheric visibility cannot be generalized to the entire population of airports around the country, the data shows it is a reasonable assumption for the purposes of this study.

The output of Box 6 is a probability of detection number. The Analytica software will store the probability number from the current trial calculation for subsequent analysis using descriptive statistics. The Analytica software will then run another trial, repeating the steps from Box 2 through Box 6 to gather a set of probability outcomes based on different, randomly selected values for the uncontrollable variables for each trial.

Box 7 represents the concluding steps taken once the Monte Carlo process completes the specified number of trials. In this final set of actions, Analytica processes and Microsoft Excel spreadsheets analyze the output data, generated by the simulation model, with descriptive statistics and graphing methods to convey the probability of UAS detection given one or more scenarios.

Figure 6 shows the graphical definition of the data and calculations used by Analytica. The magenta-colored squares represent the controllable input variables to the model. The green-colored ovals depict the uncontrollable input variables defined as distributions. These input variables supply randomly selected values to the model in accordance with the defined distribution assigned to the particular variable depicted. The light blue, rounded rectangular boxes depict calculation nodes where inputs are processed to produce some intermediate result required by the model. The yellow, rounded rectangles represent the output variables which the Analytica software gathers and saves for further statistical analysis and graphing at the conclusion of the simulation.

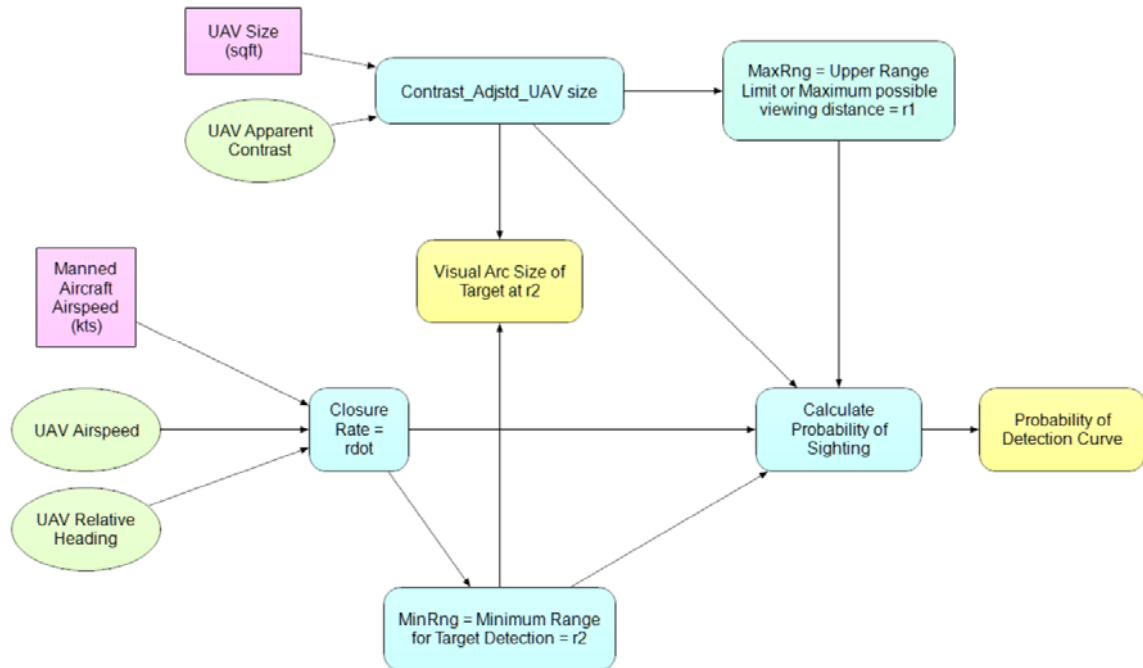


Figure 6. Conceptual layout of the mathematical model. The overall concept is defined by this graphical representation of the adaptation of the Andrews (1991a) model. This is the actual structural definition used for the Analytica® analysis software from Lumina Decision Systems.

Apparatus and materials. The Monte Carlo simulation engine used software from Lumina Decision Systems called Analytica. This study used Analytica Educational Professional release 4.6.1.30. This software allows analysts to model uncertainty and variability in the input variables and to collect the resulting outputs in a form conducive to statistical or comparative analysis. With Analytica, the researcher graphically designs the simulation model. Figure 4 shows the actual Analytica model for the mathematical process used in this study. This study also used Microsoft Excel 2013 to process the visibility data and to analyze the data used to test the reliability of the Analytica model.

Sources of the Data

The data for this model were obtained from well-known, public sources, previous research studies, or calculations based on previously reviewed models, as described in the literature review. This study did not involve any human subject interaction or experimentation. The key conceptual inputs are listed earlier in this chapter as the input variables to the design of the model. The following sections provide a more detailed description of the key constants and external data sources used in this study.

Determination of minimum visual angle. Based on Howett's (1983) work for the National Bureau of Standards, the minimum visual angle threshold of 1.0 arc minute is the smallest size of detail that humans with normal 20/20 vision can detect and recognize. While Howett acknowledges that some individuals have 20/10 vision or better and can theoretically see detail at visual angles as low as 0.5 arc minutes, such individuals are rare. The National Bureau of Standards guidance for determining letter sizing on signs uses research that finds less than two percent of the overall population have vision correctable to 20/10 or better (Howett, 1983). Hirsch and Curcio (1989) also corroborate the 1.0 arc minute finding with physiological analysis of the human retina and human subject testing. Hirsch and Curcio found the spacing of cone cells in the retina to theoretically be capable of resolving visual angles below one arc minute in a small segment of the population. However, in human subject testing they found the use of cone cell spacing tends to overestimate the level of detail humans can resolve. Hirsch and Curcio found actual visual acuity levels are less capable than the theoretical resolution suggested by cone cell density measurements.

Understanding the limit of human vision in terms of small object detection and recognition is an essential prerequisite to defining the Monte Carlo model. Since the intent of this research is to address the pilot population in general, and since the visual acuity threshold used by the National Bureau of Standards (Howett, 1983) is 1.0 arc minutes of visual angle for people with 20/20 vision, this study also used the 1.0 arc minute constant as the minimum image size that can be seen by the human eye. It is consistent with all of the human visual performance models encountered during the literature review. Andrews (1991a) also used 1.0 arc minutes as the minimum sized image visible to the human eye.

Determination of minimum distance needed to avoid a collision. The minimum distance (r_2) needed to avoid a collision is dependent upon the closure rate between the manned aircraft and the UA. This distance is determined by the minimum time before a collision occurs at which the manned aircraft pilot must be able to detect the UA visually in order to have time to react and alter the trajectory of the manned aircraft. If the pilot has not seen the target UA by the minimum time-before-collision point, there will not be enough time to maneuver clear of the UA collision point with certainty.

The amount of time required for a manned aircraft pilot to detect and avoid a collision with another aircraft is 12.5 seconds (FAA, 2016c). Table 5 depicts the breakdown of events consuming the 12.5-second requirement. The 12.5 second see-and-react time depicted in Table 5 does not include search time for an aircraft. The time period begins once the search process has resulted in visual detection. Search times vary

by the complexity of the visual search field, the contrast of the target, and the lighting conditions in the search area.

Table 5

Aircraft Identification and Reaction Time

Event	Time (seconds)	Cumulative Time (seconds)
See object	0.1	0.1
Recognize aircraft	1.0	1.1
Recognize collision course	5.0	6.1
Decide on action	4.0	10.1
Muscular reaction	0.4	10.5
Aircraft lag time	2.0	12.5

Note. This chart depicts the cumulative minimum time needed to see and react to a collision hazard in order to avoid the actual collision. This chart is adapted from the Australian Transport Safety Bureau, 1991, who based their conclusions on FAA Advisory Circular 90-48-C. The original data were derived from military research studies.

While a number of other factors also affect visual search times, this model takes a best-case approach in an attempt to find the best possible target detection performance. This study used the best-case approach because preliminary calculations of target detectability suggested targets would typically be very small and potentially difficult to see. Since this study focused on determining the limits of human visual performance for visual detection of small UA, it was important not to mask the limits with extraneous variable inputs unrelated to human vision performance.

Meteorological data. The clarity of the atmosphere affects a pilot's ability to see and detect airborne objects. When the visibility is poor, such as in foggy or misty conditions, less of the reflected light from a target object reaches the eye. The

atmospheric dispersion and absorption of transmitted light energy creates a cumulative loss of light from the target, and less light energy actually reaches the pilot's eyes. This makes it more difficult for the pilot to see the target (Lee & Shang, 2016). One variant of Andrews' model used meteorological visibility to calculate the reduction of the apparent contrast of the target against its background (Andrews, 1991a). However, Andrews (1991b) also states if the atmospheric visibility is more than two or three times the distance between the observer and the target, then the atmospheric visibility will have a minimal effect on the ability of the observer to detect the target.

This study obtained atmospheric visibility data for the three-year period from 2014 through 2016, using archived data from automated weather observation sensors located at major airports to demonstrate that, at several locations around the country, visibility is generally many times greater than the typical small UAV detection distance of less than one mile (based on preliminary calculations). As long as the visibility is generally three miles or greater, per Andrews (1991b), atmospheric visibility can be removed from the algorithm. The study gathered visibility data for airports located in 15 different cities around the country. The National Weather Service operates and maintains the visibility sensors at these airports, and Iowa State University archives these data for public access. Data for this study came from the Iowa State University archives at <http://mesonet.agron.iastate.edu/request/download.phtml>.

The reason for acquiring and analyzing these data was to ensure the assumption about atmospheric visibility, generally being much greater than three miles, is true at least at several major airports around the country. Statistical analysis of hourly visibility reports from 2014 through 2016, from 15 airports around the country, verified the belief

that visibility generally exceeds three miles at these airports (see Table 6). The data from these airports, over the last three years, shows visibility was six miles or better, 90% or more of the time, far exceeding the required three miles to justify the use of simplified formulas related to the effects of atmospheric visibility on apparent target contrast.

Table 6

Atmospheric Visibility Data from Selected Airports

Airport	Usable Observations	Missing Data	Mean Visibility	Std Dev	=> 6 Miles
KATL– Atlanta	100,693	1	9.43	1.88	94%
KBOS– Boston	67,958	6	9.07	2.40	90%
KCLT– Charlotte	99,461	75	9.53	1.68	95%
KDAB– Daytona Beach	99,691	162	9.32	1.89	94%
KDEN– Denver	101,098	35	9.44	2.00	94%
KDFW– Dallas/Fort Worth	100,149	13	9.55	1.63	95%
KEWR– Newark	98,883	22	9.39	1.86	94%
KIAD– Washington/Dulles	99,841	7	9.28	2.05	93%
KJFK– New York/Kennedy	91,406	6,960	9.35	1.95	93%
KLAX– Los Angeles	99,028	53	8.97	2.11	92%
KMIA– Miami	99,326	12	9.73	1.21	98%
KORD– Chicago/O’Hare	101,813	19	9.04	2.29	90%
KSEA– Seattle	76,010	1	9.37	1.96	94%
KSFO– San Francisco	97,616	28	9.71	1.18	97%
KSTL– St. Louis	70,347	6	9.08	2.15	90%

Note. This chart depicts the number of observations, number of missing data cases, mean visibility, standard deviation, and the percentage of observations where the visibility was six miles or greater for each of the selected airports from around the country. The data collection period was January 1, 2014 through December 31, 2016. KJFK experienced a sensor outage from August 4, 2016 to September 7, 2016. The Iowa State University Environmental Mesonet web site supplied the observations report data. The data are accessible at <http://mesonet.agron.iastate.edu/request/download.phtml>

Model reliability. To ensure the model produced consistent results over repeated simulations, the study analyzed the results from repetitive executions, with different random number generator seed values, to ensure consistency from each of the sets of simulation trials. ANOVA testing confirmed there were no significant differences

between the outputs of the reliability tests. A detailed description of the results from these tests is contained in Chapter 4.

Model validity. Two separate activity threads were used to test the validity of the model for this study. One thread ensured the mathematical computations produced the expected results. The other thread compared the probability outputs of the model to known human performance limits and other validated models from previous studies to check for convergent validity.

To ensure the integrity of the mathematical computations used in the model, all of the input distributions and computations were unit tested prior to executing the model for results analysis. This was done by statistically examining the distribution data generated by each distribution input node, to ensure the random number generators produced a set of data values that conformed to the specified input distribution profile. The Analytica software allows inspection of the internal computation and variable node outputs, so checking the distributions of the uncontrollable input variables was straightforward. Each computation and each variable node in the model was examined and verified manually to ensure it produced the expected result when executed. Nodes producing a distribution of randomly generated numbers were run in simulation mode to allow examination of both the random numbers generated and the overall distribution profile. The results of these testing procedures are detailed in Chapter 4.

The second thread of validity confirmation analysis compared the findings of this model with known limits of human visual acuity and the findings of other similar visual target detection studies. The challenge with establishing a formal comparison of results between this study and other studies is very little work has been done to determine the

probability of human visual detection of small UA in time to avoid a collision hazard. Existing similar studies do not directly address the research questions in this study. For example, Loffi et al. (2016) studied the rate of UA visual detection by human pilots but not necessarily the rate of detection constrained by the requirement to avoid a collision with the UA. Many of the sightings in the Loffi study occurred too late to allow the pilot time to avoid a collision. The Loffi et al. study also informed the pilots to look for a sUAS while flying their prescribed routes, so the pilots were in an elevated state of alertness. Other studies with published results used targets much larger than an sUAS thereby changing some of the unique challenges associated with sUAS detection. Despite these challenges, it was possible to ensure the output of this sUAS study did not contradict results from other studies in an inexplicable manner.

Background clutter. This study did not directly model the effect of background clutter on the probability of visual detection. The effect of background clutter is complex and dependent on a wide variety of variables beyond the scope of this study. To appropriately model background clutter, the model would need scenario and site specific measurements and analysis of the background. Based on data from Toet (2010) in his studies involving a variety of specific, natural background scenes, search times increased as the number and similarity of background features, comparable to the target's features, increased. In a study involving 62 participant viewers searching for objects in 44 natural scenes of varying complexity, mean search times varied from 2.2 to 29.8 seconds.

This study cannot directly use the background scenes or numeric findings from Toet's studies because Toet's data apply to specific scenes with specific features. Actual backgrounds encountered by pilots are likely to have very different kinds of features,

shapes, and contrasts. The scenes will also change with variations in seasonal, weather, and illumination conditions.

Treatment of the Data

The simulation model placed its output data in an array where it could analyze them with basic descriptive statistics. Additionally, Microsoft Excel provided a platform for additional analysis of the data. The model developed for this study produced a set of probability curves illustrating the likelihood of visual detection of the sUAS target, in time to allow the pilot to take evasive action, given different values of the controllable inputs. The study ran the simulation using multiple combinations of controllable input values to identify the sensitivity of the results to specific inputs to the model.

Additionally, the dissertation renders the results in multiple graphical forms to show how the probability of detection relates to the scenarios used to select the controllable input values for the study.

CHAPTER IV

RESULTS

A Monte Carlo simulation model, as described in Chapter 3, generated the visual detection probability data for this study. This chapter describes the results in three sections. The first section documents the data collected for verification testing of the model, as described by Anderson et al. (2015). The second section contains data depicting the reliability test results for the model. The third section describes the output of the model in both statistical and graphical formats.

Verification Testing

The simulation performed for this study was accomplished using Analytica 64-bit Educational Professional software Release 4.6.1.30—a tool by Lumina Decision Systems. In order to confirm the proper entry of the model's algorithms into the simulation software, the content of each node of the model depicted in Figure 6 was examined for proper formulation consistent with its computational objective. The computational objectives and formulas are depicted in Figure 5.

Input nodes supplying distribution data were statistically and graphically examined to verify the resulting output conformed to the specified distribution profile. The output of each computational node of the model, depicted by light blue rounded rectangles in Figure 6, was verified by comparing the node's output to the results of manual calculations using the input values from the predecessor nodes. There are three inputs to the model supplied as random numbers drawn from a specific distribution. These inputs are UAV Apparent Contrast, UAV Airspeed, and UAV relative heading.

The output of each of these distributions is examined below from a simulation run with 32,000 trials.

The UAV Apparent Contrast distribution input node generated a range of random values with a probability density conforming to a normal distribution. The distribution was truncated to ensure no contrast values below zero were possible. The resulting output produced the following distribution of values (see Figure 7).

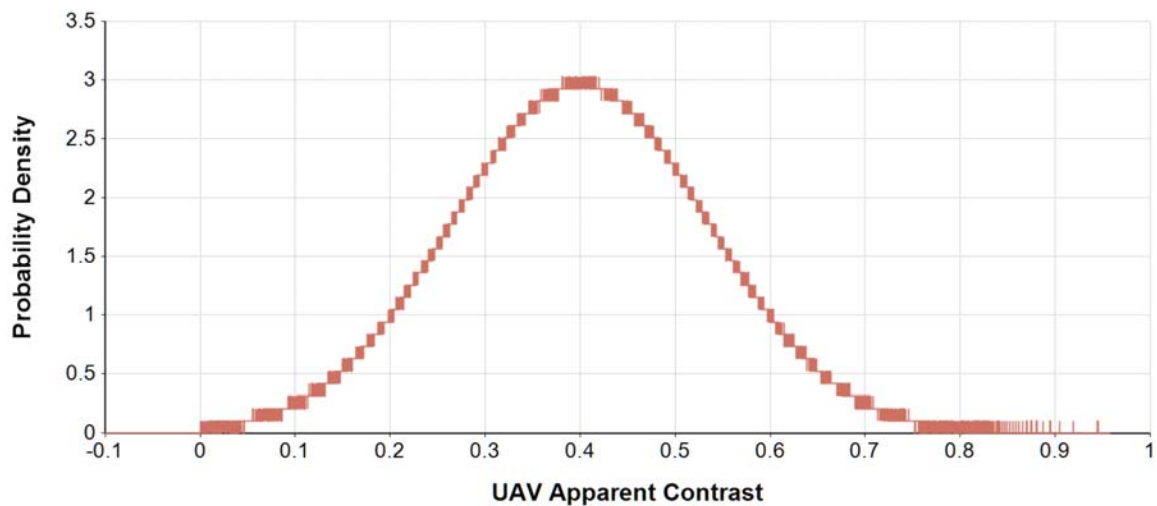


Figure 7. Probability density distribution of target contrast values. This input distribution provides random target contrast values where most of the values fall between 0.05 and 0.75 per Poe (1974). The distribution is truncated so no value below zero can be produced. As shown in this figure, the truncation does not visibly distort the normal distribution curve.

The UAV airspeed distribution input node generated a range of random values with a probability density conforming to a normal distribution with a mean of zero knots and a standard deviation of 14 knots. The distribution output was converted to an absolute value to produce a range of positive velocities from zero to around 45 knots based on a casual sampling of specifications for popular sUAS products. A table of the

specifications for these products is contained in Appendix A. The UAV airspeed generated by this distribution function represents the uncontrollable airspeed of the UAV target. It is different from the controllable airspeed of the manned aircraft which serves as the observation platform from which the human pilot must detect the UAV.

The resulting output produced the following distribution of values ranging from zero knots to 54 knots with a mean value of 11.17 knots and a standard deviation of 8.44 knots. The probability distribution curve for these values is shown in Figure 8.

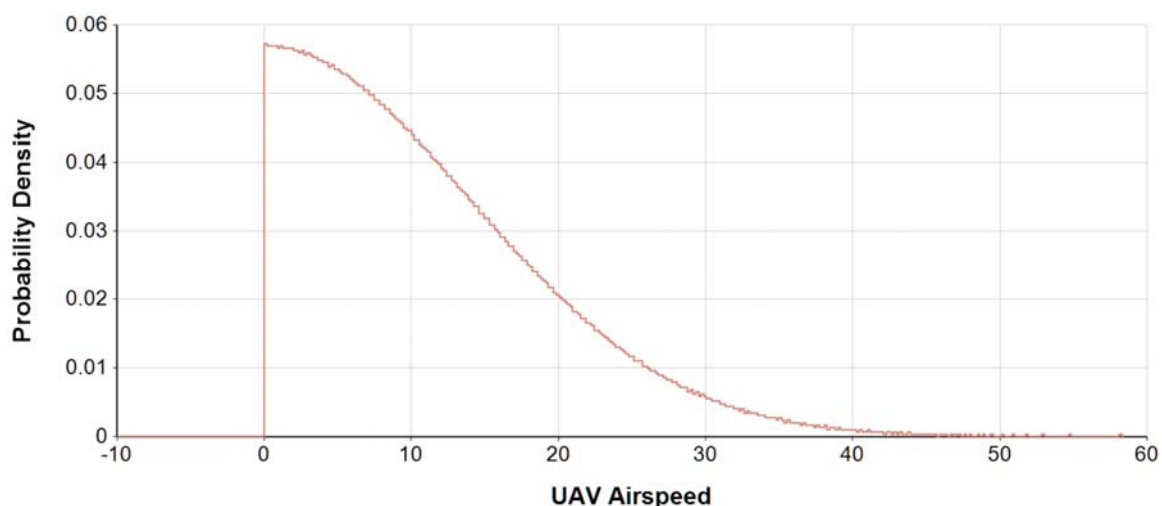


Figure 8. Probability density distribution of UAV airspeed values. This input distribution provides random UAV airspeed values ranging from zero up to around 45 knots using the positive half of a normal distribution. Only positive values are used. No value below zero can be produced.

The UAV Relative Heading distribution input node generated a range of random values with a uniform probability density producing a range of integer values from 0 to 359. The resulting output produced by the uniform distribution of values is shown in Figure 9.

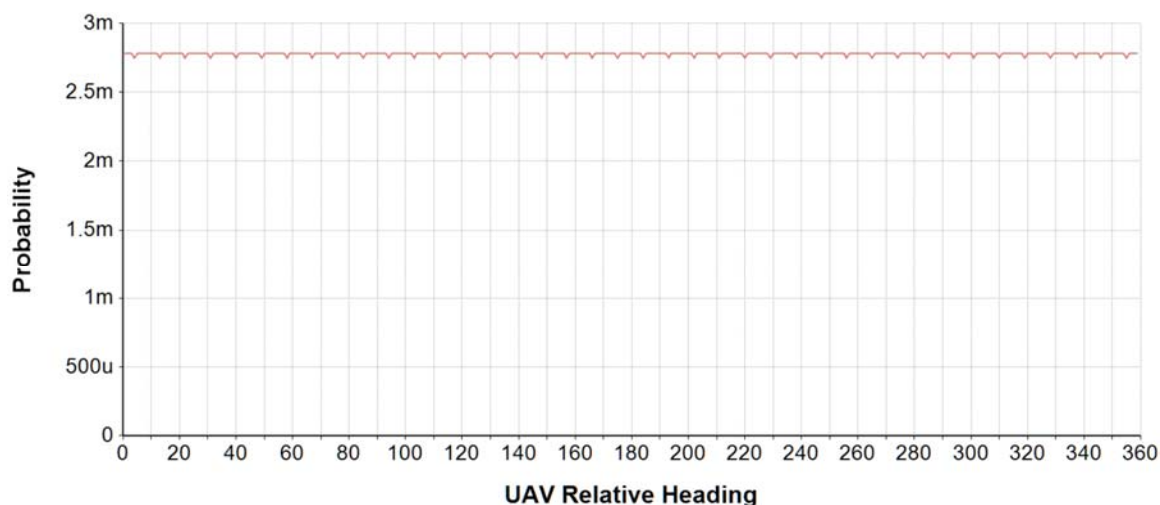


Figure 9. Probability density distribution of relative UAV heading values. This input distribution provides random UAV heading values from zero to 359 degrees relative to the observer pilot's aircraft.

Verification of the model's output for each of the computation nodes, depicted in Figure 6, is described next. For each node, a table depicts the input values, captured by the model during a test run, the output value, and the manually calculated output value. The model's output value is compared to the manually calculated value to verify the integrity of the model's calculations. This ensures no programming error occurred during the construction of the model using the Analytica tool. The verification is performed on the input values generated for three different trials of the Monte Carlo simulation.

The first node tested is the Closure Rate node where the closure rate between the UAV target and the manned aircraft with the pilot/observer resides. Table 7 depicts the input values and the calculated results from this node. Except for a slight rounding error in Trial 2, the output values calculated by Analytica match the manual calculation of the output given the input values used for the verification testing.

Table 7

Closure Rate Calculation Node Verification Results

Verification Trial Number	Manned Aircraft Speed (knots)	UAV Airspeed (knots)	UAV Relative Heading	Model Output Value	Manual Calculation Value
1	100	34.30	29	0.01944	0.01944
2	100	6.43	140	0.02914	0.02915
3	100	17.88	248	0.02964	0.02964

Note. The model output values and the manual calculation values match, verifying the model's calculations produced the expected output value. The output value for the Closure Rate Calculation node represents nautical miles per second.

The Minimum Range node in the model computes the minimum distance, in nautical miles, for detection of the UAV target by the pilot observer. The minimum range represents the distance at which only 12.5 seconds of time remain for the human pilot to take action to avoid a collision with the UAV. Table 8 depicts the input values and the calculated results from this node. Except for a slight rounding error in Trial 1, the output values calculated by Analytica match the manual calculation of the output given the input values used for the verification testing.

Table 8

Minimum Range Node Verification Results

Verification Trial Number	Closure Rate (NM/sec)	Model Output Value	Manual Calculation Value
1	0.01944	0.2431	0.2430
2	0.02914	0.3643	0.3643
3	0.02964	0.3705	0.3705

Note. The model output values and the manual calculation values match, verifying the model's calculations produced the expected output value. The output value for the Minimum Range Calculation node represents distance in nautical miles.

The Contrast-Adjusted UAV size node computes the apparent size of the UAV target adjusted for the contrast of the target against its background. Table 9 depicts the input values and the calculated results from this node. The output values calculated by Analytica match the manually calculated output values.

Table 9

Contrast-Adjusted UAV Size Node Verification Results

Verification Trial Number	UAV Size (square feet)	UAV Contrast	Model Output Value	Manual Calculation Value
1	1	0.6548	1.774×10^{-8}	1.774×10^{-8}
2	1	0.4643	1.258×10^{-8}	1.258×10^{-8}
3	1	0.4040	1.094×10^{-8}	1.094×10^{-8}

Note. The model output values and the manual calculation values match, verifying the model's calculations produced the expected output value. The output value for the Contrast-Adjusted UAV Size Calculation node represents the UAV size in square nautical miles.

The Maximum Range node computes the maximum possible range at which the UAV target can theoretically be seen. The search time for the probability of detection algorithm cannot begin until it is theoretically possible to see the UAV. The UAV, when it is further away from the observer than this maximum range, renders less than one arc minute of size on the retina and is therefore too small to be visible. Table 10 depicts the input values and the calculated results from this node. The output values calculated by Analytica match the manually calculated output values.

Table 10

Maximum Range Node Verification Results

Verification Trial Number	Contrast-Adjusted UAV Size (NM ²)	Model Output Value	Manual Calculation Value
1	1.774 x 10 ⁻⁸	0.5166	0.5167
2	1.258 x 10 ⁻⁸	0.4350	0.4351
3	1.094 x 10 ⁻⁸	0.4058	0.4057

Note. The model output values and the manual calculation values match, verifying the model's calculations produced the expected output value. There is a difference of 1/10,000 of a nautical mile due to a rounding error. The output value for the Maximum Range Calculation node represents the maximum possible sighting distance in nautical miles. Beyond this distance, the target UAV will become too small for a human eye to see.

The Probability of Sighting node uses the values computed by the other nodes in the model as shown in Equation 6. Table 11 depicts the input values and the calculated results from this node. The output values calculated by Analytica match the manual calculation of the outputs given the input values used for the verification testing.

Table 11

Probability of Sighting Node Verification Results

Trial	Closure Rate	Adjusted UAV Size	Minimum Range	Maximum Range	Model Output Value	Manual Calculation Value
1	0.01944	1.774 x 10 ⁻⁸	0.2431	0.5166	3.3%	3.3%
2	0.02914	1.258 x 10 ⁻⁸	0.3643	0.4350	0.3%	0.3%
3	0.02964	1.094 x 10 ⁻⁸	0.3705	0.4058	0.1%	0.1%

Note. The model output values and the manual calculation values match, verifying the model's calculations produced the expected output value. The output value for the Probability of Sighting Calculation node represents the probability of seeing the small UAV, within the minimum and maximum range boundaries, expressed as a percentage value.

Reliability Testing

The data used for this study are produced by a Monte Carlo simulation model using randomly selected numbers from various distributions to account for uncertainty related to several input variables. The random number generation method used for this model used a median Latin hypercube sampling method to minimize noise in the random number distributions (Lumina Decision Systems, 2015). Testing was performed with various numbers of trial runs and various random number generator seed values to ensure consistent results despite the changing random number generator control parameters.

Mean probability is the key output for this model. The mean probability output represents the probability of detection averaged over all 32,000 trials of the simulation model.

To ensure the number of trials was adequate for consistent results from the simulation, testing of the model used various numbers of trial iterations ranging from 100 trials up to 32,000 trials. While the output results varied, with noticeable aberrations in the graphs of the results data when fewer than 250 trials occurred, the results were nearly identical from test to test with more than 250 trials for a given test. The drawback of running more trials is the added computing time required (Lumina Decision Systems, 2015), though the computing time for this model was less than 2 seconds for a 32,000 trial test. Therefore, this study used 32,000 trials to compute the results documented in this dissertation.

To test the model reliability, the study compared the output from four different runs of the model—each using a different sample of random numbers for the uncontrolled input variables. In each case, 32,000 trials were executed, and the UAV

target area was set to 1.0 square feet to represent common, larger-sized retail UAV targets. Four arbitrarily selected random number generator seed values were chosen to ensure the generation of a different sequence of random numbers (see Table 12). In Analytica, the seed value determines the starting position in Analytica's random number generation function. Starting the random number generation sequence using different seed values forced Analytica to produce a different sample of random numbers for use in the simulation. The use of different samples of random numbers tests the model to see if it produces consistent results regardless of the starting point, or seed value, used in the generation of random numbers.

The model generated random numbers using the L'Ecuyer method, chosen because of the method's ability to function well with over 100,000,000 samples, according to the Analytica user's manual. The drawback of using this method is it is slower than the other methods available within Analytica (Lumina Decision Systems, 2015). With 32,000 trials completed in under 2 seconds for this study's model, processing speed was not an issue, however.

Table 12 depicts the results of the reliability testing when different samples of random numbers drove the model's uncontrollable input variables. Table 12 shows the results clustered by airspeed. For each airspeed, four different seed values generated four different samples of random numbers. The model ran 32,000 trials, producing 32,000 results for each of the four different samples of random numbers. Table 12 also shows the mean and standard deviation for each of these runs.

Since no significant differences appeared among the four different sets of results, the results are considered statistically reliable. This study used ANOVA to test for

differences across the four groups (Hoyt, 1941). Table 12 shows the ANOVA F -statistic and P -value for each of the four sets of results.

Assumptions for ANOVA were tested. The large sample size of the data fulfills the normality assumption. Levene's testing verified the satisfaction of the homogeneity assumption. A non-significant Levene's statistic test ($p > 0.05$) indicates the homogeneity of variance among the test groups. Levene's testing identified the lack of homogeneity of variance for the 160-knot scenario; therefore, reliability testing for the 160-knot scenario data used Welch's ANOVA because Welch's ANOVA does not require homogeneity of variance. Levene's testing on the remainder of the airspeed scenarios produced results confirming homogeneity of variance; therefore, standard ANOVA testing is appropriate for all but the 160-knot scenario.

As shown in Table 12, the P -values for all cases are greater than 0.05 indicating there are no significant differences among the four samples; therefore, the model results are statistically reliable.

Table 12

Comparison of Results with Different Random Number Seed Values

Manned Aircraft Speed and Seed Value	Mean	Standard Deviation	ANOVA <i>F</i>	ANOVA <i>P</i> -value
60 – Seed=422	3.00	2.67	0.5887	0.62
60 – Seed=2017	3.03	2.81		
60 – Seed=8888	3.01	2.78		
60 – Seed=13579	3.02	2.76		
80 - Seed=422	1.09	0.96	0.3847	0.76
80 - Seed=2017	1.10	0.99		
80 - Seed=8888	1.09	0.96		
80 - Seed=13579	1.09	0.97		
100 - Seed=422	0.37	0.43	0.3734	0.77
100 - Seed=2017	0.38	0.44		
100 - Seed=8888	0.37	0.43		
100 - Seed=13579	0.38	0.43		
120 - Seed=422	0.10	0.18	0.3484	0.79
120 - Seed=2017	0.10	0.19		
120 - Seed=8888	0.10	0.18		
120 - Seed=13579	0.10	0.18		
140 - Seed=422	0.01	0.06	0.3838	0.76
140 - Seed=2017	0.02	0.06		
140 - Seed=8888	0.01	0.06		
140 - Seed=13579	0.01	0.06		
160 - Seed=422	0.00	0.01	0.911 _w	0.435 _w
160 - Seed=2017	0.00	0.01		
160 - Seed=8888	0.00	0.01		
160 - Seed=13579	0.00	0.01		

Note. This table shows the results of the model for a 1.0 square foot target at each manned aircraft airspeed from 60 knots to 160 knots in 20 knot increments. Each airspeed appears four times, once for each result produced by four different random number seed values as shown in the table. The *F*-statistic and *P*-value shown, from ANOVA processing of the four means for each group of airspeeds, indicate there is no significant difference between the means. Therefore, the model is reliable. The ANOVA results from the 160 knot scenario are marked with a ‘_w’ to indicate these results were produced by Welch’s ANOVA.

Descriptive Statistics of the Results

The scenarios used to generate input values for the simulation model all used a list of manned aircraft flight speeds ranging from 60 knots to 160 knots in 20 knot increments; therefore, six different airspeeds are utilized in each scenario representing aircraft from small sport-category aircraft to large transport-category aircraft operating at approach or departure-appropriate airspeeds. Each test scenario ran the model through 32,000 trials to generate the output dataset. The Analytica software tool computed each trial case with all six airspeeds, capturing the output from each of the airspeeds in a separate results matrix for each airspeed. This allowed the model to compute probability results for each of the airspeeds using the same random UAS airspeed, UAS heading, and UAS contrast values for a given simulation trial.

The probability data produced by the simulation model are shown in the following tables and graphs. A table and a graph were produced for each of the following sUAS sizes as measured in square feet for the sUAS's horizontal profile (see Table 13). Unlike fixed wing aircraft, when viewed from the same altitude as the target sUAS, the viewable area does not change radically. The horizontal profile areas depicted in Table 14 are estimated values based on measurements and specifications for popular sUAS products. The products used to develop these estimated sizes are listed in Appendix A. They were assembled as a convenience sample from retail outlet and product manufacturer websites by a student in the Northshore Community College Aviation Science program. The information was initially gathered in March of 2017 and was verified in April of 2017 by checking additional online-accessible sources. Since these data are intended to provide a conceptual approximation of the types of products available and the range of sizes

associated with these types of products, excessive validation of the input was not required.

Table 13

Area of Small UAS Side View Profile

General sUAS Size Class	Size (square feet)
Very Small sUAS	0.2
Common Hobby sUAS	0.7
Commercial Video UAS	1.0
Professional Video UAS	1.5
Larger Video UAS	3.5
Very Large sUAS platform	10.8

Note. These size values are not statistically derived values. They represent the viewable surface area of actual sUAS products based on measurements from common products listed in Appendix A. The products described in Appendix A represent a small convenience sample of sUAS quadcopter products found at popular retail outlets.

The Monte Carlo simulation model was repeatedly run for each of the UA profile sizes shown in Table 13. The following sets of tables and figures depicts the output from each of the model runs. The results shown in each of the following tables and graphs represents the mean probability of a human pilot visually detecting a small UA in time to be able to maneuver clear of a collision with it, if needed. The numbers shown are the probability in terms of percentage. Therefore, 0.10% means a probability of 0.0010 in decimal fraction form.

Table 14 and Figure 10 show the probability results from the model for a very small UAV rendering only 0.2 square feet of visible, horizontal profile. A pilot flying an aircraft similar to a light sport aircraft or a Piper Cub, flying slowly at 60 knots, will only have a 0.10% chance of spotting the very small UA in time to avoid colliding with it. At

speeds faster than 60 knots, the pilot won't be able to see the small UA in time to steer clear of a collision with it, if a collision is going to occur. While it is remotely possible that the UA may be flying away from the slow moving manned aircraft at a high rate of speed, thereby giving the pilot an extended opportunity to spot and avoid colliding with it, such a scenario is unlikely. The scenario above explains why there was an instance where the model predicted an 86% chance of detection at 60 knots; however, the mean of the values for chance of detection is only 0.10%.

Table 14

Probability of Sighting a 0.2 Square Foot sUAS

Statistic	Airspeed of the Manned Aircraft (in Knots)					
	60	80	100	120	140	160
Mean	0.10%	0.00%	0.00%	0.00%	0.00%	0.00%
Standard Deviation	0.63	0.05	0.01	0.00	0.00	0.00
Minimum	0.00%	0.00%	0.00%	0.00%	0.00%	0.00%
Maximum	86.42%	5.52%	0.87%	0.00%	0.00%	0.00%

Note. This chart depicts the mean percentage and standard deviation of detection probability as computed by the Monte Carlo simulation model when executed with 32,000 trials.

Figure 10 presents this same information graphically. While it appears there is a much greater chance of seeing this very small UA if the manned aircraft pilot is only flying at 60 knots, the probability number is only 0.10% so the probability of detection is virtually zero, even at 60 knots.

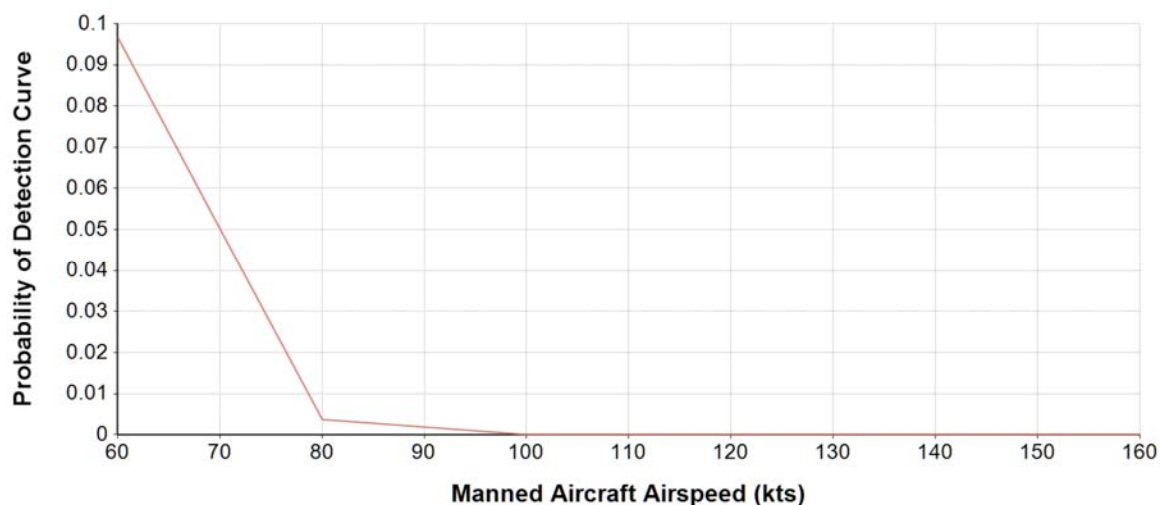


Figure 10. Probability of detection curve: 0.2 square foot target. The probability of detection, in time to avoid a collision, mapped against the manned aircraft speed. Probability values are shown in terms of percentage. The vertical axis shows a range of 0.01 percent to 0.10 percent or 0.0001 to 0.0010 in decimal fraction form.

Table 15 depicts the mean, standard deviation, minimum, and maximum of the values for the probability of detection when the UA has a visible profile of 0.7 square feet. This profile size approximates the visible profile of common hobby sUAS vehicles such as the DJI Phantom 3. At a slow, 60 knot airspeed, possible with a Piper Cub or light sport aircraft, there is a 1.78% chance the manned aircraft human pilot will see the sUAS in time to avoid colliding with it. At higher manned aircraft speeds, common for small general aviation, the likelihood of visual detection in time to avoid a collision drops to less than 1.0% and is 0.0% at airliner operating airspeeds. Figure 11 depicts this same information graphically for small, hobby-sized sUAS with visible profiles of 0.7 square feet.

Table 15

Probability of Sighting a 0.7 Square Foot sUAS

Statistic	Airspeed of the Manned Aircraft (in Knots)					
	60	80	100	120	140	160
Mean	1.78%	0.51%	0.11%	0.01%	0.00%	0.00%
Standard Deviation	2.00	0.62	0.22	0.06	0.01	0.00
Minimum	0.00%	0.00%	0.00%	0.00%	0.00%	0.00%
Maximum	99.93%	22.71%	6.14%	2.22%	0.84%	0.24%

Note. This chart depicts the mean percentage and standard deviation of detection probability as computed by the Monte Carlo simulation model when executed with 32,000 trials.

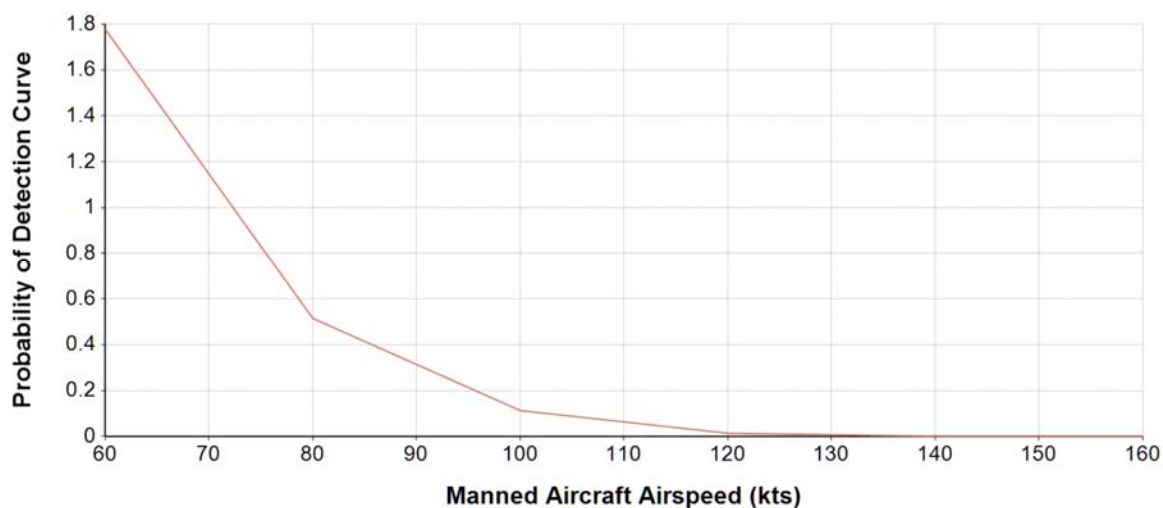


Figure 11. Probability of detection curve: 0.7 square foot target. The probability of detection, in time to avoid a collision, mapped against the manned aircraft speed.

Table 16 and Figure 12 show the probability of detection statistics for slightly larger, commercial-grade sUAS with a visible profile of 1.0 square feet. At this size, the mean value for probability of detection is higher, though it is still only 3.03% for pilots on a slow, manned aircraft flying at 60 knots. For pilots flying in manned aircraft at airliner airspeeds of 140 knots or greater, the probability of detection is nearly 0.0%.

Table 16

Probability of Sighting a 1.0 Square Foot sUAS

Statistic	Airspeed of the Manned Aircraft (in Knots)					
	60	80	100	120	140	160
Mean	3.03%	1.10%	0.38%	0.10%	0.02%	0.00%
Standard Deviation	2.81	0.99	0.44	0.19	0.06	0.01
Minimum	0.00%	0.00%	0.00%	0.00%	0.00%	0.00%
Maximum	100.00%	31.87%	9.46%	3.75%	1.66%	0.73%

Note. This chart depicts the mean percentage and standard deviation of detection probability as computed by the Monte Carlo simulation model when executed with 32,000 trials.

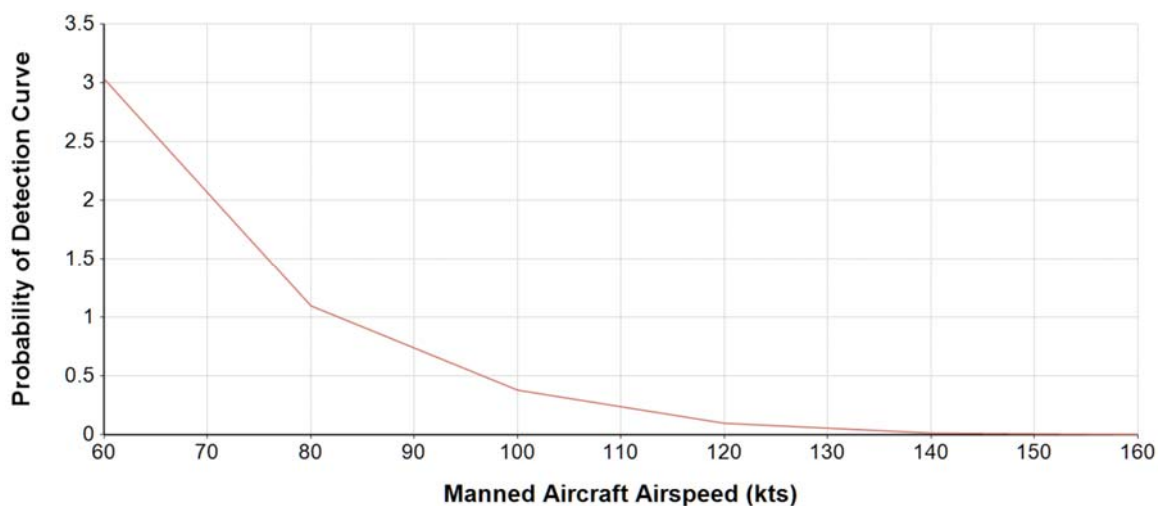


Figure 12. Probability of detection curve: 1.0 square foot target. The probability of detection, in time to avoid a collision, mapped against the manned aircraft speed.

Some professional sUAS camera platforms are larger and render more visible target area for detection by the human, manned aircraft pilot. These larger sUAS range from 1.5 square feet up to 10.8 square feet of visible profile area. Table 17 and Figure 13 illustrate there is a larger mean value for the probability of detection numbers generated by the Monte Carlo model. However, at 1.5 square feet, the mean probability of detection ranges from 5.20% when the manned aircraft is flying at 60 knots, to 0.03%

when the manned aircraft is flying at 160 knots. These numbers are far below 50%; therefore, the human pilot is unlikely to see the target sUAS most of the time. The maximum value computed during the 32,000 trials of the model was 100% at 60 knots of airspeed for the manned aircraft; however, high probability of detection numbers were rarely produced as indicated by the mean of 5.20% and the standard deviation of 4.09.

Table 17

Probability of Sighting a 1.5 Square Foot sUAS

Statistic	Airspeed of the Manned Aircraft (in Knots)					
	60	80	100	120	140	160
Mean	5.20%	2.18%	0.97%	0.41%	0.14%	0.03%
Standard Deviation	4.09	1.59	0.78	0.42	0.21	0.09
Minimum	0.00%	0.00%	0.00%	0.00%	0.00%	0.00%
Maximum	100.00%	45.01%	14.91%	6.38%	3.12%	1.61%

Note. This chart depicts the mean percentage and standard deviation of detection probability as computed by the Monte Carlo simulation model when executed with 32,000 trials.

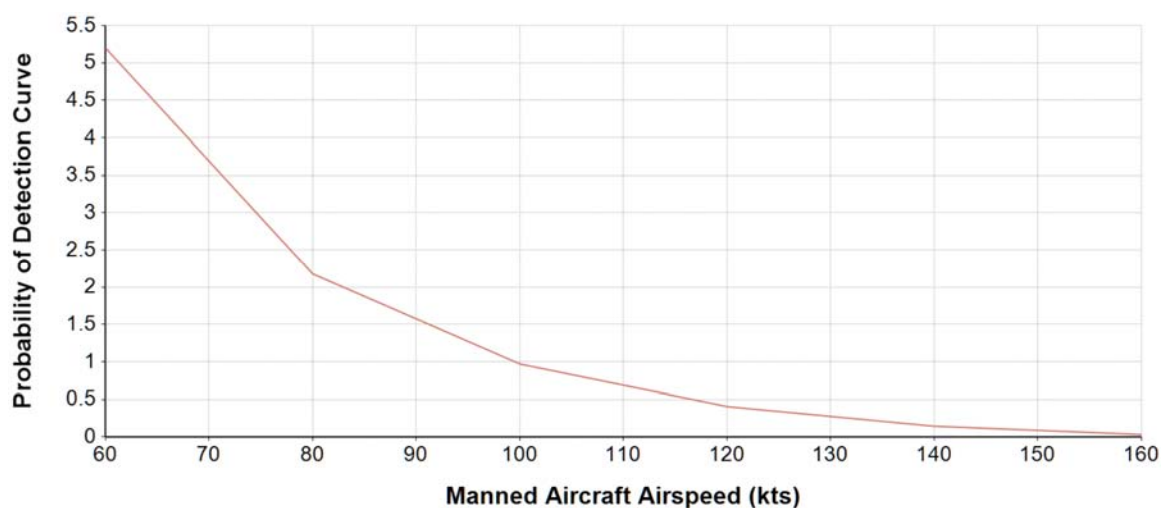


Figure 13. Probability of detection curve: 1.5 square foot target. The probability of detection, in time to avoid a collision, mapped against the manned aircraft speed.

Larger sUAS targets, with 3.5 square feet of visible profile area, resulted in a mean probability of detection of 13.8% when the manned aircraft is flying at 60 knots. Table 18 and Figure 14 show the probability of detection drops to 6.85% when the manned aircraft operates at 80 knots, and the probability of detection is only 1.29% at 140 knots. The larger-sized sUAS with 3.5 square feet of visible profile represents sUAS products such as commercial videography platforms in the \$12,000 to \$24,000 range.

Despite their comparatively large size, and the corresponding higher probability of visual detection, the mean visual detection probability is well below 50% at slow airspeeds and close to zero percent at airliner approach speeds. In a few isolated trials during the 32,000 iterations of the Monte Carlo simulation, the model identified cases where the probability of detection for these larger sUAS was likely if the manned aircraft airspeed was low. Table 18 depicts this for the maximum value of the 60-knot scenario. Those trial results were rare, however, as shown by the mean and standard deviation.

Table 18

Probability of Sighting a 3.5 Square Foot sUAS

Statistic	Airspeed of the Manned Aircraft (in Knots)					
	60	80	100	120	140	160
Mean	13.80%	6.85%	3.76%	2.18%	1.29%	0.76%
Standard Deviation	8.24	3.84	2.10	1.29	0.85	0.58
Minimum	0.00%	0.00%	0.00%	0.00%	0.00%	0.00%
Maximum	100.00%	77.13%	34.39%	16.86%	9.30%	5.55%

Note. This chart depicts the mean percentage and standard deviation of detection probability as computed by the Monte Carlo simulation model when executed with 32,000 trials.

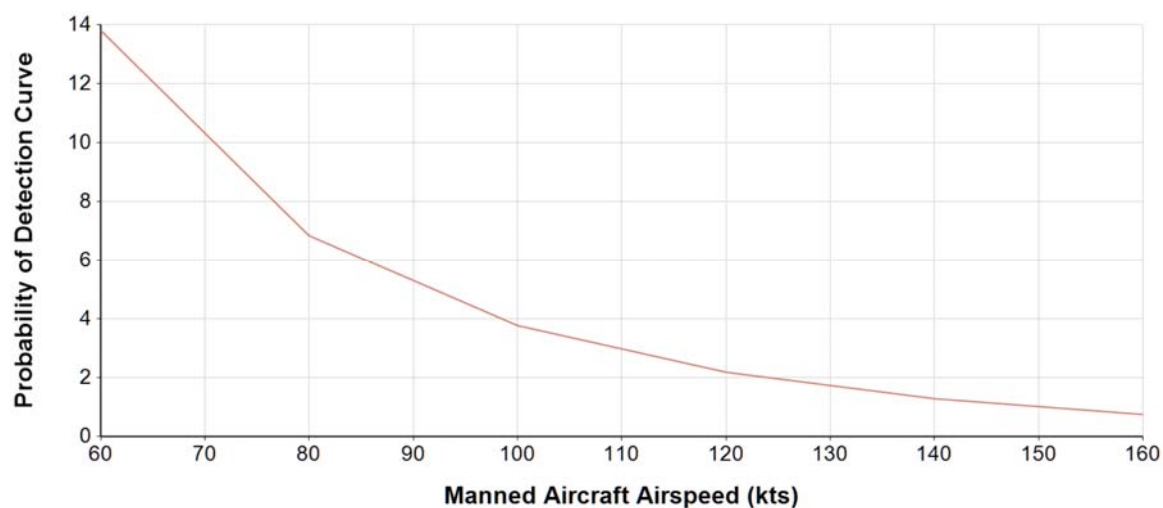


Figure 14. Probability of detection curve: 3.5 square foot target. The probability of detection, in time to avoid a collision, mapped against the manned aircraft speed.

For very large sUAS aircraft with a visible profile of 10.8 square feet, the probability of detection in time to avoid a collision is much greater. Table 19 and Figure 15 show the large visible profile produces model results with mean probabilities of detection over 39% at 60-knots, 23.15% at 80 knots, and 4.7% at 160 knots. Though these mean percentages are noticeably larger than the mean probabilities of detection for smaller hobby-sized sUAS, they are still all less than 50%.

Table 19

Probability of Sighting a 10.8 Square Foot sUAS

Statistic	Airspeed of the Manned Aircraft (in Knots)					
	60	80	100	120	140	160
Mean	39.10%	23.15%	14.52%	9.60%	6.62%	4.70%
Standard Deviation	15.72	9.92	6.31	4.24	3.00	2.21
Minimum	0.00%	0.00%	0.00%	0.00%	0.00%	0.00%
Maximum	100.00%	99.14%	75.65%	47.67%	30.29%	20.11%

Note. This chart depicts the mean percentage and standard deviation of detection probability as computed by the Monte Carlo simulation model when executed with 32,000 trials.

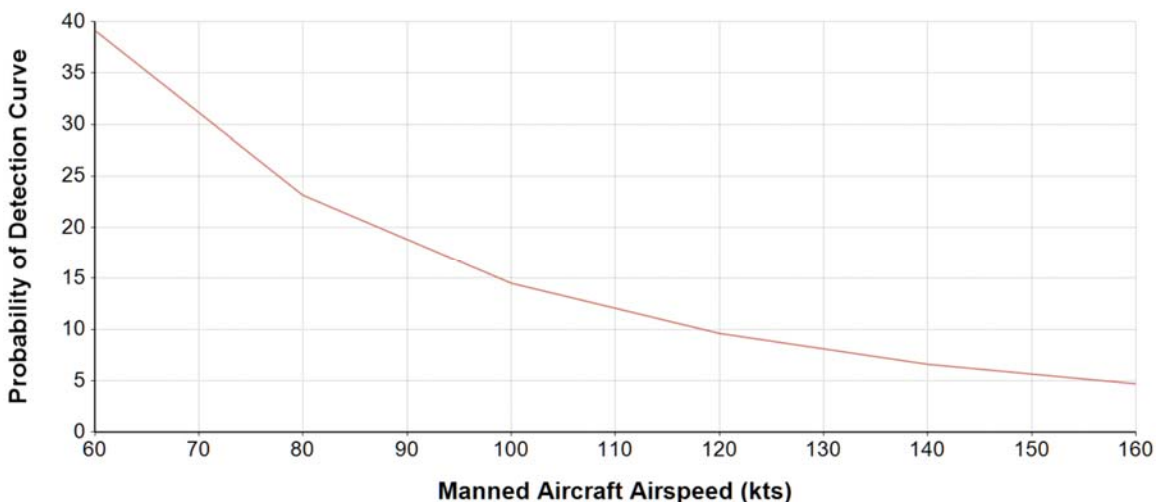


Figure 15. Probability of detection curve: 10.8 square foot target. The probability of detection, in time to avoid a collision, mapped against the manned aircraft speed.

In addition to the low probability of visual detection previously illustrated by the results in Figures 10 through 15, this study showed small UA render very small image sizes on the human eye. These UA targets, when viewed from the minimum distance (r_2), a distance which allows a pilot to have time to react and turn the aircraft away from a collision with the small UA, render image sizes near or below the 1.0 arc minute limit for

human visual acuity. Figure 16 shows the image size of a target UA, at r_2 , for different UA sizes as seen from manned aircraft flying at airspeeds ranging from 60 knots to 160 knots. The human eye cannot generally resolve images below 1.0 arc minutes in size (Hirsch and Curcio, 1989; Howett, 1983) and objects rendering images below 12.0 arc minutes may be difficult to recognize (ATSB, 1991).

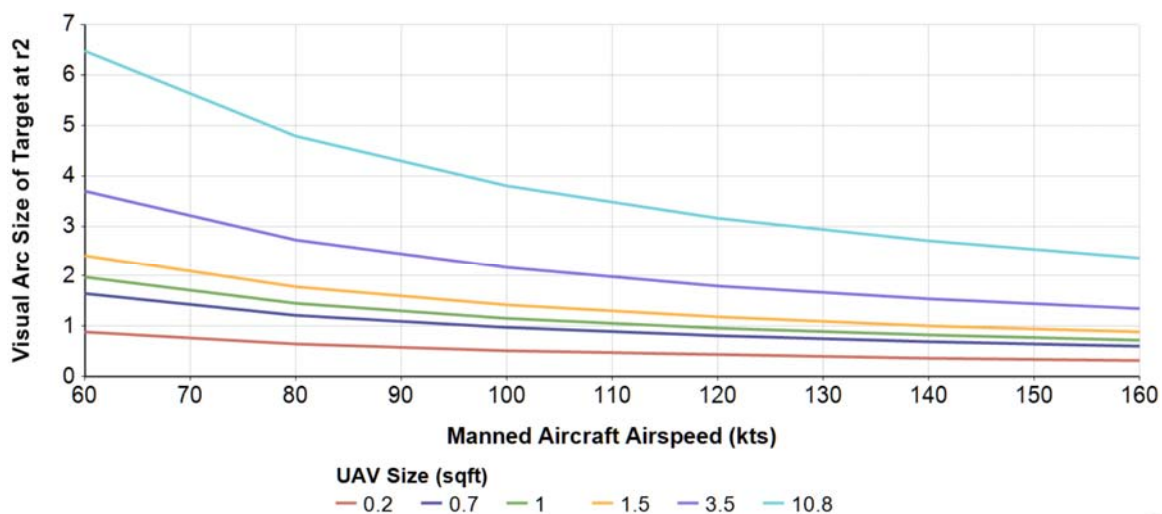


Figure 16. Average arc size of image at latest possible detection time. This graph shows the arc size of the target UA image rendered at the human eye at r_2 —the minimum target detection range allowing the manned aircraft pilot time to see and avoid a target UA.

Since the collision avoidance maneuver requires a minimum of 12.5 seconds, the pilot must detect the small UA 12.5 seconds or more before the two aircraft would collide. The r_2 distance between the two aircraft, 12.5 seconds before they collide, varies from approximately 316 feet to 4,325 feet depending on the rate of closure between the two aircraft. The mean r_2 values in this study ranged from 1,266 feet for aircraft flying at 60 knots to 3,375 feet for aircraft flying at 160 knots.

High Contrast Testing

Typical contrast levels for airborne aircraft targets range from 0.05 to 0.75 for daylight target detection (Poe, 1974). This study treats the contrast of the target UAS against its background as an uncontrollable variable and therefore randomly selects a contrast value for each trial from a normally distributed range of values ranging from 0.05 to 0.75 with a mode of 0.40.

For exploratory purposes, an alternative version of the model used contrast values fixed at very high values of 0.8 and 1.0 to determine how much detection improvement the alternative model would produce if the UA contrast were consistently and unusually high. While the scenario of a consistent, unusually high contrast is unrealistic, this test provides insight regarding the effect of contrast on the visibility of the sUAS aircraft. Table 20 and Figure 17 depict the results from the high contrast testing of a medium-sized sUAS with a visible profile of 1.0 square feet.

Table 20

Probability of Sighting a 1.0 Square Foot sUAS, Contrast = 0.8

Statistic	Airspeed of the Manned Aircraft (in Knots)					
	60	80	100	120	140	160
Mean	7.34%	3.26%	1.58%	0.76%	0.31%	0.07%
Standard Deviation	4.15	1.40	0.61	0.31	0.17	0.09
Minimum	0.94%	0.42%	0.12%	0.00%	0.00%	0.00%
Maximum	91.18%	25.84%	9.18%	4.05%	1.96%	0.96%

Note. This chart depicts the mean percentage and standard deviation of detection probability as computed by the Monte Carlo simulation model when executed with 32,000 trials.

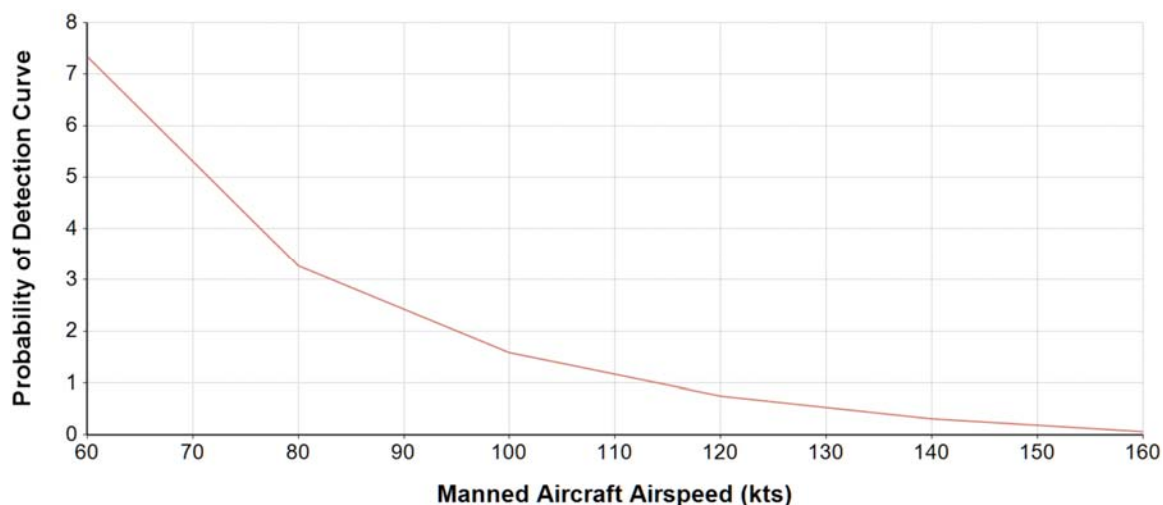


Figure 17. Probability of detection curve: 1.0 square foot target, contrast= 0.8.

An additional run of the high contrast test, with a very high fixed contrast value of 1.00, resulted in increases in the mean probability of detection as shown in Table 21 and Figure 18. The mean probability of detection values increased between 30 percent at 60-knots airspeed for the manned aircraft, to 271 percent at 160-knots airspeed.

Table 21

Probability of Sighting a 1.0 Square Foot sUAS, Contrast = 1.0

Statistic	Airspeed of the Manned Aircraft (in Knots)					
	60	80	100	120	140	160
Mean	9.54%	4.43%	2.27%	1.20%	0.61%	0.26%
Standard Deviation	4.99	1.77	0.79	0.41	0.23	0.14
Minimum	1.44%	0.75%	0.34%	0.10%	0.00%	0.00%
Maximum	95.32%	31.83%	11.86%	5.44%	2.77%	1.47%

Note. This chart depicts the mean percentage and standard deviation of detection probability as computed by the Monte Carlo simulation model when executed with 32,000 trials.

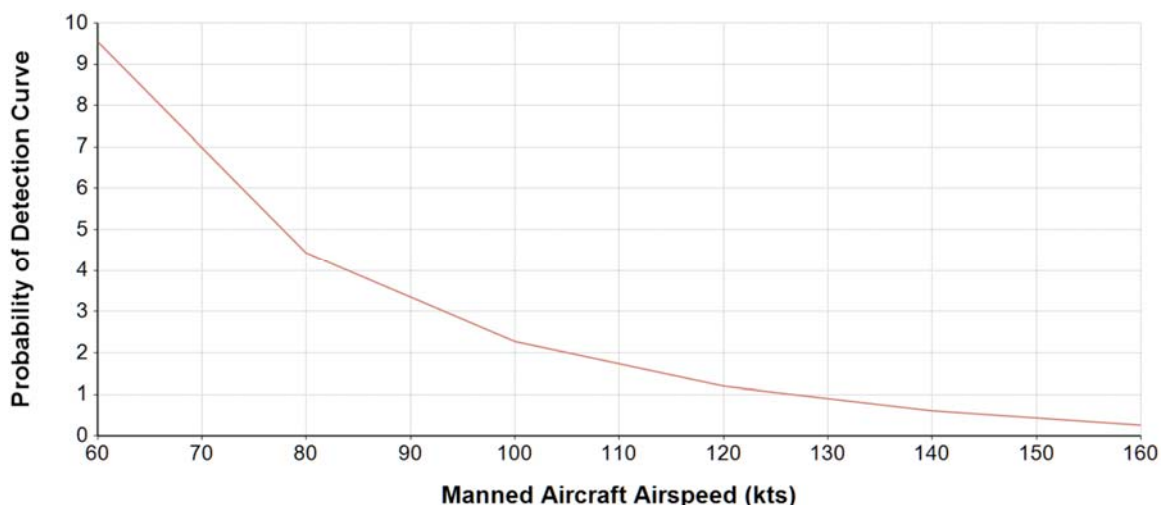


Figure 18. Probability of detection curve: 1.0 square foot target, contrast= 1.0.

While the percentage increase in the mean probability of detection values seems large, the actual probability of detection figures remained low. At 60-knots, the mean probability of detection rose from 7.34 percent to 9.54 percent—still far below 50 percent. At 160-knots, the mean probability of detection rose from 0.07 percent to 0.26 percent. In both cases, at 160-knots, the probability of detection is under one percent.

High contrast testing was limited to values of 0.8 and 1.0. While it is possible to create higher levels of contrast, it requires very intense lighting—greater than 100,000 candelas for higher contrast values in full daylight. Most existing aircraft strobe lights produce only 100 to 400 candelas of light (ATSB, 1991).

Results Summary

The results of this study illustrate the mean probability of seeing a small UA in time to avoid colliding with it ranges from 39 percent to 0.0 percent based on the visible profile area of the target aircraft and the airspeed of the manned aircraft. For smaller-sized UA with a visible profile area of 0.7 to 1.0 square feet, the mean probability of

timely detection varies from 3.0 percent to 0.0 percent depending on the airspeed of the manned aircraft. The target UA image size rendered at the human observer's eye, when the manned aircraft is as close to the UA as possible while still allowing time for evasive action, ranges from 3.00 arc minutes to less than 0.01 arc minutes at the human eye.

Exploratory testing of relatively large-sized small UAS vehicles (near the 55-pound regulatory weight limit) showed the mean probability of detection ranging from 39 percent to five percent depending on closure rates. Consistent, very high contrast testing resulted in mean probability of detection values ranging from 9.5 to 0.0 percent for sUAS with a 1.0 square foot visible profile area. The mean probability of detection was less than 50 percent for all of the practical scenarios tested during this study.

CHAPTER V

DISCUSSION, CONCLUSIONS, AND RECOMMENDATIONS

This chapter discusses the results described in Chapter IV and addresses the research questions from Chapter I. The chapter describes the data produced by the simulation model developed for this study, discusses the analysis of the data, and states the study's conclusions. The chapter also discusses the limitations of the study and provides recommendations for future research.

The purpose of this study was to determine the key variables related to the ability of a manned aircraft pilot to visually detect a small UA with adequate time to maneuver clear of a collision. The study focused on the variables related to the limits of human visual performance since the visual detection of small UA demands visual performance levels close to those physical limits.

The study derived the probability of visual detection of small UA aircraft targets, at a great enough distance to allow a manned aircraft pilot to avoid colliding with the target, from a Monte Carlo simulation model designed for this study. This study extended concepts, from those used in older models developed by Andrews (1991a), Howett (1983), and Poe (1974), to create a simulation model capable of answering the study's research questions concerning small UAS aircraft targets. A Monte Carlo simulation allowed for the treatment of uncontrollable uncertainties, relevant to real-world operating conditions a manned aircraft pilot would face during an encounter with a small UA. These uncertainties included varying target UA contrast values due to changing lighting and background conditions, unknown UA airspeed, and unknown UA course direction. The model created for this study also produced visual arc size output

data to provide information on the arc size of the image rendered in the human eye when the target is 12.5 seconds away from a collision impact. This arc size data provides further insight into the physical issues related to a human pilot in a manned aircraft seeing a small UAV in time to avoid colliding with it. Data found during the literature review provided the information needed to choose constants related to the physiological constraints of human vision and to verify the assumptions used in the incorporation of concepts from Andrews' (1991a) model, which was designed for full-sized aircraft target detection.

Discussion

In order to gather useful data about the probability of visual detection for small UA, it was necessary to define multiple, scenario-driven values for the input variables used by the research model. Since this study focused on exploring the limits of human visual performance in the context of seeing small UAS aircraft, the intent of the chosen scenarios was to represent typical operations as opposed to scenarios in which visual detection would be unusually challenging. The scenarios used for this study all assumed daylight and high-visibility weather conditions. The scenarios also involved aircraft generally departing from or approaching an airport or performing other lower altitude operations. The manned aircraft could range from light sport-category aircraft to airliner-sized aircraft, and the unmanned aircraft could range from recreational hobby sUAS vehicles to large, commercial filming platforms near the upper end of the sUAS weight limit of under 55 pounds.

Combining the graphs in Figures 10 through 15 results in the composite graph shown in Figure 19. Very small sUAS aircraft are unlikely to be visible in time to avoid

a collision. This is true at any of the airspeeds used in this study's scenarios. The mean probability of sighting a sUAS aircraft drops quickly as the sUAS vehicle becomes smaller and as the manned aircraft speed increases. In all cases, the mean probability of detection is less than 50% suggesting, more often than not, manned aircraft pilots will not see a small UA in time to avoid colliding with it.

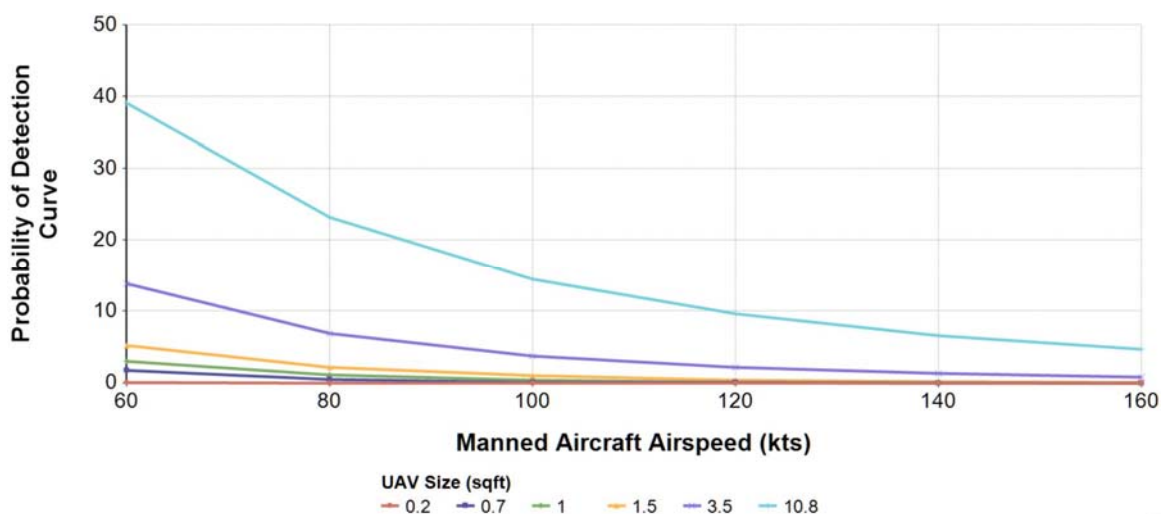


Figure 19. Composite probability of detection graph. This graph combines information from Figures 10 through 15 in Chapter 4. Very large sUAS aircraft have up to a 39 percent probability of timely detection. Smaller hobby and photo-mission UAs are detectable less than 10 percent of the time and are virtually undetectable at higher manned aircraft speeds.

Focused discussion on findings related to the size of the UA, the manned aircraft speed, search time constraints, and contrast follow. Findings related to these variables provide strong insight regarding the relationship between the variables and the probability of visual detection.

sUAS size. The visible profile of the sUAS aircraft has a direct influence on the ability of the human pilot, in a manned aircraft, to see the sUAS vehicle in time to avoid

colliding with it. The mean probability of detecting a very small UA (0.2 square feet of visual profile) is 0.10 percent when the human pilot is flying at 60 knots and 0.00 percent for all faster airspeeds (as shown in Chapter 4, Table 14). Investigation of the internal model variables shows the cause for this low likelihood of visual detection is the minimum acceptable search time for detection. The pilot's search time is constrained between the point at which the image of the UA first becomes big enough to see from a distance, to the point at which there are only 12.5 seconds left to see and avoid the UA. If the distance needed to avoid a collision with the sUAS vehicle is greater than the distance at which the sUAS vehicle first becomes visible, there is no time for the pilot to search for the UA target. In other words, by the time the object is close enough to render at least 1.0 arc minute of image size on the retina, it is already too close to avoid.

Increasing the size of the UA makes it more visible. Table 15 and Table 16 in Chapter 4 show that larger-sized small UA, such the DJI Phantom 3 or the Yuneec Typhoon H, have a better chance of being seen. These common types of sUAS aircraft present visual profiles ranging between 0.7 to 1.0 square feet when they are candidate targets for a collision. The model results show these UA have between a 1.78 percent to a 3.03 percent chance of being seen when the manned aircraft is flying at 60 knots. The same tables show the mean probability of detection drops below 1.00 percent at manned aircraft speeds of 100 knots.

Very large-sized, small UA, encroaching on the upper allowable weight limit for sUAS aircraft, can have a 39.10 percent chance of being detected if the manned aircraft is only flying at 60 knots. At 160 knots, the mean probability of detection drops to 4.70 percent. Increasing the size of the UA's visible profile increases the probability of visual

detection but not enough to achieve reliable or even frequent detection. Even the large sUAS aircraft, near the maximum allowable weight limit of less than 55 pounds, only has a 39.10 percent to 4.70 percent chance of being seen. Exploratory testing of the model revealed the visible profile of the target UA would need to approach 100 square feet to be reliably spotted in time to avoid a collision at low to medium airspeeds (see Table 22). Such an UA would need to present a horizontal profile similar to a Piper PA28 when viewed from the side. This is unrealistic because the weight of the UA would likely exceed the less than 55 pound regulatory constraint for sUAS aircraft. It would also be cost-prohibitive for most recreational and low-cost commercial operators.

Table 22

Probability of Sighting a 100 Square Foot sUAS

Statistic	Airspeed of the Manned Aircraft (in Knots)					
	60	80	100	120	140	160
Mean	96.81%	89.84%	79.03%	67.04%	55.90%	46.38%
Standard Deviation	7.43	11.64	14.42	15.16	14.49	13.18
Minimum	0.00%	0.00%	0.00%	0.00%	0.00%	0.00%
Maximum	100.0%	100.0%	100.0%	99.82%	97.83%	92.19%

Note. This chart depicts the mean percentage and standard deviation of detection probability computed for an unrealistically large sUAS aircraft presenting at 100 square foot visible profile.

Manned aircraft airspeed. Figures 10 through 18 in Chapter 4 all illustrate the effect the speed of the manned aircraft has on the probability of detection. As the speed of the manned aircraft increases, the minimum range from which the target UA must be spotted in order to leave enough time to avoid a collision also increases. The increased minimum range has two effects. It causes the rendered image size of the UA to be smaller on the retina, in many cases challenging the one arc minute resolution limit of the

human eye (as shown in Figure 16 in Chapter 4), and when combined with the increased closure rate between the aircraft, it shortens the amount of time available for the search activity (as shown in Figure 20). These both reduce the probability of sighting the small UA in time to avoid colliding with it. While slowing the manned aircraft's airspeed may be an option for some general aviation aircraft, for business jets, larger cabin-class airplanes, and airliners, flying at slow speeds of 80 knots or less is not an option.

Search time. Search time is not one of the explicit input variables for the model used for this study. However, allowable search time has an impact on the human pilot's probability of detecting a small UA from a manned aircraft. The search time starts once the manned aircraft has closed in on the small UA enough so that it becomes theoretically visible. The UA becomes theoretically visible when it renders an image of at least 1.0 arc minutes of size on the retina. The allowable search time ends 12.5 seconds before collision so the human pilot has enough time to sense and react to maneuver the manned aircraft away from a collision. Figure 20 depicts the relative differences in available search time, in seconds, given a specific sUAS visible profile size (or cross section) and given manned aircraft airspeed.

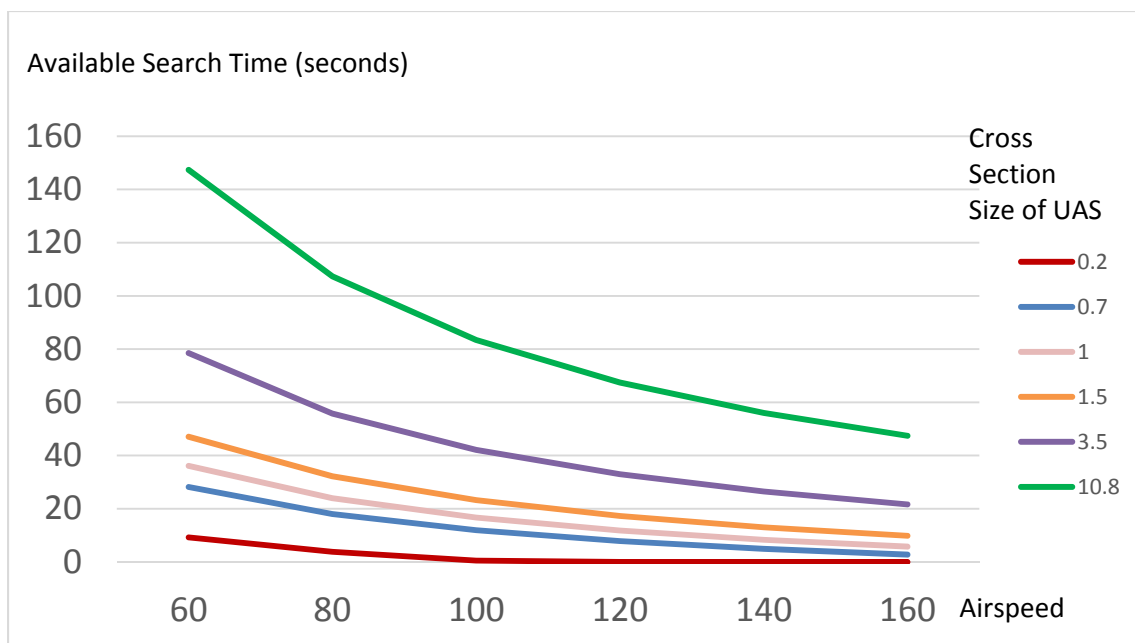


Figure 20. Available search time. For a given airspeed, ranging from 60 to 160 knots, the search time available to the manned aircraft’s pilot ranges from a maximum of 147 seconds to a low of 0.0 seconds, assuming excellent target contrast. The search time is reduced if the target contrast is reduced.

The available search time for a 0.2 square foot UA is small—ranging from 9.3 seconds to 0.0 seconds at high airspeeds where the UA does not become visible until the 12.5-second collision-avoidance maneuvering deadline has already passed. Since it is not possible for the pilot or the UAS operator to change the available search time, the purpose of this section is only to illustrate the short time the human pilot has for the task of detecting small UA, especially when flying faster aircraft.

sUAS contrast. The effect of contrast on the probability of detection model is that it modifies the apparent size of the UA visible profile. In other words, if the visible profile area of the target UA is 1.0 square feet and the contrast ratio is 0.5, then the apparent size of the UA becomes $0.5 \times 1.0 = 0.5$ square feet. When the contrast is 0.5, the size of the UA would need to double in order for it to be just as visible as the UA

would be given a high contrast of 1.0 with its background (Andrews, 1991b). Poe (1974) says the contrast of an airborne target is subject to “substantial variation” (p. 11) over the course of its flight. Poe further states that contrast values of 0.05 to 0.75 are common. As shown in Figure 7, this study used contrast values ranging from 0.05 to 0.75 selected from a normally distributed population at random. The mean for this population was 0.40, and the standard deviation was 0.13. Each of the 32,000 trial runs for each scenario drew a random number for the contrast ratio from this population to simulate the uncertainty and the varied nature of target versus background contrast.

As an exploratory test to see how much the mean probability of detection would improve if the target contrast were improved, testing was repeated with the UA target contrast value set as a constant value: 1.00 for a small UA with a 1.0 square foot visible profile. Locking the contrast ratio at 1.00 for a consistently high contrast target improved the mean probability of detection by 30 percent at 60-knots and by 271 percent at 160-knots. However, the improved probability of detection was still only 9.54 percent at 60-knots and 0.26 percent at 160-knots. Though the high contrast test resulted in a large 271 percent improvement in the probability of detection for manned aircraft flying at 160 knots, the improvement did not make a practical difference since the probability of detection remained well under one percent. Even with a consistent, high contrast value for the UA target against its background, manned aircraft pilots are unlikely to spot the small UA in time to avoid colliding with it.

If it were possible to create an extraordinary contrast ratio of 100.0 for the small UA target against its background, a small UA with a 1.0 square foot profile would become much more visible. This extreme contrast would be 100 times greater than the

high contrast test described in the previous paragraph. Extreme contrast modeling, at a contrast ratio of 100.0, revealed the mean probability of detection rises well above 50 percent to nearly 100 percent for aircraft operating at slower airspeeds (see Figure 21). An augmented contrast of this magnitude would give the UA an inherent level of visibility similar to a full-sized Piper PA28 aircraft with an excellent contrast of 1.0.

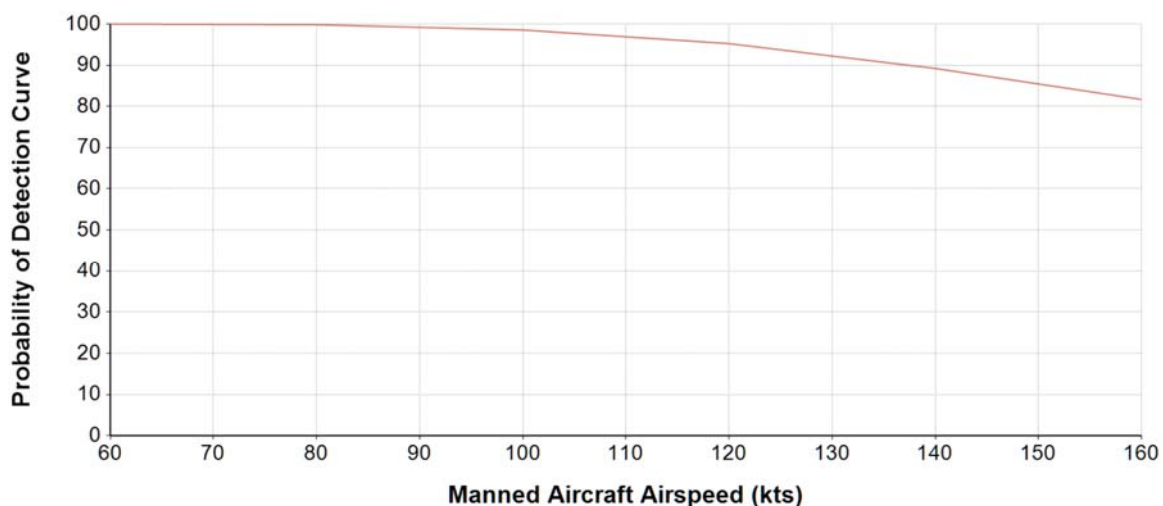


Figure 21. Extreme contrast test – contrast = 100. When the contrast ratio is increased to an extreme value of 100.0, the probability of detection for a small UA with 1.0 square feet of visible profile rises to nearly 100 percent at slower manned aircraft airspeeds and is above 80 percent at 160 knot airspeeds.

To achieve a contrast ratio of 100.0 against a fair weather, daytime sky, the small UA would need to emit 101,000 foot-lamberts of luminance. This finding is similar to anti-collision light findings published by the Australian Transportation Safety Bureau (ATSB, 1991). Chisum (1977) recommended adding light sources capable of emitting 200,00 to 300,000 foot lamberts to produce a solar-like glare to make small targets more visible in full daylight conditions on a clear day. The ATSB states most existing aircraft

strobe lights only produce a small fraction of the light intensity required to create detection in daylight conditions (ATSB, 1991).

Conclusions

This study explored the relationship of five key variables on the probability of a human pilot in a manned aircraft, visually detecting a small UA in time to avoid colliding with it, using a Monte Carlo simulation model. Two of the five variables, UA visible profile size and unmanned aircraft speed, are controllable inputs to the model. The other three variables, UA airspeed, UA relative heading, and UA contrast relative to its background, are uncontrollable values, which the Monte Carlo simulation model selected at random from pre-defined populations of possible values.

Figure 19 illustrates the overall conclusion that human pilots are unlikely to spot a small UA in time to avoid colliding with it. At slower airspeeds, the mean probability of detection is higher, though the probability of detection is far below 50 percent. At faster airspeeds, the probability of detection is zero for faster moving manned aircraft. The conclusions for each of the three research questions follow next.

Research Question 1: What key variables in the Andrews probability of detection model, related to the physical features of a small UAS or the manner in which pilots operate their manned aircraft, limit a manned aircraft pilot's ability to see a small UAV in time to avoid colliding with it?

The key variables limiting the pilot's ability to see a small UAV in time to avoid colliding with it are the visible profile area or size of the UAV and the speed at which the manned aircraft moves. The speed at which the manned aircraft moves determines the minimum distance from which the pilot must be able to spot the small UA. The literature

is consistent about the use of 1.0 arc minutes, as the minimum size of a visual feature one should expect a person with normal 20/20 vision to see (Andrews, 1991a; Hirsch and Curcio, 1989; Howett, 1984). Given the speeds at which typical general aviation and commercial airliner aircraft move, pilots must be able to spot small UA from thousands of feet away. Viewing a small UA with a visual profile of one or two square feet, or less, from thousands of feet away renders a tiny image on the human retina close to the 1.0 arc minute resolution limit. Other variables, such as contrast, atmospheric visibility, and perspective angle contribute to the overall solution but are less influential due to the distance between the UA and the observer. The distance between the UA and the observer is too short to allow atmospheric visibility to be influential in fair weather conditions, and the distance is too great for the observation perspective to be other than horizontal (or head-on). Changing the contrast affects the apparent size of the image but the image is still very small given the required viewing distance of multiple thousands of feet. This study has demonstrated the adjustment of variable inputs to the model helps small UA be more visible but not enough to be detectable most of the time.

Research Question 2: Given different scenarios determined by the controllable input variables, what is the probability a manned aircraft pilot will see a small UAV, in time to avoid colliding with it?

The probability of a manned aircraft pilot visually detecting a small UA in time to avoid colliding with it is very low as shown in Figure 19. Even when the small UA is physically very large, at the upper end of the allowable weight limit for small UA, the probability of detection is well under 50 percent at slow airspeeds. For the more common hobby and lower-cost commercial UA, ranging in visible profile area size from 0.7 to 1.0

square feet, the probability of visual detection in time to avoid a collision is under four percent down to zero percent when the manned aircraft is moving at airliner approach airspeeds above 120 knots.

Research Question 3: What simulation model parameters, if changed, would improve the manned aircraft pilot's ability to see and avoid a small UAV?

Exploratory testing, as described in Chapter 4, resulted in improvement in the manned aircraft pilot's ability to see and avoid small UAs when the contrast ratio of the small UA target versus its background was consistently higher. Exploratory testing, described in the discussion section of this chapter, determined the use of extreme contrast values, made possible by very intense lighting, could make the probability of detection for small 1.0 square foot UA aircraft rise well above the 80 percent level. However, the technology for producing and powering such an intense emission of light is not generally available in a form suitable for small UA weighing only one to eight pounds. Increasing the visible profile area of the small UA also helped raise the probability of detection. However, the change was not enough to make the probability of detection rise above 50 percent at the faster manned aircraft airspeeds. The exploratory testing found no other options for improvement.

Methodology and data. This study demonstrated a useful approach for the extension of Andrews' (1991a) Air-to-Air Visual Acquisition model in the presence of varying input value due to uncertainty. The use of a Monte Carlo simulation enabled the model to function and to produce realistic results despite the range of possible values for UA airspeed, relative heading, and changing UA target contrast against its background

due to the variety of possible illumination levels from both the sky and reflected light from the ground.

There were additional variables the model could have incorporated into its calculations. Given the tiny sizes of the target images rendered on the retina, most of those other variables became secondary or irrelevant. These included color of the target, clarity of the atmosphere, and orientation of the UA in terms of the visual profile it presented to the observer. The visual profile would be more significant for fixed wing sUAS aircraft, and this will be discussed in the recommendations section. However, the methodology and the model developed for this study will work well for the study of fixed wing aircraft.

The methodology and the model developed for this study can be applied to a variety of future visual search research studies since it is flexible, easily adaptable, and capable of handling uncertainty in its input values. If the nature of search task is altered, however, human subject testing will be required to determine the correct value of β , the search effectiveness constant, for use in the new application.

Validity. The results from this model were found to be consistent with the results described by other studies on the probability of visual detection for airborne targets. Greening (1976) examined multiple models for the prediction of visual target acquisition where the background contained more ground features than sky features. Based on Greening's findings relating target subtense, or visual angle image size, mapped to the probability of detection, all of the results produced by this study should render a finding of less than 50 percent probability of detection. Greening compared several visual detection models which all came to the same conclusion.

Chisum's (1977) nomographs suggest visual detection of a 1.0 square foot target should be possible at distances ranging from 1,200 feet to approximately 2,400 feet. While Chisum used a different type of chart to convey the results of her analysis of airborne target visibility, the distance numbers are comparable—though Chisum's predictions are even less favorable for target detection of small airborne objects.

Poe's (1974) studies of visual detection of aircraft by ground observers had higher rates of detection. However, the targets in Poe's studies were full-sized manned aircraft instead of small UAs, and the observers reported augmentation of their search efforts by use of smoke trails and noise signatures. Therefore, Poe's results are not directly comparable.

The low probability of detection is also consistent with Howett's (1983) recommendations for the minimum size of lettering on signs for readability. In all cases, the visual arc size of the UA at the minimum range point (the point at which visual detection must have occurred in order for the pilot to have time to avoid a collision) ranges from 0.3 arc minutes to 6.5 arc minutes for the very large UA (10.8 square feet) in the 60-knot airspeed scenario, as shown in Figure 16 in Chapter 4. Given the 1.0 square foot UA size, the visual arc size at the minimum range point varies from 0.7 to 2.0 arc minutes rendering a poor target for recognition.

The generally consistent alignment of this study's results to results from other studies identified in the literature suggests the model is valid. Loffi, Wallace, Jacob, and Dunlap (2016) concluded the general aviation pilots in their study could have time to avoid a larger-sized Anaconda fixed-wing UAV when searching from a Cessna Skyhawk flying at 100 knots; however, the general aviation pilots were unlikely to have time to

avoid a collision with the smaller, quad-copter UAV used in their study. Since the pilots in the Loffi et al. study were aware there would be a UAV encounter in their path of flight, they were pre-alerted. Even with the larger Anaconda UA used in the Loffi et al. (2016) study, the available reaction time was 15.42 seconds (p. 23) which provides the pilot with less than three seconds of time before the 12.5 second reaction time limit, described by the FAA (FAA, 2016c), is reached. Though statistical comparisons of model results are not possible because of the different structure of the output data and the different sizes of the targets used in the other studies, no inconsistencies were found between this study's results and the results of other studies found in the literature.

Practical implications. This study has contributed practical, data-driven knowledge to the question of small UA visibility and the degree to which the human pilots in manned aircraft can be expected to visually detect and avoid small UA in flight. This is the first study to specifically relate small UA visibility to the physical limits of the human eye using a mathematical modeling tool that addresses the multitude of potential contrast values between the small UA and its background as they operate in different regions under different weather and lighting conditions. This study indicates pilots of manned aircraft are unlikely to see a small UA in time to avoid a collision. Though pilots have described the task of visually detecting small UA as difficult (Loffi, et al., 2016), the explanation of why the visual detection task is so difficult has not been described in-depth. This study demonstrates why it is important for small UAS aircraft to have the intelligence and ability to detect and avoid manned aircraft—because manned aircraft pilots are unable to see and avoid the small UAS aircraft.

This study also explored the extreme conditions required to make small UA targets visually detectable in time to avoid a collision, most of the time. Though the results of this study's exploratory testing found the requirements to make small UA reliably visible to the human pilot's eyes impractical, the model can help future researchers with other questions related to small UA visual detection and visibility. Additionally, since advancement in electronic technology will produce ADS-B and other technologies with lower, more practical payload and power demands, the industry focus should be on the deployment of those types of solutions as soon as possible.

Theoretical implications. This study has also built upon previously proven air-to-air target acquisition models to create a new, useful model for small airborne target detection, in cases where researchers seek to understand the probability of visual detection, when uncertainty exists for one or more input values. The study connects previously conducted physiological research on the human eye with mathematical calculations of the target image size, from the observer's vantage point, to explain how the visual detection of small UA pushes the limits of human visual acuity. The study demonstrates the utility of using a Monte Carlo simulation as an approach for handling uncertainty in the values of important input parameters and provides researchers with a means of describing the range of possible outcomes. Describing the potential outcomes in this manner allows the study to provide useful answers while simultaneously acknowledging the results of specific, actual sUAS encounters may occasionally be different due to the uncertainties involved.

Additionally, the study provides more specific insight regarding the effect of contrast, aircraft size, and visibility-enhancing features related to the visual detection of

very small aircraft targets. Many of the considerations that apply to large aircraft to enhance their visual detectability, don't apply well to sUAS aircraft because the image rendered on the eye's retina is so small. While color, contrast, and increases in size generally make a difference for larger aircraft, when searching for sUAS aircraft at a distance great enough to maneuver clear of a collision, even large improvements in contrast, distinctive coloration, and increased aircraft visual profile sizes result in visual detection probabilities that remain very small because the image size is so small to begin with. The study emphasizes the unique visual detection dynamics related to small targets that remain near the threshold of human visual acuity throughout the search time interval. Unlike manned aircraft, these sUAS aircraft target images rarely grow large enough to be seen in time to allow pilots to avoid colliding with them.

Limitations. The Monte Carlo simulation model developed for this study draws upon concepts from the Andrews (1991a) aircraft visual acquisition model and adds extensions to create a new model appropriate for small UAS aircraft detection and uncertainty in multiple input variable values. The model uses Andrews' β constant to account for many of the human factors considerations related to pilot search effectiveness. $\beta=17,000$ was determined experimentally by Andrews (1991a) for un-alerted, normal search and low workload. The assumptions tied to the β value of 17,000, as described by Andrews (1991a), apply well to the scenarios in this study. Though the results of the model are consistent with the results inferred by other models for visual object recognition, the accuracy of the model used for this study is dependent upon the quality of Andrews' research in determining the value of β .

This study also modeled contrast uncertainty between the sUAS target and its background, using a normal distribution of values for the range of contrast values described by Poe (1974). Poe described the difficulty of determining target contrast values for use in models such as this. Poe states concerns about the effect of contrast on the detection of airborne targets. This study found even high contrast target values still produced low probabilities of detection; however, additional data regarding actual contrast values would add value to the model's predictions for future studies related to improving the visibility of small UA.

In addition to the study's limited access to actual contrast data, this study did not explicitly model the effects of background clutter and target confusion related to background features with similar shape and contrast attributes as the target. Background clutter and feature similarity create confusion and increased search time requirements (Toet, 2010). Though the model does not specifically address the effects of background clutter and feature similarity, future incorporation of these attributes into the model will only reduce the probability of target detection further.

Recommendations

The results of this study demonstrate it is unlikely a pilot of a manned aircraft will consistently see and have time to avoid colliding with a small UA. Therefore, regulators and educators should inform pilots of manned aircraft about the limitations of their ability to visually detect small UA in time to avoid colliding with them. If a manned aircraft pilot sees a small UA, the pilot should immediately report the presence of the UA to an air traffic control facility so other pilots can be warned and law enforcement officials can be dispatched to take action.

Since manned aircraft pilots cannot be expected to see and avoid small UAS aircraft, regulators and manufacturers must give more attention and greater urgency to the deployment of technology-based solutions to keep small UAS aircraft away from manned aircraft. Given the increasing rate of small UA sales and the simultaneous, albeit slower, increase in the rate of UAS target sightings, there is likely a growing collision hazard forming as long as new sUAS products do not have the technology needed to ensure they will remain clear of manned aircraft. Additionally, consideration should be given to technologies on sUAS products that enable warning information to be made available to manned aircraft pilots in a manner similar to existing traffic information service, ADS-B, or traffic collision avoidance systems.

Educational programs are essential for sUAS operators, and the educational programs in place today appear to be effective, to some degree, based on the fact that the number of reported UAS sightings per month is rising less rapidly than the number of sUAS aircraft sold. However, the number of UAS sighting reports continues to rise (FAA, 2017b; Volpe, 2017). Therefore, education alone does not appear to be a complete solution to the sUAS aircraft collision hazard.

This study revealed aircraft with larger visible profile areas are easier to visually detect. Loffi, et al. (2016) conducted visual detection testing with a fixed-wing Anaconda UAS and found it was both easier to see and it was visually detected in time to avoid a collision. Though the Loffi et al. study pre-alerted the manned aircraft pilots to the presence of small UA operating in the vicinity, giving the pilots in the study an unusual advantage in the visual detection task, the results of their study confirmed the concept that larger sUAS aircraft are easier to visually detect than smaller sUAS aircraft.

This suggests there may be safety advantages available if sUAS aircraft are designed to present larger visual profiles to increase their visibility from larger distances. This could be accomplished through the addition of side panels to increase the visual profile area of the aircraft. Such panels might not be aerodynamically reasonable or sound.

Alternatively, a smoke discharge system could make the small UA more visible, though such a system may not be reasonable from a payload perspective. Chisum (1977) suggested the addition of mirror-like reflectors to reflect sunlight off of the target UA might increase the contrast of the vehicle to make it more visible from large distances.

Future research opportunities. Chapter 1 of this dissertation describes a number of limitations and delimitations for this study. This section of Chapter 5 describes opportunities for future research to further explore both the capabilities of the model and the options for improving the accuracy of the model's predictions.

The model uses an important constant referred to as β to represent the search effectiveness of the manned aircraft pilot(s). Andrews (1991a) determined several values for β based on data gathered from actual flight tests. While the results of this study appear to be consistent with the results of other visual detection studies, additional confidence could be obtained through flight testing with human pilots, in a controlled data gathering experiment designed to validate or refine the β constant for the model.

Additional testing could be conducted to refine the range of contrast values used for the apparent contrast distribution in the Monte Carlo model. The normal distribution of contrast values used in the model for this study provides contrast values within the range described by Poe (1974). However, the use of photometric sensors and data gathered from flight testing experiments would potentially provide a more accurate

model. Photometric testing of fixed wing vs. multi-rotor sUAS aircraft would also provide useful information on the detectability of small fixed wing UAVs. When this comparative testing is conducted, an additional uncontrolled variable should be added to account for the uncertainty of the fixed wing UAV's attitude since its attitude will alter its visible profile area or apparent size. It should be noted that high contrast testing of the model failed to improve sUAS visibility enough to result in a different conclusion from what is stated in this chapter.

The use of photometric data gathering to more accurately define the apparent contrast distribution used by the Monte Carlo simulation, could also gather the data needed to enable repurposing of the model to predict sUAS visibility from the ground by a UAS observer or operator. It is recommended that consideration be given to the use of this model as a means to forecast the probability of visual tracking of sUAS aircraft by the UAS operator and/or observer on the ground.

The final recommendation of this study is to explore the use of more sophisticated algorithms or methods for assessing the effect of background clutter, and target confusion due to similarly shaped objects in the background, on search effectiveness and search time. There are existing studies on the effects of background clutter and target confusion; however, none of the studies could be directly applied to the model in this study without extensive human subject testing and the collection of wide variety of background scenes, due to a wide range of possibilities applicable to the detection of small UA from an airplane. The availability of such data would enable the model to be more precise and accurate in its predictions.

REFERENCES

- Academy of Model Aeronautics (AMA). (2016). *An analysis of the FAA's March 2016 UAS sightings*. Retrieved from <http://amablog.modelaircraft.org/amagov/files/2016/06/AMA-Analysis-FINAL-6-1-16.pdf>
- Akerman, III, A. & Kinzly, R. E. (1979). Predicting aircraft visibility. *Human Factors*, 21(3), 277-291. Retrieved from <http://hfs.sagepub.com.ezproxy.libproxy.db.erau.edu/content/21/3/277.full.pdf>
- Anderson, D. R., Sweeney, D. J., Williams, T. A., Camm, J. D., & Martin, K. (2012). *An introduction to management science: Quantitative approaches to decision making*. Mason, OH: South-Western Cengage Learning.
- Andrews, J. W. (1984). *Air-to-air visual acquisition performance with TCAS II*. (MIT Lincoln Laboratory Report No. ATC-130). Retrieved from https://www.ll.mit.edu/mission/aviation/publications/publication-files/atc-reports/Andrews_1984_ATC-130_WW-15318.pdf
- Andrews, J. W. (1991a). *Air-to-air visual acquisition handbook*. (MIT Lincoln Laboratory Report No. ATC-151). Retrieved from https://www.ll.mit.edu/mission/aviation/publications/publication-files/atc-reports/Andrews_1991_ATC-151_WW-15318.pdf
- Andrews, J. W. (1991b). *Unalerted air-to-air visual acquisition* (MIT Lincoln Laboratory Report No. ATC-152). Retrieved from https://www.ll.mit.edu/mission/aviation/publications/publication-files/atc-reports/Andrews_1991_ATC-152_WW-15318.pdf

- Australian Transportation Safety Bureau (ATSB). (1991). *Midair collisions: Limitations of the see-and-avoid concept*. (Australian Transportation Safety Bureau report, ISBN 0 642 16089 9). Retrieved from https://www.atsb.gov.au/media/4050593/see_and_avoid_report_print.pdf
- Australian Maritime Safety Authority (AMSA). (2016). *National search and rescue manual*. Canberra, Australia: AMSA. Retrieved from <https://natsar.amsa.gov.au/documents/NATSAR-Manual/2016AustralianNationalSARManual.pdf>
- Boeing Aircraft. (2016). *FAA reference code and approach speeds for Boeing aircraft, 30 March 2016*. Retrieved from <http://www.boeing.com/assets/pdf/commercial/airports/faqs/arcandapproachspeeds.pdf>
- Campbell, P. (2012, October). *Challenges to using ground based sense and avoid (GBSAA) for UAS operations*. Paper presented at the 2012 IEEE/AIAA 31st Digital Avionics Systems Conference (DASC), Williamsburg, VA. Retrieved from <http://ieeexplore.ieee.org.ezproxy.libproxy.db.erau.edu/document/6383116/>
- Chang, H., & Zhang, J. (2006). Evaluation of human detection performance using target structure similarity clutter metrics. *Optical Engineering*, 45(9), 096404-1-7. Retrieved from <http://opticalengineering.spiedigitallibrary.org.ezproxy.libproxy.db.erau.edu/article.aspx?articleid=1076970>
- Chisum, G. T. (1977). *Prediction of airborne target detection*. (Naval Air Development Center Report NADC-77102-40). Retrieved from <http://www.dtic.mil/cgi-bin/GetTRDoc?Location=U2&doc=GetTRDoc.pdf&AD=ADA041428>

- Cohn, T. E. (1981). Absolute threshold: analysis in terms of uncertainty. *Journal of the Optical Society of America*, 71(6), 783-785. Retrieved from <https://www.osapublishing.org/josa/issue.cfm?volume=71&issue=6>
- Consiglio, M. C., Chamberlain, J. P., Muñoz, C. A., & Hoffler, K. D. (2012, September). *Concept of integration for UAS operations in the NAS* (NASA Technical Report: NF1676L-13199). Report presented at ICAS 2012 – 28th Congress of the International Council of the Aeronautical Sciences, Brisbane, Australia. Retrieved from <http://ntrs.nasa.gov/search.jsp?R=20120015770>
- De Veaux, R. D., Velleman, P. F., & Bock, D. E. (2012). *Stats: Data and models*. Boston, MA: Pearson Education, Inc.
- Doll, T. J., McWhorter, S. W., Wasilewski, A. A., & Schmieder, D. E. (1998). Robust, sensor-independent target detection and recognition based on computational models of human vision. *Optical Engineering*, 37(7), 2006-2021. doi:10.1117/1.601898
- Erickson, R. A., & Burge, C. J. (1974). *Modeling air-to-air visual search*. (Naval Weapons Center Report NWC TP 5709). Retrieved from www.dtic.mil/dtic/tr/fulltext/u2/b001148.pdf
- Esler, D. (2015, September 25). What a business aviation flight department needs to know about UAS. *Aviation Week & Space Technology*. Retrieved from <http://aviationweek.com/bca/what-business-aviation-flight-department-needs-know-about-uas>

- Embry-Riddle Aeronautical University (ERAU). (2016). *Cessna Skyhawk: Standard operating procedures and maneuvers, Revision 3*. Daytona Beach, FL: Embry-Riddle Aeronautical University.
- Federal Aviation Administration (FAA). (2013). *Integration of civil unmanned aircraft systems (UAS) in the National Airspace System (NAS) roadmap*. FAA news release. Retrieved from http://www.faa.gov/uas/media/uas_roadmap_2013.pdf
- Federal Aviation Administration (FAA). (2016a). *FAA releases updated UAS sighting reports*. Retrieved from https://www.faa.gov/news/updates/?newsId=85229&omniRss=news_updatesAoc&cid=101_N_U
- Federal Aviation Administration (FAA). (2016b). *FAA aerospace forecast: Fiscal years 2016-2036*. Retrieved from http://www.faa.gov/data_research/aviation/aerospace_forecasts/media/FY2016-36_FAA_Aerospace_Forecast.pdf
- Federal Aviation Administration (FAA). (2016c). *Pilot's role in collision avoidance (AC No. 90-48D)*. Retrieved from https://www.faa.gov/documentLibrary/media/Advisory_Circular/AC_90-48D_CHG_1.pdf
- Federal Aviation Administration (FAA). (2017a). *FAA releases updated drone sighting reports*. Retrieved from <https://www.faa.gov/news/updates/?newsId=87565>
- Federal Aviation Administration (FAA). (2017b). *UAS sightings report*. Retrieved from https://www.faa.gov/UAS/resources/uas_sightings_report/
- Fisher, J. (2017, February 21). The best drones of 2017. *PCMag*. Retrieved from <http://www.pcmag.com/roundup/337251/the-best-drones>
- Frew, E. W., & Brown, T. X. (2008). Airborne communications networks for small unmanned aircraft systems. *Proceedings of the IEEE*, 96(12), 2008-2027.

Retrieved from <http://ieeexplore.ieee.org.ezproxy.libproxy.db.erau.edu/stamp/stamp.jsp?tp=&arnumber=4745652>

Frisby, J. P., & Stone, J. V. (2010). *Seeing: The computational approach to biological vision*. Cambridge, MA: The MIT Press.

Gettinger, D., & Michel, A. H. (2015). *Drone sightings and close encounters: An analysis*. Annondale-on-Hudson, NY: Center for the Study of the Drone at Bard College. Retrieved from <http://dronecenter.bard.edu/files/2015/12/12-11-Drone-Sightings-and-Close-Encounters.pdf>

Gibb, R., Gray, R., & Scharff, L. (2010). *Aviation visual perception: Research, misperception, and mishaps*. Burlington, VT: Ashgate Publishing.

Google.com. (2017, March). *The best drones reviews of March 2017 – we rate the top quadcopters*. Retrieved from <https://sites.google.com/site/bestdronesreview/>

Graham, W. (1989). *See and avoid/cockpit visibility*. (FAA Technical Center Report. DOT/FAA/CT-TN89/18). Atlantic City, NJ: Retrieved from <http://www.dtic.mil/dtic/tr/fulltext/u2/a214214.pdf>

Greening, C. P. (1976). Mathematical modeling of air-to-ground target acquisition. *Human Factors*, 18(2), 111-148. Retrieved from <http://hfs.sagepub.com.ezproxy.libproxy.db.erau.edu/content/18/2/111>

Hirsch, J., & Curcio, C. A. (1989). The spatial resolution capacity of human foveal retina. *Vision Research Journal*, 29(9), 1095-1101. Retrieved from http://fmri.org/publications/Hirsch_Curcio_Spatioal_resolution.pdf

Howett, G. L. (1983). *Size of letters required for visibility as a function of viewing distance and observer visual acuity* (National Bureau of Standards Technical Note

- 1180). Washington, DC: Government Printing Office. Retrieved from <https://www.gpo.gov/fdsys/pkg/GOVPUB-C13-ff8dc22d75e66f29ebdb2bb2085ee683/pdf/GOVPUB-C13-ff8dc22d75e66f29ebdb2bb2085ee683.pdf>
- Hoyt, C. (1941). Test reliability estimated by analysis of variance. *Psychometrika*, 6(3), 153-160.
- Itti, L., & Koch, C. (1999). A saliency-based search mechanism for overt and covert shifts of visual attention. *Vision Research*, 40(2000), 1489-1506. Retrieved from <http://www.sciencedirect.com.ezproxy.libproxy.db.erau.edu/science/article/pii/S0042698999001637>
- Jones, D. B., Freitag, M., & Collyer, S. C. (1974). D. C. Middledauff (Ed.). *Air-to-ground target acquisition source book: A review of the literature*. Orlando, FL: Martin Marietta Corp. Retrieved from <http://www.dtic.mil/dtic/tr/fulltext/u2/a015079.pdf>
- Lai, J., Mejias, L., & Ford, J. J. (2011). Airborne vision-based collision-detection system. *Journal of Field Robotics*, 28(2), 137-157. doi:<http://dx.doi.org/10.1002/rob.20359>
- Lee, Z., & Shang, S. (2016). Visibility: How applicable is the century-old Koschmieder model? *Journal of the Atmospheric Sciences*, 73(11), 4573-4581. Retrieved from <http://journals.ametsoc.org/doi/abs/10.1175/JAS-D-16-0102.1>
- Le Tallec, C. (2005). VFR general aviation aircraft and UAV flights deconfliction. *Aerospace Science and Technology*, 9(6), 495-503. Retrieved from <http://www.sciencedirect.com.ezproxy.libproxy.db.erau.edu/science/article/pii/S1270963805000040>

- Loffi, J., Wallace, R. J., & Ison, C. S. (2016). Analysis of the Federal Aviation Administration's small UAS regulations for hobbyist and recreational users. *International Journal of Aviation, Aeronautics, and Aerospace*, 3(1), Article 3. Retrieved from <http://commons.erau.edu/cgi/viewcontent.cgi?article=1111&context=ijaaa>
- Loffi, J. M., Wallace, R. J., Jacob, J. D., & Dunlap, J. C. (2016) Seeing the threat: Pilot visual detection of small unmanned aircraft systems in visual meteorological conditions. *International Journal of Aviation, Aeronautics, and Aerospace*, 3(3), Article 13. Retrieved from <http://commons.erau.edu/cgi/viewcontent.cgi?article=1142&context=ijaaa>
- Lumina Decision Systems, Inc. (2015). *Analytica user guide – Analytica 4.6*. Retrieved from http://downloads.analytica.com/ana/UserGuide4_6_1.pdf
- Mcfadyen, A., & Mejias, L. (2015). A survey of autonomous vision-based see and avoid for unmanned aircraft systems. *Progress in Aerospace Systems*, 80, 1-17. Retrieved from <http://www.sciencedirect.com.ezproxy.libproxy.db.erau.edu/science/article/pii/S0376042115300208/pdf?md5=c6e2fc63aab297e300cae1b3ef36405d&pid=1-s2.0-S0376042115300208-main.pdf>
- McKee, S. P., & Nakayama, K. (1984). The detection of motion in the peripheral visual field. *Vision Research*, 24(1), 25-32. Abstract retrieved from <https://www.ncbi.nlm.nih.gov/pubmed/6695503>
- Morris, C. (2005). Midair collisions: Limitations of the see-and-avoid concept in civil aviation. *Aviation, Space, and Environmental Medicine*, 76(4), 357-365. Retrieved from <http://docserver.ingentaconnect.com.ezproxy>.

libproxy.db.erau.edu/deliver/connect/asma/00956562/v76n4/s7.pdf?expires=1469484551&id=88247521&titleid=8218&acname=Embry-Riddle+Aeronautical+University&checksum=545A1612DE20DB0DAA5BA9001DB0569F

NPD Group. (2016) *Year-over-year drone revenue soars*. Press release. Retrieved from <https://www.npd.com/wps/portal/npd/us/news/press-releases/2016/year-over-year-drone-revenue-soars-according-to-npd/>

Operation and Certification of Small Unmanned Aircraft Systems; Final Rule. 81 Fed. Reg. § 124 (June 28, 2016) (to be codified at 14 CFR Parts 21, 43, 61,91, 101, 107, 119, 133, and 183). Retrieved from <https://www.gpo.gov/fdsys/pkg/FR-2016-06-28/pdf/2016-15079.pdf>

Papadopoulos, C. E., & Yeung, H. (2001). Uncertainty estimation and Monte Carlo simulation method. *Flow Measurement and Instrumentation*, 12(2001), 291-298. Retrieved from <http://www.sciencedirect.com.ezproxy.libproxy.db.erau.edu/science/article/pii/S0955598601000152>

Poe, A. C. (1974). *A model for visual detection of aircraft by ground observers*. U.S. Army Missile Command technical report RD-75-30. Washington, DC. Retrieved from <http://www.dtic.mil/dtic/tr/fulltext/u2/a017599.pdf>

Regan, D. (2000). *Human perception of objects*. Sunderland, MA: Sinauer Associates

Registration and Marking Requirements for Small Unmanned Aircraft; Final Rule, 80 Fed. Reg. § 241 (December 16, 2015) (to be codified at 14 CFR Parts 1, 45, 47, 48, 91, and 375). Retrieved from <https://www.gpo.gov/fdsys/pkg/FR-2015-12-16/pdf/2015-31750.pdf>

- Senate Passes Transportation, HUD Funding Bill: Includes Hoeven Provisions For Williston Airport, ND UAS Research.* (2016). Lanham: Federal Information & News Dispatch, Inc. Retrieved from <http://search.proquest.com.ezproxy.libproxy.db.erau.edu/docview/1790488345?accountid=27203>
- Toet, A. (2010). Structural similarity determines search time and detection probability. *Infrared Physics & Technology*, 53(2010), 464-468. Retrieved from <http://www.sciencedirect.com.ezproxy.libproxy.db.erau.edu/science/article/pii/S1350449510000745>
- Veneri, G., Pretegianni, E., Federighi, P., Rosini, P., Federico, A., & Rufa, A. (2010, November). Evaluating human visual search performance by Monte Carlo methods and heuristic model. *Proceedings of the 10th IEEE International Conference on Information Technology and Applications in Biomedicine*, 1-4. Retrieved from <http://ieeexplore.ieee.org.ezproxy.libproxy.db.erau.edu/xpl/articleDetails.jsp?arnumber=5687697>
- Volpe National Transportation Systems Center. (2017). *Presentation on the Number of Mandatory Occurrence Reports Filed for UAS Sightings per Month*. Unpublished analysis of Federal Aviation Administration Mandatory Occurrence Reports data.
- Warwick, G. (2016, February 15). Counter-UAS special report: The small UAV problem. *Aviation Week & Space Technology*. Accession Number 112987573. Retrieved from <http://web.b.ebscohost.com.ezproxy.libproxy.db.erau.edu/ehost/detail/detail?vid=2&sid=4b4fb84f-9e83-45e2-a289-79a9e61d80a4%40sessionmgr104&bdata=JnNpdGU9ZWwhvc3QtbGl2ZQ%3d%3d#db=bth&AN=112987573&anchor=AN0112987573-3>

- Weaver, M. E. (1981). *Target acquisition during a manned real-time reconnaissance mission* (Wright-Patterson Air Force Base, Operations Research Group – Mission Analysis Report ASD/XRM-TR-81-5021). Retrieved from <http://handle.dtic.mil/100.2/ADA100570>
- Westheimer, G. (2010). Visual acuity and hyperacuity. *Handbook of Optics*. Retrieved from <http://citeseerx.ist.psu.edu/viewdoc/download?doi=10.1.1.438.6210&rep=rep1&type=pdf>
- Wulfeck, J. W., Weisz, A., & Raben, M. W. (1958). *Vision in military aviation* (United States Air Force Report 58-399). Wright Air Development Center, Air Research and Development Command. Retrieved from <http://www.dtic.mil/dtic/tr/fulltext/u2/207780.pdf>
- Yu, X., & Zhang, Y. (2015). Sense and avoid technologies with applications to unmanned aircraft systems: Review and prospects. *Progress in Aerospace Sciences*, 74(2015), 152-166. Retrieved from http://ac.els-cdn.com/S0376042115000020/1-s2.0-S0376042115000020-main.pdf?_tid=64a855b4-ee1d-11e5-a67c-00000aab0f6c&acdnat=1458424751_749ae35bbe29ba8cc168f917f9bb7517

APPENDIX A

Common Small UAS Products and Specifications

Convenience Sample of Popular UAV Products for Consumers									Last Updated: 4/29/2017
Source	Mfg	Model	Primary Color	Size (in inches)			Weight (lbs)	Max Speed	Notes
				Width	Height	Depth			
DJI Website / Amazon	DJI	Phantom 3 Standard	WHITE	15	8.2	14	2.7	36 MPH	Aircraft can be personalized with small colored stripes
DJI Website / Amazon	DJI	Phantom 3 Advanced	WHITE	18	8	13	2.8	36 MPH	Aircraft can be personalized with small colored stripes
DJI Website / Amazon	DJI	Phantom 3 Professional	WHITE	18	8	13	2.8	36 MPH	Aircraft can be personalized with small colored stripes
DJI Website / Amazon	DJI	Phantom 3 4K	WHITE	18	8	13	2.8	36 MPH	Optional gold stickers available
DJI Website / Amazon	DJI	Phantom 4	WHITE	15	8	12.7	3	44 MPH	No stickers, body is completely white
DJI Website / Amazon	DJI	Phantom 4 Pro	WHITE	14.5	8	14	3.1	45 MPH	No stickers, body is completely white
DJI Website / Amazon	DJI	Mavic Pro	DARK GREY	11.4	7.1	9.4	1.62	40 MPH	Has small gold stripes painted on aircraft, no sticker options available

Convenience Sample of Popular UAV Products for Consumers

Last Updated: 4/29/2017

Source	Mfg	Model	Primary Color	Size (in inches)			Weight (lbs)	Max Speed	Notes
				Width	Height	Depth			
Amazon	Parrot	Bebop	BLACK*	13.2	3.8	14.4	0.88	31 MPH	Choice of red or blue with black
Amazon / Parrot Website	Parrot	Bebop 2	WHITE / BLACK	12.9	3.5	12.9	1.1	37 MPH	
Amazon / Parrot Website	Parrot	Disco	WHITE / BLACK	45.2	4.7	22.8	1.65	50 MPH	Dimensions are correct - not a quadcopter drone, it has two long wings
Amazon	Parrot	AR Drone 2.0	BLACK	23	5	23	0.9	25 MPH	
Best Buy / YUNEEC Website	YUNEEC	Typhoon 4K	BLACK	16.5	8.3	16.5	2.4	18 MPH	
YUNEEC Website	YUNEEC	Breeze	WHITE	7.7	2.5	7.7	0.85	11.2 MPH	
YUNEEC Website	YUNEEC	Typhoon H	BLACK	20.5	12.2	18.2	4.3	43.5 MPH	
YUNEEC Website	YUNEEC	Tornado H920	BLACK	31.4	18.1	36.2	11	25 MPH	Hexacopter
Best Buy / Autel	Autel Robotics	X-Star Premium	MULTIPLE*	6.8	8	5.1	3.13	35 MPH	Options of white or orange
Best Buy	EHANG	Ghostdrone 2.0 VR	MULTIPLE*	7.9	3.5	13.8	2.54	37 MPH	Options of white, black, or orange
DJI Website / Amazon	DJI	Inspire 1	WHITE / BLACK	16.5	2.8	18.9	6.74	49 MPH	Weight can vary with cameras

Convenience Sample of Popular UAV Products for Consumers

Last Updated: 4/29/2017

Source	Mfg	Model	Primary Color	Size (in inches)			Weight (lbs)	Max Speed	Notes
				Width	Height	Depth			
DJI Website / Amazon	DJI	Inspire 2	BLACK / SILVER	18	12	21	7.25	58 MPH	MTOW - 8.82 lbs.
xFold Website	xFold	Spy x8	BLACK	15.9	15	17.4	3.4	33.5 MPH	Drone is \$3,499
xFold Website	xFold	Travel x12	BLACK	31	38	22.6	10.3	Unavailable	Drone is \$12,999
xFold Website	xFold	Cinema x12	BLACK	34	39.2	27	24.9	Unavailable	Drone is \$23,999
xFold Website	xFold	Dragon x12	BLACK	53.7	28.3	62	42.5	Unavailable	Drone is \$31,599